Evaluating the consequences of polynucleotide kinase/phosphatase (PNKP) mutations in neurological diseases

by

Bingcheng Jiang

A thesis submitted in partial fulfillment of the requirements for the degree of

Doctor of Philosophy

in

Cancer Sciences

Department of Oncology
University of Alberta

Abstract

Genomic stability is extremely important for developing or maintaining normal neurological functions, as the nervous system is constantly suffering from endogenous DNA damage. To maintain such stability, living cells are protected by several different DNA repair pathways. Polynucleotide kinase/phosphatase (PNKP) is a bifunctional DNA repair enzyme that possesses both the DNA 3'-phosphatase and DNA 5'-kinase activities. It is involved in several different repair pathways including the single strand break repair and the non-homologous end joining pathways. Mutations in *PNKP* have been found to be responsible for different neurological diseases, including Microcephaly, seizures and developmental delay (MCSZ), and Ataxia-ocular motor apraxia 4 (AOA4).

Our focus was directed towards three different PNKP mutations reported in clinical cases. The first two mutations were found in a 3-year-old male MCSZ patient with cerebellar glioblastoma. Genetic screening for mutations associated with his clinical features showed that he carried 2 germline point mutations in *PNKP*, which caused two different single amino acid alterations in the protein (P101L and T323M). This is the first report of human cancer found in a patient with MCSZ. While the latter mutation has recently been identified in an MCSZ patient, the P101L mutation has not been previously reported. We have investigated the consequences of these mutations at the biochemical and cellular levels. Biochemically, the P101L variant retains relatively

robust DNA kinase and phosphatase activity, but the alteration at T323 significantly diminishes both enzymatic activities, especially the phosphatase activity. This is due in part to the reduced affinity for DNA substrates. Expressing the mutated proteins in HeLa PNKP-knockout cells revealed that the P101L PNKP variant localizes primarily to the cytoplasm rather than the nucleus. We established that this is the result of the creation of a novel nuclear export signal. An increase in cytoplasmic PNKP was also observed in tissue from the patient. Further analysis indicated that cells expressing P101L and T323M variants have a slower repair of radiation-induced DNA single strand breaks than cells reconstituted with the wild-type protein, and that the repair of radiation-induced double strand breaks is particularly slow in T323M-expressing cells. We also observed a significant increase in cellular transformation by the cells expressing the mutant proteins using the soft agar assay, which may reflect an increased propensity for oncogenic transformation.

To expand the spectrum of *PNKP* mutations and understand the molecular basis of AOA4, we picked one of the most frequently identified *PNKP* mutations associated with AOA4, G1123T, which gives rise to a G375W change in the protein. *In vitro* kinase and phosphatase assays revealed that the G375W PNKP mutant lacks kinase but retains near normal phosphatase activity. Furthermore, our results indicate that the loss of kinase activity can be attributed to near elimination of ATP binding, while DNA binding affinity remained unchanged. Cellular studies showed that the G375W-PNKP has the same subcellular localization as the wild type PNKP. It partially rescues radiation sensitivity in mutant cells compared to the PNKP knockout cells. Interestingly, G375W-

PNKP increases paraquat sensitivity more than PNKP knockout cells. Further study

showed mitochondria in G375W cells are more sensitive to paraquat treatment,

indicating mitochondria in the mutant cell lines could be the main target during the

disease's development.

Together, our study explored the consequences of different PNKP mutations found in

MCSZ and AOA4, and provided evidence for different mechanisms underlying the

development of these diseases. Understanding these consequences could lead to more

targeted treatment in the future.

Preface

Chapter 1 provides an introduction about different pathways of DNA damage and repair, neurological diseases linked with mutations of DNA repair genes, characteristics and functions of PNKP, neurological diseases caused by PNKP mutations, and pediatric glioblastoma.

Chapter 2 is collaborative work among the University of Alberta, Seattle Children's Hospital, University of Washington, Tulane University, University of California Los Angeles, and University of Texas. A manuscript describing this work entitled "Mutations of the DNA repair gene PNKP in a patient with Microcephaly, Seizures, and Developmental Delay (MCSZ) presenting with a high-grade brain tumor" was recently submitted to Scientific Reports. The clinical components of the study were provided by Seattle Children's Hospital and the University of Washington. Most of the experiments and manuscript preparation were designed and conducted by Bingcheng Jiang under the supervision of Dr. Michael Weinfeld. Rajam S. Mani conducted the DNA binding assays and circular dichroism analysis. Cameron Murray in Dr. Mark Glover's laboratory conducted the XRCC4 peptide binding assays.

Chapter 3 encompasses original work by Bingcheng Jiang. Most of the experiments and manuscript preparation were designed and conducted by Bingcheng Jiang under the supervision of Dr. Michael Weinfeld. Rajam S. Mani conducted the DNA binding assays and circular dichroism analysis.

Chapter 4 summarizes the main topics of this thesis, discusses the related areas in neurological diseases and cancer development. Finally, we discuss future experimental procedures required to optimize the work done in this thesis.

Appendix includes the published paper by Bingcheng Jiang, Mark Glover, and Michael Weinfeld. "Neurological disorders associated with DNA strand-break processing enzymes" on *Mechanisms of Ageing and Development* 161 (2017) 130-140.

Acknowledgements

Table of Contents

List of Tables

List of Figures

Abbreviations

3'-OH	3'-hydroxyl
3'-P	3'-phosphate
3'-PUA	3'-α,β unsaturated aldehyde
53BP1	p53 binding protein 1
5'-OH	5'-hydroxyl
5'-P	5'-phosphate
5'-dRP	5'-deoxyribose phosphate
8-oxo-dG	8-hydroxydeoxyguanosine
Aβ	Amyloid beta
AAV	Adeno-associated virus
ABCA1	ATP binding cassette subfamily A member 1
AD	Alzheimer's disease
ANOVA	Analysis of variance
AOA	Ataxia-ocular motor apraxia
AP	Apurinic/apyrimidinic
APE1	Apurinic/apyrimidinic endonuclease 1
APP	Amyloid-beta precursor protein
APTX	Aprataxin
ATM	Ataxia Telangiectasia Mutated
ATP	Adenosine triphosphate
ATR	Ataxia telangiectasia and Rad3-related protein
ATRX	ATP-dependent helicase
ATXN3	Ataxin 3
BDNF	Brain-derived neurotrophic factor
BER	Base excision repair

BRCA2	Breast cancer type 2 susceptibility protein
BTICs	Brain tumor initiating cells
CD	Circular dichroism
CF	Cystic fibrosis
CFTR	Cystic fibrosis transmembrane conductance regulator
CK2	Casein kinase 2
CMT	Charcot-Marie-Tooth
CNS	Central nervous system
CRM1	Chromosomal Maintenance 1, Exportin 1
cRNA	Complementary RNA
CT	Computed tomography
DDR	DNA damage response
D-loop	Displacement loop
DM	Double Mutant
DNA	Deoxyribonucleic acid
DNA-PKcs	DNA-dependent protein kinase catalytic subunit
DSB	Double-strand break
DSBR	Double-strand break repair
DTT	Dithiothreitol
EDTA	Ethylenediaminetetraacetic acid
EGFR	Epidermal growth factor receptor
EVD	External ventricular drain
EXO1	Exonuclease 1
FEN1	Flap endonuclease 1
FHA	Forkhead-associated
FP	Fluorescence polarization

GBM	Glioblastoma multiforme
GFAP	Glial fibrillary acid protein
GFP	Green fluorescent protein
H2AX	H2A histone family member X
HD	Huntington's disease
HDL	High-density lipoproteins
HGG	High-grade gliomas
His	Histidine
HMSN	Hereditary motor and sensory neuropathy
HR	Homologous recombination
HTT	Huntingtin
HTV-1	Human immunodeficiency virus type 1
IPTG	Isopropyl-β-D-1-thiogalactopyranoside
Ku	Ku70/Ku80 heterodimer
LB	Lysogeny broth
LIG1	DNA ligase I
LIG3	DNA ligase III
LIG4	DNA ligase IV
LMB	Leptomycin B
lpSSBR	long-patch single-strand break repair
MCPH	Microcephaly
MCSZ	Microcephaly, seizures and developmental delay
MED25	Mediator Complex Subunit 25
MGMT	O^6-methylguanine methyltransferase
MLH1	MutL homolog 1
MNCV	Motor nerve conduction velocities

mNPCs	Murine neuroepithelial progenitors
MRN	MRE11/RAD50/NBS1 protein complex
MRIs	Magnetic resonance imaging scans
MSH2	MutS homolog 2
mtDNA	Mitochondrial DNA
MYH9	Myosin-9 protein
NBS	Nijmegen breakage syndrome
NBS1	Nibrin
NEIL1	Endonuclease VIII-like 1
NEIL2	Endonuclease VIII-like 2
NER	Nucleotide excision repair
NES	Nuclear export signal
NF1	Neurofibromin 1
NHEJ	Non-homologous end joining
NLS	Nuclear localization signal
NPC	Nuclear pore complexes
nsSNPs	Non-synonymous SNPs
NTR	Near-total resection
OGG1	8-Oxoguanine DNA glycosylase
PARP1	Poly(ADP-ribose) polymerase I
PCNA	Proliferating cell nuclear antigen
PD	Parkinson's disease
PDGFRA	Platelet-derived growth factor receptor-α
PG	Phosphoglycolate
PI3Ks	Phosphoinositide 3-kinase
PIK3R5	Phosphoinostitide-e-kinase regulatory subunit 5
PINK1	Parkinson disease-related protein
PKI	Protein kinase inhibitor

PMP22	Peripheral myelin protein 22
PMSF	Phenylmethylsulfonyl fluoride
PNKP	Polynucleotide kinase/phosphatase
Pol β	DNA polymerase β
Pol δ	DNA polymerase δ
Pol ε	DNA polymerase ε
Pol λ	DNA polymerase λ
Pol μ	DNA polymerase μ
PTEN	Phosphatase and tensin homolog
RAD51	RAD51 recombinase
RB1	Retinoblastoma protein 1
RNA	Ribonucleic acid
ROS	Reactive oxygen species
RPA	Replication protein A
SAM	S-adenosylmethionine
SCA3	Spinocerebellar ataxia type3
SCAN1	Spinocerebellar ataxia with axonal neuropathy
SDSA	Synthesis-dependent strand annealing
SETX	Senataxin
SNPs	Single nucleotide polymorphisms
spSSBR	short-patch single-strand break repair
SSB	Single-strand break
TCR	Transcription-coupled DNA repair
TDP1	Tyrosyl-DNA phosphodiesterase 1
TERT	Telomerase reverse transcriptase
TOP1	DNA topoisomerase I
TP53	Tumour protein 53

UV	Ultraviolet
WT	Wild-type
WHO	World Health Organization
XLF	XRCC4-like factor
XP	Xeroderma pigmentosum
XRCC1	X-ray repair cross-complementing protein 1
XRCC4	X-ray repair cross-complementing protein 4

1 Chapter 1: Introduction

1.1 DNA damage and repair

DNA, the central repository of genetic information in a living cell, is essential to life. Even without exogenous agents such as ionizing radiation, ultraviolet (UV) light, and genotoxic chemicals, DNA is continuously under attacks from endogenous agents (1). As the most common endogenous DNA damaging agent, reactive oxygen species (ROS) are formed continuously in the course of cellular metabolism. ROS can directly interact with DNA bases or the backbone to generate various oxidative DNA lesions (2), for example 8-hydroxydeoxyguanosine (8-oxo-dG), the most common oxidatively modified DNA nucleoside, ranging from 0.1 to 100 per 10^5 guanines (3). Besides ROS, reactive metabolites can also trigger DNA lesions. S-adenosylmethionine (SAM) is a reactive methyl group donor required for physiological enzymatic DNA methylation (4). However, intracellular SAM may also generate mutagenic DNA adducts such as 7-methylguanine and O^6-methylguanine (5). In addition to direct modification, the DNA alterations induced by endogenous agents could also lead to further damage to DNA during attempted repair. For example, in the course of repairing modified DNA bases, abasic sites are generated by cleavage of glycosidic bonds in DNA. The abasic sites caused by such a process are estimated to occur 10,000 lesions/human cell/day (6). The plethora of DNA lesions arising from all the scenarios can compromise the integrity of cellular DNA. To maintain genetic stability, living cells are equipped with a signaling network, termed the DNA damage response (DDR).

1.1.1 Base excision repair (BER)

Smaller DNA base modifications, such as those produced by ROS and smaller alkylating agents, constitute one of the most common classes of lesions. BER is the repair pathway that actively responds to such damages throughout the cell cycle (**Fig. 1.1**). The first step is initiated by a damage-specific DNA glycosylase that detects the damaged base (7). There are two main groups of DNA glycosylases: monofunctional and bifunctional glycosylases. Monofunctional DNA glycosylases will flip the base out of the double helix and cleave the N-glycosylic bond that links the DNA base to the sugar-phosphate backbone to generate an abasic site (8). The abasic site will then be cleaved by Apurinic/apyrimidinic (AP) endonuclease 1 (APE1) to create a DNA single-strand break (SSB) harboring a 5'-deoxyribose phosphate (5'-dRP) residue (9). Bifunctional DNA glycosylases possess N-glycosidic bond cleaving activity and an additional AP lyase activity. There are two types of AP lyase eliminations by human bifunctional DNA glycosylases: β-elimination and β,δ-elimination. β-elimination is carried out by glycosylases such as Endonuclease III homolog 1 (NTH1) and 8-Oxoguanine DNA glycosylase (OGG1), generating a 3'-α,β unsaturated aldehyde (3'-PUA), which will then be removed by APE1, resulting in a strand break with a 3'-OH terminus. β,δ-elimination glycosylases, such as Endonuclease VIII-like 1 (NEIL1) and Endonuclease VIII-like 2 (NEIL2), generate strand breaks with 3'-phosphate termini, which cannot be processed by APE1 and require the action of Polynucleotide kinase/phosphatase (PNKP) to convert them into 3'-OH termini (10).

Overall, BER utilizes multiple proteins, and goes through different routes, to convert base damage into indirect SSB. Both indirect SSB and those generated directly by attack on the sugar-phosphate backbone are repaired either by the short-patch single-strand break repair (spSSBR) or the long-patch single-strand break repair (lpSSBR) pathways.

1.1.2 spSSBR and lpSSBR

spSSBR starts with the involvement of poly(ADP-ribose) polymerase I (PARP1). After PARP1 binds to the specific DNA end structure with its zinc finger domain (Zn1 to the 5'-end, Zn2 to the 3'-end), PARP1 undergoes allosteric activation and catalyzes poly (ADP-ribose) synthesis: PARylation (11). The PARylation occurs on several acceptor proteins, such as histones (12), DNA topoisomerase I (TOP1) (13), and itself: auto-PARylation (14). The accumulation of negatively charged PAR polymers facilitates chromatin decondensation, allowing the accession to damage sites by downstream repair proteins (15). The PAR chain also flags the damage sites for recruiting repair proteins such as X-ray repair cross-complementing protein 1 (XRCC1) (16). XRCC1 acts as a scaffold for other SSBR proteins, such as PNKP (17), DNA polymerase β (Pol β) (18), and DNA ligase 3 (LIG3) (19). PNKP converts the 3'-phosphate and 5'-OH termini into 3'-OH and 5'-phosphate (20). Pol β, with its intrinsic dRP-lyase activity, removes the blocking 5'-dRP generated by APE1 (21). Once all the termini have the correct chemical form, Pol βadds one nucleotide to replace the damaged nucleotide (22). Finally, LIG3 seals the nick to complete the repair process in spSSBR (23).
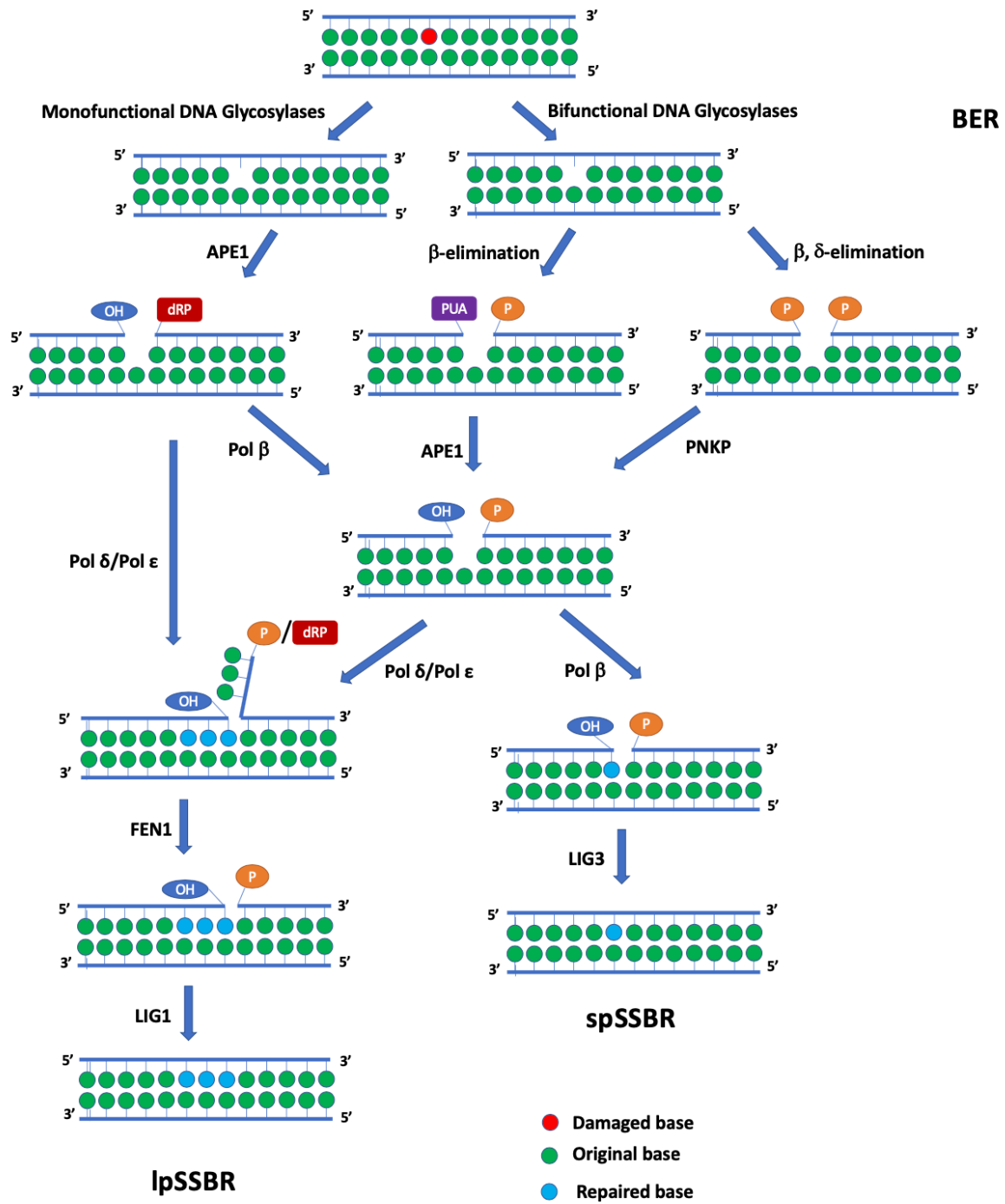
Figure 1.1 Graphical representation of BER, spSSBR and lpSSBR.

Graphical representation of major steps involved in BER, spSSBR and lpSSBR. Details are outlined in 1.1.1 and 1.1.2.

In contrast to the spSSBR, the lpSSBR incorporates multiple nucleotides ranging from 2 to 12 during the DNA synthesis step. This synthesis step is carried out by DNA polymerase δ (Pol δ) and DNA polymerase ε (Pol ε), with the help of proliferating cell nuclear antigen (PCNA) (24). The synthesized strand displaces the downstream 5'-DNA end to form a flap intermediate. As a structure specific nuclease, Flap endonuclease 1 (FEN1) excises the displaced oligonucleotides (25). DNA ligase I (LIG1) then seals the nick to finish the lpSSBR process (26). The decision to go through lpSSBR instead of spSSBR appears to be influenced by multiple factors. For example, lpSSBR occurs if termini, such as X-ray damage generated 2-deoxyribonolactone, cannot be processed by spSSBR (27). lpSSBR also occurs more frequently at low ATP concentration, where the ATP dependent ligation process cannot immediately proceed (28). In addition, cell cycle and differentiation also contribute to the choice between lpSSBR and spSSBR (29).

1.1.3 Non-homologous end joining (NHEJ)

A DNA double-strand break (DSB) arises when two SSB occur on the opposing strand simultaneously within 10-20 bp (30). Similar to other forms of DNA damage, DSB can arise from a wide range of exogenous and endogenous factors. Unlike other DNA lesions, DSBs directly disrupt the genome's physical continuity and integrity (31). DSBs are mainly repaired by two different pathways, non-homologous end joining (NHEJ) and homologous recombination (HR).
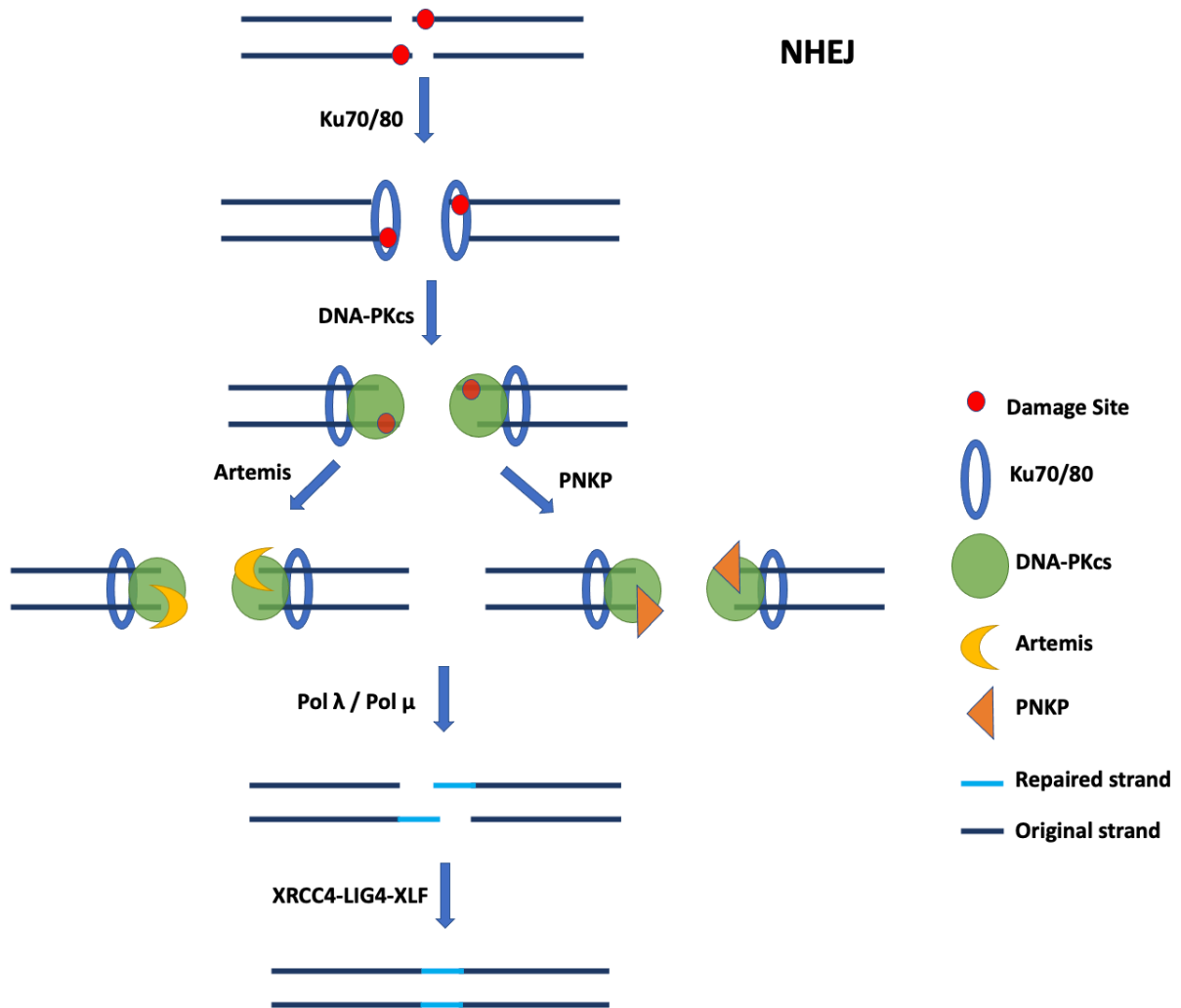
Figure 1.2 Graphical representation of NHEJ.

Graphical representation of major steps involved in NHEJ. Detailed steps are outlined in **1.1.3**.

NHEJ (**Fig. 1.2**) is active throughout the cell cycle and is the major double-strand break repair pathway being responsible for approximately 75% of DSB repair while HR handles approximately 25% in proliferating cells (32). One of the primary sensing proteins in NHEJ is the Ku70/Ku80 heterodimer (Ku). By binding to the broken DNA termini, Ku aligns both strands and protects them from degradation while still allowing access of other downstream repair proteins (33). The scaffold created by Ku recruits and activates DNA-dependent protein kinase catalytic subunit (DNA-PKcs) (34). After Ku loads onto DNA strand break termini, it moves inward by one helical turn to allow DNA-PKcs to bind to the 10-bp region at both broken termini (35). The recruited DNA-PKcs initiates a cascade of phosphorylation targeting itself and Ku, followed by phosphorylation of multiple participating proteins, such as Artemis, X-ray repair cross-complementing protein 4 (XRCC4), XRCC4-like factor (XLF), and DNA ligase IV (LIG4) (36). Similar to the BER and SSBR process, compatible DNA termini (3'-OH and 5'-phosphate) can be directly used for DNA synthesis and ligation. However, incompatible DNA termini require the termini to be processed as well. Two key NHEJ end-processing enzymes are PNKP(37, 38) and the Artemis endonuclease. Once activated by DNA-PKcs, Artemis removes single-stranded overhanging DNA ends containing damaged nucleotides to generate blunt or near-blunt ends DSB (39, 40). Once the correct termini are formed, the gap-filling process is completed by DNA polymerase λ (Pol λ) (41) and/or DNA polymerase μ (Pol μ) (42). The final step in NHEJ is carried out by the XRCC4-LIG4-XLF complex. Interaction with XRCC4 stabilizes LIG4 (43) and stimulates its activity (44). The binding between XLF and XRCC4 facilitates the stabilizing of broken DNA ends (45). XLF also

helps the synthesis process of Pol λ and Pol μ by aligning DNA termini in the repair complex (46).

Overall, NHEJ utilizes multiple proteins to repair DSBs without the requirement of a sister chromatid template. Thus, NHEJ has been regarded as "error-prone" in the past since it "simply" cleans up the damaged termini and ligates them. However, the majority of autosomal genes are biallelically expressed, and a recent study indicated that nascent RNA transcribed from the other (undamaged) allele can provide the template for NHEJ, thereby mediating error-free repair (47).

1.1.4 Homologous recombination (HR)

In contrast to NHEJ, HR requires the sister chromatid as a template to repair DSBs (**Fig. 1.3**). Thus, it only occurs during the late S/G2 phase of the cell cycle. HR can be divided into three stages: presynapsis, synapsis, and postsynapsis (48). Presynapsis is made up of the damage recognition and end resection process, achieved by multiple proteins including the MRE11/RAD50/NBS1 (MRN) protein complex, Exonuclease 1 (EXO1), and Replication protein A (RPA). The MRN complex plays the key structural role of binding broken DNA termini (49). In addition, MRE11 carries out the endonuclease activity to create the initial nicked sites for the ensuing bidirectional resection (50) mediated by the 3'-5' exonuclease activity of MRE11 and the 5'-3' exonuclease activity of EXO1 (51). During presynapsis, the MRN complex also recruits Ataxia Telangiectasia Mutated (ATM) (52). As a major serine/threonine protein kinase, ATM phosphorylates various DNA repair proteins, including MRN and EXO1. The phosphorylation of MRN and EXO1 by ATM
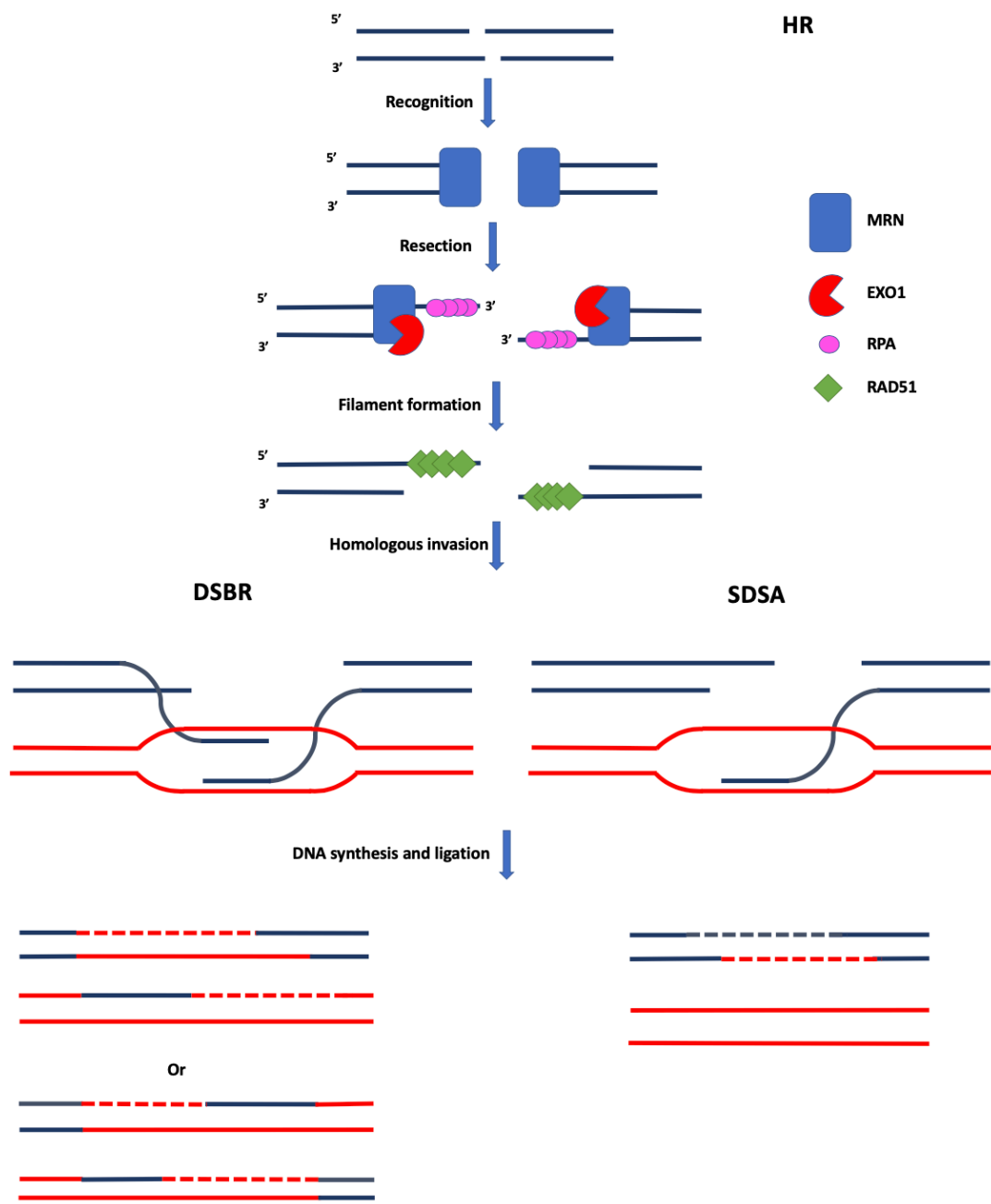
Figure 1.3 Graphical representation of HR.

Graphical representation of major steps involved in HR. Details of the steps are outlined in **1.1.4**. Damaged strands are in dark blue, template strands are in red, original strands are in solid lines, newly synthesised strands are in dotted lines.

determines the extent of resection to prepare an optimal substrate for subsequent steps (53). The resection process creates two 3'- ssDNA overhangs, which bind to RPA to prevent possible secondary structure or degradation (54). RPA is then replaced by the RAD51 recombinase (RAD51) to form a RAD51-ssDNA filament, referred to as the presynaptic complex (55). During the synapsis stage, the presynaptic complex is responsible for searching DNA homologous to the 3'-overhang. Once it has located the template, the protein-coated 3'-overhang invades the homologous DNA to form a displacement loop (D-loop). DNA polymerase η then copies the genetic information from the template to extend the 3' strand (56). During the postsynapsis stage, the second DSB end can become involved in the D-loop to form a DNA intermediate that contains two Holliday junctions, referred to as double-strand break repair (DSBR). Alternatively, the extended single-strand end can be annealed, followed by the other strand's gap-filling DNA synthesis and ligation, referred to as synthesis-dependent strand annealing (SDSA) (57). The repair products of SDSA are always non-crossover, while the products of DSBR can be either crossover or non-crossover (58-60).

1.2 Nuclear import and export machinery

DNA replication and protein synthesis are separated by the double membranous nuclear envelope in eukaryotic cells. It is important to have selective and regulated machinery to transport proteins between the nucleus and cytoplasm. Proteins enter and exit the nucleus through the nuclear pore complexes (NPC). In mammals, NPC is a 125 MDa macromolecular complex inserted in the nuclear envelope (61). Proteins that are

smaller than 40 kDa can pass through the NPC's 10-nm diameter single transport

channel by passive diffusion. At the same time, the active transport channel of NPC can

expand to 35 nm, allowing rapid translocation of larger proteins with appropriate signals

(62). Efficient active transport requires nuclear transport receptors that bind to proteins

and mediate their translocation, in particular, the karyopherins family (63). Karyopherins

weigh 95 to 145 kDa and can interact with NPC proteins. So far, 14 karyopherins have

been identified in yeast and at least 20 have been found in mammals (64). Karyopherins

mediate the import or export process via recognition of the nuclear localization signal

(NLS) or nuclear export signal (NES) in the cargo proteins (65).

The nuclear import process starts with the interaction between the cargo protein's NLS

motif and import karyopherins (importins). The classical NLS is a lysine/arginine-rich

sequence that falls into two categories: monopartite NLS, such as P<u>KKKRK</u>VE from

simian virus 40 large T antigen (66), or bipartite NLS, such as <u>KR</u>PAATKKAGQA<u>KKKK</u>

from *Xenopus* nucleoplasmin (67). Once the cargo protein is bound by its NLS,

importins can then interact with NPC and translocate the cargo protein to the nucleus.

The interactions between cargo protein and importins are regulated by the GTPase

Ran. Ran cycles between Ran-GTP and Ran-GDP bound states. Once in the nucleus,

the importins will associate with Ran-GTP and dissociate from the cargo protein, thus

finishing the transportation process (68). Similar to the import process, the nuclear

export process starts with the interaction of the cargo protein's NES sequence and

export karyopherins (exportin). The most common NES is a conserved leucine-rich

motif, such as <u>L</u>PP<u>L</u>ER<u>L</u>T<u>L</u> in human immunodeficiency virus type 1 (HIV-1) Rev protein

(69). In contrast to importin, the association between exportin and cargo protein requires the interaction with Ran-GTP. After the recognition step, the exportin-cargo-Ran-GTP complex will then transport from the nucleus to the cytoplasm. After the Ran-GTP is hydrolysed to Ran-GDP in the cytoplasm, the complex is dissociated and the export process is completed (70). It is worth noting that there is signal-independent transportation machinery as well. For example, β-catenin, which contains no NLS, is imported into the nucleus by directly binding to NPC without the help of karyopherins (71).

The nuclear transportation machinery is a prerequisite for the functions of DNA repair proteins. Many DNA repair proteins contain classical or putative NLS, such as XRCC1 (SPKGKRKLDLNQEEKKTPSKPPAQLSPSVPKRPKLP) (16, 72), PNKP (LPKKRMRKSNP) (73, 74), and XRCC4 (PSRKRRQRM) (75). DNA repair proteins that do not contain an NLS sequence can be translocated through the co-import mechanism. For example, mismatch repair protein MSH2 does not contain a classical NLS sequence, but it forms a complex with EXO1 (IVKRPRSA) containing an NLS to facilitate the import process (76). The NER protein XPD also lacks an NLS sequence and be imported into the nucleus in association with other NLS-containing proteins (77).
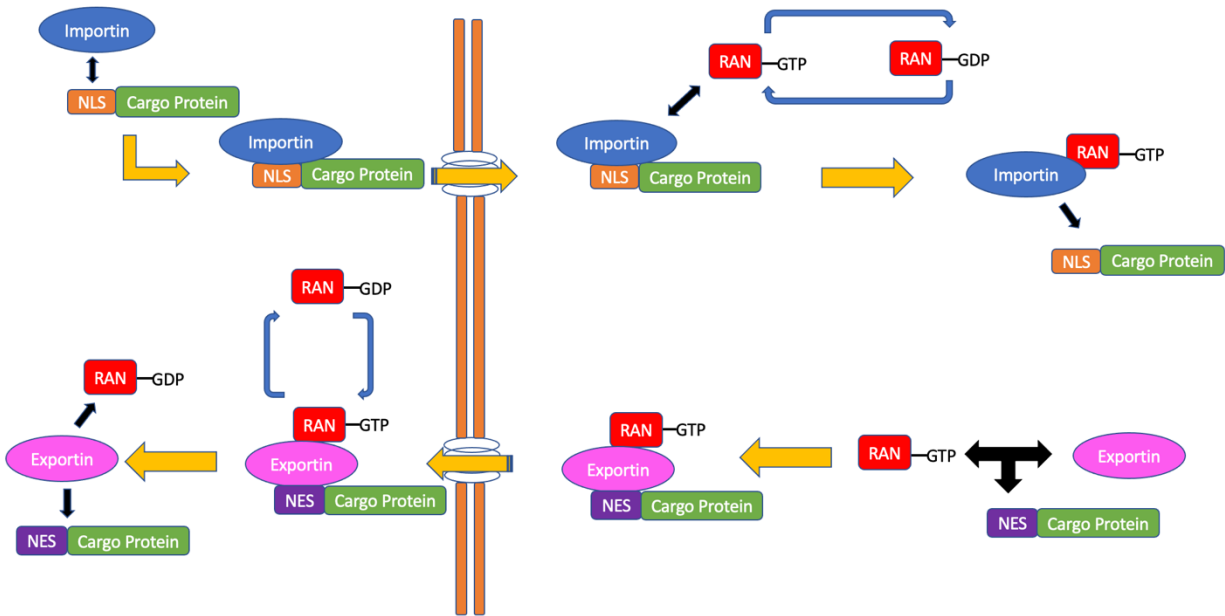
Figure 1.4 Graphical representation of nuclear import and export machinery.

Graphical representation of major steps involved in nuclear import and export process.

Details of the steps are outlined in **1.2**. NLS represents nuclear localization signal, NES

represents nuclear export signal.

1.3 Neurological diseases linked with DNA instability

The nervous system constantly suffers from endogenous DNA damage arising from neurogenesis (78), physiologic activities (79), and the aging process (80). Thus, genome stability is extremely important for maintaining normal neurological functions. Various neurological symptoms can arise from DNA instability and affect different nervous system regions at different life stages.

Neurodevelopmental disorders are a group of disorders caused by the disruption of the nervous system's normal development, leading to the inability to acquire motor, cognitive, or emotional functions (81). A large number of neurodevelopmental disorders are found associated with DNA instability. For example, Nijmegen breakage syndrome (NBS) is a rare autosomal recessive disorder characterized by developmental defects, including microcephaly and retardation, immunodeficiency, and cancer predisposition (82). NBS has been linked to mutations in the *NBN* gene, which codes for the protein Nibrin (NBS1) (83). NBS1 is part of the MRN protein complex, which plays an important role in initiating double-strand DNA break repair (84). Ataxia telangiectasia and Rad3-related protein (ATR) is a serine/threonine-specific protein kinase that participates in sensing single-strand DNA breaks and stalled replication forks, activating cell cycle arrest and DNA repair (85). Mutations in *ATR* are linked to one form of Seckel syndrome, an autosomal recessive disorder characterized by microcephaly, mental retardation, and growth defect (86).

Unlike the early onset of neurodevelopmental disorders, the neurodegenerative diseases usually occur at later ages. Neurodegenerative diseases are disorders resulting from progressive deterioration of selected neurons in the nervous system (87). Ataxia telangiectasia, an autosomal recessive syndrome, is characterized by progressive cerebellar degeneration, premature aging, telangiectasia, immunodeficiency, and predisposition to cancer (88). Ataxia telangiectasia is caused by mutations in *ATM* (89). ATM belongs to the phosphoinositide 3-kinase (PI3Ks) superfamily, the same family as ATR. As discussed above, ATM is recruited by the MRN complex and involved in double-strand DNA break repair (52). Spinocerebellar ataxia with axonal neuropathy (SCAN1) is also an autosomal recessive disorder. Its symptoms include slowly progressing cerebellar ataxia, loss of reflexes, and peripheral neuropathy. SCAN1 is caused by mutations in *TDP1* gene, which encodes tyrosyl-DNA phosphodiesterase 1 (TDP1), a DNA strand-break processing enzyme (90). TDP1 acts on the covalent TOP1-DNA dead-end complexes formed by incomplete reaction of TOP1 with DNA (91). It also releases a variety of 3'-adducts to generate a 3'-phosphate terminus for further DNA repair processing (92).

The road from DNA defects to neurological disorders is still not clear. It is interesting that proteins that act in the same DNA repair pathway, like NBS1 and ATM, or proteins from the same superfamily, like ATM and ATR, could lead to different symptoms, while similar symptoms, such as progressive cerebellar degeneration, are caused by mutations in proteins from different DNA repair pathways, like ATM and TDP1.

1.4 PNKP

PNKP is a bifunctional DNA repair enzyme that possesses both the DNA 3'-phosphatase and DNA 5'-kinase activities (**Fig. 1.5**) required to process both 3'-phosphate and 5'-hydroxyl strand break termini in DNA (93-95).
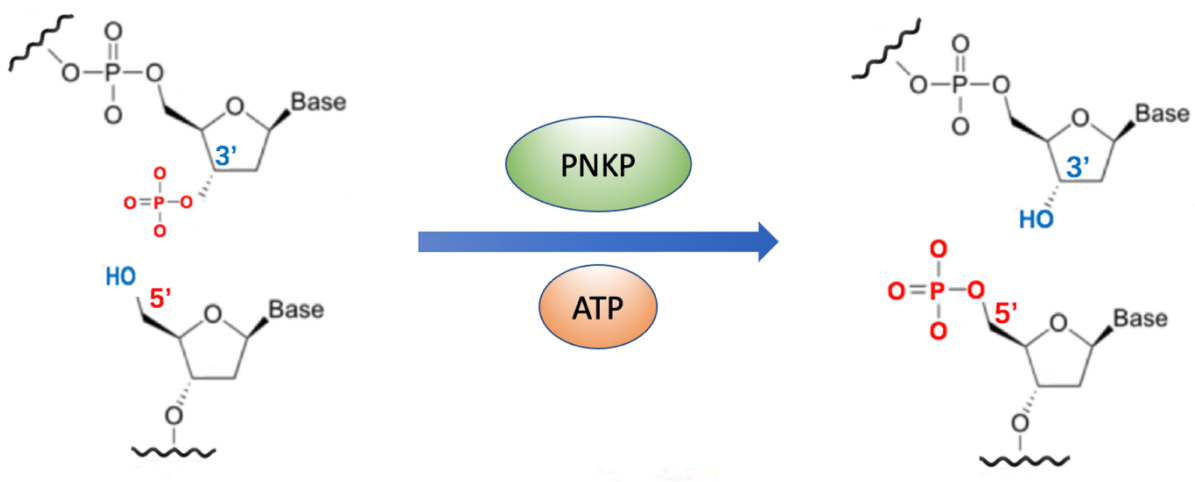
Figure 1.5 The enzymatic activities of PNKP.

The activities of PNKP including both DNA 3'-phosphatase and DNA 5'-kinase activities. PNKP catalyzes the phosphorylation of 5′-OH termini, using ATP as the phosphate donor, and the dephosphorylation of 3′-phosphate termini (96).
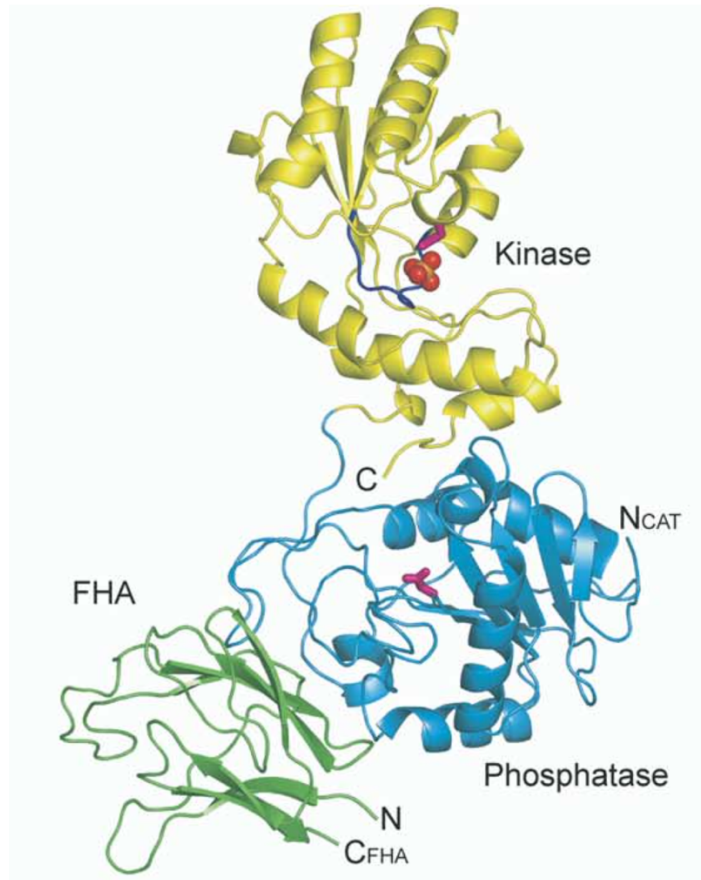
Figure 1.6 Structure of murine PNKP.

Structures of murine PNKP, with kinase domain in yellow, phosphatase domain in blue, FHA domain in green. Catalytic residues (Asp170 and Asp396 in the phosphatase and kinase, respectively) are in pink, the ATP binding P loop is in navy blue, and the sulfate bound at the P loop is in orange and red spheres (97).

PNKP protein is conserved through different organisms. The amino acid sequence of murine PNKP shares over 80% similarity to human PNKP (97), and even the homologs of PNKP in *Caenorhabditis elegans* and *Schizosaccharomyces pombe* share ~30% similarity to the human protein (95). So far only the structure of murine PNKP has been crystallized, as shown in **Figure 1.6**. Human PNKP is a 57.1-kDa multidomain protein that consists of an N-terminal forkhead-associated (FHA) domain and a catalytic subunit, attached to each other by a flexible linker region (97). The FHA domain selectively binds to acidic casein kinase 2 (CK2)-phosphorylated regions of the scaffold proteins XRCC1 (98) and XRCC4 (37), key components of BER and NHEJ, respectively. Such interactions facilitated by the FHA domain help direct PNKP to the DNA damage site (20, 97). The catalytic subunit includes the phosphatase domain and the C-terminal kinase domain. Although named independently, the phosphatase and kinase domains are tightly associated with each other in structure and function. The crystal structure of murine PNKP (97) shows the kinase and phosphatase domain tightly associate with each other through a large interface and cannot be separated by proteolysis. Moreover, the two catalytic active sites (Asp 170 and Asp 396 in the phosphatase and kinase domain, respectively) in murine PNKP are positioned on the same side of the protein. One study showed that in human PNKP, mutated phosphatase active sites (D171A or D173A) disrupts both phosphatase and kinase activities while mutated kinase active site (K378A) does not affect the phosphatase activity (99).

As a key DNA terminus processing protein, PNKP is involved heavily in BER, SSBR, and NHEJ (17, 38, 100) but is not required for HR (101, 102). Strand breaks with 3'-phosphate and 5'-hydroxyl termini can arise directly when exposing cells to damaging agents such

as hydroxyl radicals and ionizing radiation (103, 104). During different DNA repair processes, 3'-phosphate and 5'-hydroxyl termini can also be produced as intermediate products. A large number of PNKP substrates arise as the products of DNA glycosylases or endonucleases, as mentioned above in **1.1.1**. The end product of TDP1 also requires processing by PNKP prior to ligation. Topoisomerase I poison such as camptothecin prevent the DNA nick rejoining by TOP1, leaving a TOP1-DNA "dead-end" complex. Hydrolysis of this complex by TDP1 creates a DNA nick with 3'-phosphate and 5'-OH termini. Another important role of TDP1 is converting 3'-phosphoglycolate (PG) into 3'-phosphate (105). 3'-PG is produced by ionizing radiation, bleomycin, and enediyne compounds such as neocrazinostatin (20). PNKP, in combination with TDP1, can efficiently process 3'-PG, especially at 3'-overhangs and blunt-ends (106).

1.5 Neurological diseases caused by *PNKP* mutation

Mutations in *PNKP* have been found to be responsible for three different neurological diseases: the autosomal recessive neurodevelopmental disorder Microcephaly, seizures and developmental delay (MCSZ) (OMIM 613402) (107), the autosomal recessive neurodegenerative disease Ataxia-ocular motor apraxia 4 (AOA4) (OMIM 616267) (108), and the hereditary peripheral neuropathy Charcot-Marie-Tooth disease subtype 2B2 (CMT2B2) (OMIM 605589) (109).

1.5.1 Microcephaly, seizures and developmental delay (MCSZ)

In 2010, Shen et al. reported a previously unknown autosomal recessive disease in seven unrelated kindreds with Middle Eastern and European origin. Brain magnetic resonance imaging scans (MRIs) showed the signature feature of this disorder to be primary microcephaly without apparent structural abnormalities or degeneration (107). Primary microcephaly is characterized by reduced skull circumference with corresponding reduced brain volume at birth, in the absence of environmental or maternal aetiologies. The degree of microcephaly is correlated with the risk and severity of mental retardation (110). So far, there are two groups of protein malfunctions related to microcephaly. The first group is comprised of autosomal recessive primary microcephaly (MCPH) proteins, all of which are involved in centrosome function. Disruption of MCPH proteins can delay centrosome maturation or spindle orientation, thereby depleting the progenitor pool and limiting the total number of neurons that can be generated (111). Another group of proteins that contributes to microcephaly is involved in the DNA damage response. Besides *PNKP*, mutations in several DNA repair genes are responsible for microcephaly, such as *ATR* mutation, which causes Seckel syndrome 1 (OMIM 210600) (86); Breast cancer type 2 susceptibility protein (*BRCA2*) mutation causing Fanconi anemia complementation group D1 (OMIM 605724) (112); *NBS1* mutation causing Nijmegen breakage syndrome (OMIM 251260) (83); and *LIG4* mutation responsible for LIG4 syndrome (OMIM 606953) (113).

In addition to the microcephaly, MRI showed a preserved or slightly simplified gyral pattern and proportionately reduced cerebellum, indicating an absence of neuronal migration or other structural abnormalities. In contrast to other diseases featuring

21

microcephaly, the affected MCSZ individuals showed several different traits: (a) MCSZ patients did not develop ataxia or any other neurological symptom; (b) clinical evidence of immunodeficiency was not observed, with normal frequency of common or uncommon infections; (c) all the individuals showed development delay, seizures (first onset ranging from 1 to 6 months) and variable behavioral problems, particularly hyperactivity (107).

In the original seven families discovered to have MCSZ individuals, two kinds of point-mutations and two kinds of frame-shift mutations in *PNKP* were identified. *PNKP* mutation types include homozygous and compound heterozygous mutations in MCSZ individuals. The mutation patterns include different combinations in the PNKP's catalytic domain: (a) homozygous mutations only in the phosphatase domain (E326K + E326K); (b) homozygous mutations only in the kinase domain (T424Gfs48X + T424Gfs48X); (c) compound heterozygous mutations in the kinase domain (T424Gfs48X + Exon15Δfs4X); (d) compound heterozygous mutations in both domains (L176F + T424Gfs48X) (107). Later, several studies of individuals with MCSZ from the Middle East, Europe, East Asia, and South Asia revealed eight other mutations (114-121). Mutations in *PNKP* associated with MCSZ are shown in **Figure 1.7**. All the MCSZ individuals showed similar clinical phenotypes with different ranges of severity. Like the first seven families, *PNKP* mutations identified later in the MCSZ patients appear mostly in the catalytic domain. Only three PNKP-FHA domain mutations have been found before our study, which will be discussed later in **1.5.4**.
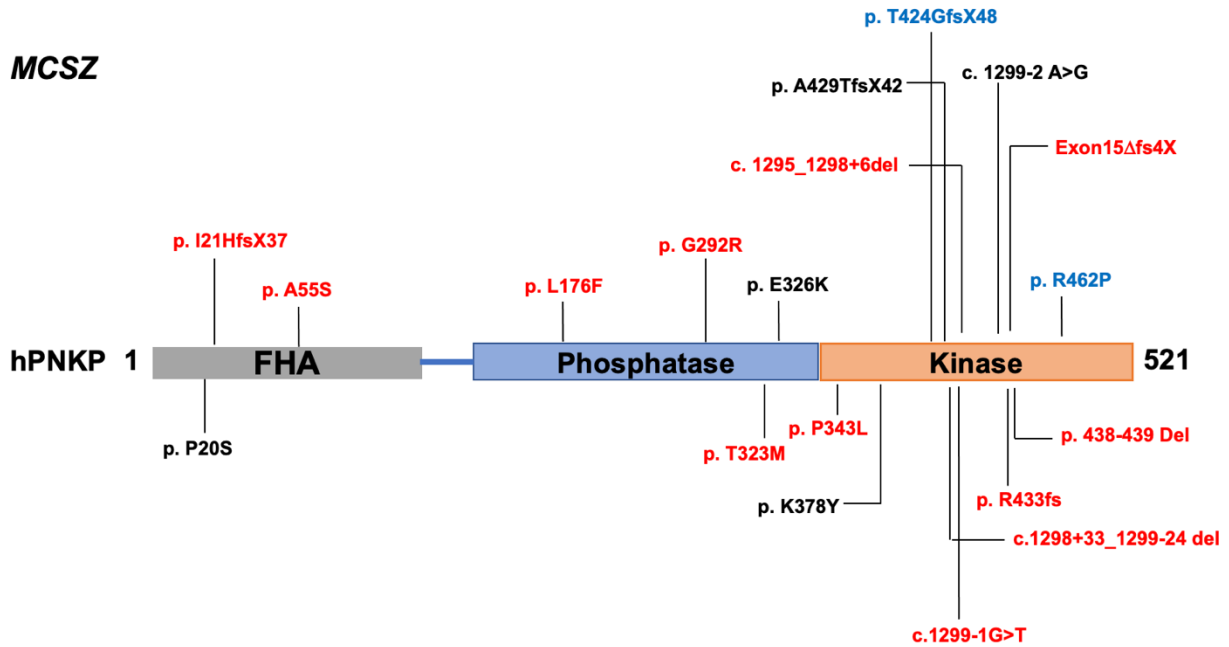
Figure 1.7 Mutations associated with MCSZ.

Black mutations only have been found in homozygous mutation form. Red ones have been found only in compound heterozygous mutation form. Blue ones have been found in both homozygous and heterozygous forms.

The most direct consequences of mutations in the catalytic domain could be alterations in PNKP's enzymatic activities. To test PNKP's enzymatic activities, a few biochemical studies have been performed using recombinant PNKP engineered with MCSZ mutations or extracts from patient-derived lymphoblastoid cells or fibroblasts (116, 122). All the PNKP

mutations that have been tested did affect the PNKP enzymatic activities. Some of the consequences are predictable, such as two kinase domain mutants (T424GfsX48 and Exon 15 del), exhibit near-normal phosphatase activities and greatly reduced kinase activities. However, as predicted by PNKP's tightly intertwined phosphatase-kinase linker region (97), the affected enzymatic functions are not always limited to one activity only. Two phosphatase domain mutants, L176K and E326K, showed disruption in both phosphatase and kinase activities (122). Extracts from patient-derived fibroblasts harboring compound heterozygous mutation (I21HfsX37 in FHA domain + part of exon/intron 14 del in the kinase domain) reduced both phosphatase and kinase activities as well (116).

Importantly, although the biochemical studies of recombinant PNKP showed direct impacts due to mutation, the altered enzymatic activity in cells could also be affected by the total cellular PNKP protein level. Indeed, Epstein-Barr virus (EBV)-transformed lymphocytes derived from affected MCSZ individuals (E326K and T424GfsX48) showed decreased PNKP protein content (107) in the cell extract. Low PNKP protein levels were also observed in the patient-derived fibroblasts carrying the I21HfsX37 + part of exon/intron 14 del mutations (116). Thus, although the exact reason for the

neurodevelopmental disorder is still not clear, it could arise from the combination of reduced protein activities and protein levels.

Animal-based study of MCSZ mutation is limited. Like some other key DNA repair proteins such as XRCC1 (123), inactivation of *PNKP* in mice results in embryonic death. Even *PNKP* inactivation restricted to the nervous system resulted in early neonatal lethality. Interestingly, these prematurely deceased mice showed a reduced cortex and cerebellum size, similar to MCSZ patients. In contrast to the lifespan of human MCSZ patients, it has not been possible to extend the lifespan of MCSZ mouse models. Homozygous MCSZ mutation (T424GfsX48) in mice induced similar embryonic death to total *PNKP* inactivation (124). It seems that while low/mutant PNKP protein is still able to support the survival of MCSZ human individuals, PNKP plays more critical roles in murine development.

1.5.2 Ataxia-oculomotor apraxia 4 (AOA4)

In 1988, Aicardi et al. found a progressive neurological syndrome in 14 patients from 10 families (125). The syndrome is similar to Ataxia-Telangiectasia with progressive neurodegeneration and loss of Purkinje cells (126), but without extra-neurological features such as telangiectasia, immunodeficiency, and susceptibility to malignancies (125, 127). This syndrome was then termed as Ataxia-ocular motor apraxia (AOA). Symptoms included progressive ataxia, choreoathetosis, and ocular motor apraxia (125). Since then, four subtypes of AOA disorder have been identified, each associated with mutations in different genes: AOA1 (OMIM 208920) is linked to mutations in Aprataxin

(*APTX*) (128, 129), AOA2 (OMIM 606002) is linked to mutations in Senataxin (*SETX*) (130), AOA3 (OMIM 615217) is linked to mutations in Phosphoinostitide-e-kinase regulatory subunit 5 (*PIK3R5*) (131), and AOA4 (OMIM 616267) is linked to mutations in *PNKP* (108).

AOA4 was first identified in eight Portuguese families. It affects nearly 40% of the identified Portuguese AOA population (108). None of the AOA4 individuals showed the signature symptoms of MCSZ patients, such as microcephaly and epilepsy. The age of onset ranged from 1 to 9 years instead of at birth. The first and most prominent symptom of most AOA4 patients is dystonia. Dystonia is a movement disorder featuring sustained muscle contractions, repetitive twisting movement, and abnormal postures (132). In all the patients, dystonia attenuated with the progression of the disease. The second common symptom among AOA4 patients is ataxia, characterized as impairment of gait. Individuals with severe disease could not stand or walk without assistance (133). Another signature symptom is oculomotor apraxia. Oculomotor apraxia is a rare oculomotor disturbance characterized by the inability to initiate horizontal eye movement; head rotation is usually needed to fix the gaze (134). Other symptoms of AOA4 include polyneuropathy and cognitive impairment. Brain MRIs revealed cerebellar atrophy.

In the eight families identified with AOA4 initially, G375W mutation is the most common mutation, present both in homozygous and compound heterozygous mutation forms. All the other PNKP mutations identified in the eight families are all present as compound heterozygous mutation forms. Mutations include frameshift (T424GfsX48, Q517LfsX24,

R439GfsX51, G442AfsX27) and deletion (T408del). Later, several studies of AOA4 patients from Europe and the Middle East revealed more PNKP mutation types (135-141), as shown in **Figure 1.8**. In contrast to MCSZ, almost all the AOA4 mutations identified are limited to the kinase domain. The only FHA domain mutation will be discussed later in **1.5.4**.

Interestingly, among all the identified PNKP mutations, T424GfsX48 frameshift mutation showed up in both MCSZ and AOA4 cases. All the T424GfsX48 frameshift mutations found in AOA4 patients are present in compound heterozygous mutation form, accompanied by another AOA4 specific point mutation (G375W, Y515X, or L399P) (108, 135, 138). However, T424GfsX48 mutations found in MCSZ patients are presented in both homozygous (107, 118, 120, 142) and compound heterozygous (107, 114, 142) forms.

Based on the mutation locations, the AOA4 mutant might only disrupt the kinase activity of PNKP. However, so far, the only AOA4 mutation that has been biochemically studied is the T424GfsX48 mutation, which was observed more frequently in MCSZ individuals.

1.5.3 Charcot-Marie-Tooth disease subtype 2B2 (CMT2B2)

Unlike MCSZ and AOA4, Charcot-Marie-Tooth (CMT) disease is one of the commonest inherited neuromuscular disorders. Also known as hereditary motor and sensory neuropathy (HMSN), it was first described in 1886 (143).
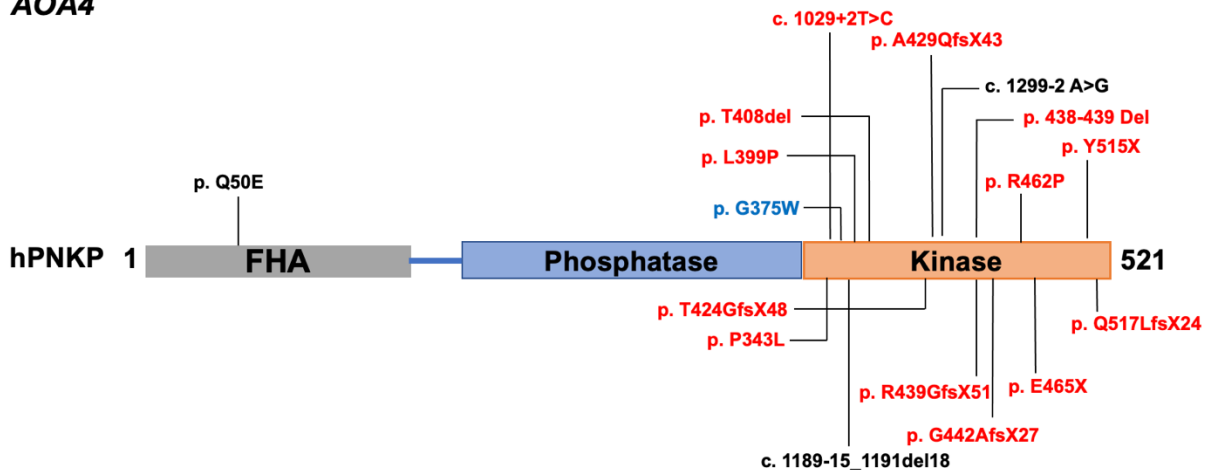
Figure 1.8 Mutations associated with AOA4.

Black mutation only has been found in homozygous mutation form. Blue mutation has been found in both homozygous and heterozygous form. Red ones have been found only in compound heterozygous mutation form.

Before the availability of genetic testing, CMT was classified into two subtypes based on their causes: CMT1, also known as "demyelinating" CMT, is caused by damage to the myelin sheath covering nerves. CMT2, also known as "axonal" CMT, is caused by damage to the nerve axons themselves (144). In 1991, Peripheral myelin protein 22 (PMP22) became the first causative gene identified in CMT, linked with subtype CMT1A, the most common CMT type (60%-90% of CMT1) (145, 146). Since then, more than 30 genes linked with CMT have been identified. CMT's complexity is not limited to numerous causative genes but also various inheritance patterns: Both CMT1 and CMT2 subtypes include autosomal dominant, autosomal recessive, and X-linked forms (147).

Classic CMT patients usually present with muscle weakness and atrophy, leading to lower limb symptoms such as ankle sprains and foot deformity. Sensory loss is another signature symptom, also commonly seen in the lower limb (148). Due to the differences of damage sites, motor and sensory nerve conduction velocities are different between CMT1 and CMT2: CMT1 subtypes usually have slower motor nerve conduction velocities (MNCV) compared to CMT2 patients. Although not always accurate, a cut off value of 38 m/s in the MNCV test is widely used to distinguish CMT1 from CMT2 (149). Additionally, the onset age is usually later, and sensory loss is less severe in CMT2 (150). It is noticeable that various CMT subtypes are often accompanied by specific phenotypes besides the classic symptoms. However, it is hard to distinguish different subtypes based solely on the symptoms because of the degree of overlap. The current diagnosis of CMT combines both clinical and genetic approaches (147).

In comparison to the high incidence of some CMT subtypes such as CMT1A, reports of CMT2B2 are quite rare. In 2001, Leal et al. identified CMT2B2 for the first time in a large consanguineous Costa Rican family comprising 18 affected individuals out of 31 family members, with a mean age of onset at 33.8 years (151). Although correctly mapped to chromosome 19q13, the causative gene of CMT2B2 was erroneously identified as a homozygous mutation in Mediator Complex Subunit 25 (MED25) (152). In 2015, Pedroso et al. reported a 17-year-old Brazilian male presenting CMT symptoms. A homozygous T408del mutation in *PNKP* was mapped in this patient. The T408del mutation has been found among AOA4 cases in a compound heterozygous form (108). However, it presented in a homozygous form in this CMT individual. Unlike AOA4 patients, this individual never had oculomotor apraxia symptoms, but an electrophysiologic examination was consistent with CMT2's axonal neuropathy (153). In 2018, a re-evaluation of the original Costa Rica families led to the identification of a homozygous Q517X mutation in PNKP instead of MED25. And five unrelated Costa Rican CMT2 individuals initially identified as MED25 mutations were found to be compound heterozygous for PNKP (Q517X + T408del) as well (109). In 2019, Gatti et al. reported three patients with novel PNKP mutations, one of them showed CMT-like symptoms with new compound heterozygous PNKP mutation, expanded the mutation map of CMT2B2 (120). All the mutations associated with CMT2B2 so far are shown in **Figure 1.9**.
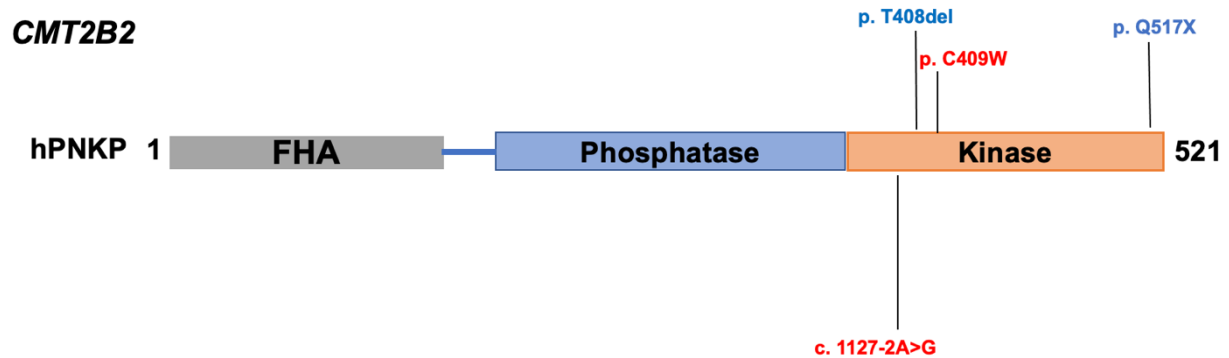
Figure 1.9 Mutations associated with CMT2B2.

Red ones have been found only in compound heterozygous mutation form. Blue one has been found in both homozygous and heterozygous form.

1.5.4 Diseases associated with *PNKP* mutations in the FHA domain

Because of the low incidence of neurological disorders linked with *PNKP* mutation, it is worth mentioning a few special mutations in the FHA domain. As mentioned above, most PNKP mutations are located in the catalytic domain. There are four recorded PNKP-FHA domain mutations that have been identified to date. Two of them are homozygous forms, and the other two are compound heterozygous forms.

In 2014, a targeted resequencing study of 500 patients with a range of epileptic encephalopathy phenotypes revealed a *PNKP* homozygous FHA domain mutation (121). This patient was carrying a homozygous P20S mutation in PNKP and was diagnosed as unclassified epileptic encephalopathy. Although categorized as MCSZ, this patient's symptoms did not entirely fit with MCSZ. He did not have microcephaly or developmental delay but did have multiple seizure symptoms. In 2020, another homozygous PNKP-FHA domain mutation Q50E was found in a patient categorized as AOA4 (154). Similar to the P20S patient mentioned above, the symptoms of this patient did not completely fit with AOA4 either. He did not show any dystonia, and the age of onset was over 50 years old. In contrast, most AOA4 patients have an early onset age ranging from 1 to 9 years old. Both of the PNKP-FHA homozygous mutations showed mild symptoms.

The other two compound heterozygous PNKP-FHA mutations were both identified in MCSZ patients. In one case, the patient was carrying a A55S mutation in the FHA domain accompanied by a G292R mutation in the phosphatase domain (117). The other patient

harboured a I21HfsX37 mutation in the FHA domain together with part of exon14 and intron 14 deletions in the kinase domain (c. 1295_1298+6del) (116). It is likely the other mutations in the catalytic domain play a bigger role in resulting symptoms. Due to limited clinical evidence and biochemistry study, it is still unclear how FHA domain mutation impacts the individual.

1.5.5 Other neurological diseases associated with impaired PNKP function

Besides MCSZ, AOA4, and CMT2B2, impaired PNKP function has been observed in other neurological disorders. Similar to AOA4, Spinocerebellar ataxia type3 (SCA3) is an autosomal dominant neurodegenerative disease. It is also the most common inherited ataxia worldwide. SCA3 is caused by mutant Ataxin 3 (*ATXN3*) involving the expansion of C-terminal polymorphic CAG repeats, causing poly-glutamine aggregation (155). Interestingly, deleting *Atxn3* does not create neurological abnormalities in mice, indicating it might not be essential for neurological development and function (156). The prevalent hypothesis is that not ATXN3 itself, but the changes of ATXN3's interacting proteins contribute to the pathology of SCA3, either by aberrant interaction or loss of function (157). In 2015, PNKP was found to be one of ATXN3's native interacting proteins and in the poly-glutamine aggregates in the SCA3 mouse brain (158). The same group noticed that both wild type and mutant ATXN3 associate with PNKP in cells and brain tissues in mice and humans. However, while wild type ATXN3 stimulates, mutant ATXN3 leads to the inactivation of PNKP's phosphatase activity, resulting in the accumulation of DNA

damage (159). Further study using nuclear extracts confirmed PNKP's activity is abrogated in SCA3 mice and patients' brain (160).

A few years after the linkage between SCA3 and PNKP was discovered, another poly-glutamine aggregation related disease was also found associated with PNKP. Huntington's disease (HD) is an autosomal dominant neurodegenerative disease caused by CAG repeat expansion in Huntingtin (HTT). Similar to SCA3, the mechanism of how mutant HTT causes HD is still not clear (161). A recent study showed that HTT forms a transcription-coupled DNA repair (TCR) complex with PNKP and facilitates DNA repair during transcriptional elongation. The mutant HTT with an extended poly-glutamine tail impairs such interaction, resulting in inefficient DNA repair (162). Interestingly, ATXN3 is part of this TCR complex as well (160, 162). As mentioned earlier in **1.1.3**, a recent model of NHEJ indicated that the transcription process could improve the accuracy of NHEJ repair machinery by providing the RNA template (47). The precise machinery of this transcription coupled NHEJ pathway is still under study. However, it is clear that PNKP could contribute to neurological diseases not just by genetic mutations, but also by altered interactions with its associated proteins in DNA repair pathways.

1.6 Mutations of DNA repair genes and cancer initiation

As mentioned in **1.3**, neurological diseases are not the only problem caused by the mutations of DNA repair genes: it also plays a vital role in cancer initiation. Although mutations in DNA repair genes are not frequently termed "driver" mutations, the term

typically describes mutations that render a growth advantage to the cells carrying them (163). Mutated DNA repair genes play more of an invisible role during cancer initiation. The intact DNA repair machinery is essential for cells to cope with endogenous and exogenous DNA damage, thus avoiding the starting point of carcinogenesis, i.e., oncogene activation or tumor suppressor gene deactivation. However, DNA lesions indirectly caused by impaired DNA repair machinery could quickly accumulate, leading to activation of key "driver" mutations, thus driving cells to carcinogenic transformation (164, 165).

The first linkage between the mutations of DNA repair genes and cancer initiation was recognized in Xeroderma pigmentosum (XP), an autosomal recessive syndrome caused by impaired nucleotide excision repair (NER) pathway (166). Mutations in several NER proteins render them unable to remove UV-induced photodimers in DNA, which creates the particular skin cancer predisposition observed in XP patients, who have a 1000 fold increased chance of developing skin cancer(167). After that, more mutated DNA repair genes were found associated with cancer predisposition. Mutations in DNA mismatch repair genes, such as MutL homolog 1 (*MLH1*) and MutS homolog 2 (*MSH2*), were associated with Lynch syndrome (168, 169). Lynch syndrome, also named Hereditary nonpolyposis colorectal cancer, is associated with a high risk of colon cancer and endometrial, gastric, ovarian, and pancreatic cancers (170). Mutations in the HR pathway gene *BRCA2* are found associated with Fanconi anemia, which is also strongly associated with cancer development, especially acute myelogenous leukemia (171).

Interestingly, many of the genetic mutations associated with neurological diseases, as mentioned in **1.3**, are also linked to cancer predisposition. For example, NBS patients (linked with *NBS1* mutation) have a higher risk of cancer, especially B cell lymphoma development during childhood (172). Ataxia telangiectasia patients (linked with *ATM* mutation) have a higher lifetime risk of cancers, particularly lymphomas, leukemia, and breast cancer (173). Although *PNKP* is a prominent player in the DNA repair arena and a gene linked with neurological diseases, so far only two cases have been found linked with cancer development. One patient with AOA4 was diagnosed with cerebellar pilocytic astrocytoma (low grade brain tumor) at the age of 23 years (138) and a second AOA4 patient developed a cerebellar hemangioblastoma resulting from a concurrent mutation in the von Hippel-Lindau gene (142), but until now no cancer has been reported in an MCSZ patient.

1.7 Pediatric GBM

Glioblastoma multiforme (Glioblastoma, GBM) is the most aggressive malignant primary brain tumour. Based on prognostic and survival correlates, GBM is classified as grade IV tumours of the central nervous system (CNS) according to the World Health Organization (WHO) (174). GBM is the most common CNS tumour in the USA and Europe (175). Primary GBM, which usually develops in a short time without a precursor lesion or clinical signs, contributes to 95% of all GBM, also known as de novo GBM (176). Secondary GBM only accounts for 5% of all GBM, usually developing from low-grade gliomas such as diffuse astrocytoma or anaplastic astrocytoma (176, 177). The mean age of primary

GBM patients is 62 years, while the mean age of secondary GBM is 45 years (178). However, the incidence of all GBM increases with age (peak age between 75 and 84 years). It is rare to see GBM in younger patients. Only 0.8 per 100,000 children (aged below 19) are estimated to develop high-grade gliomas (HGG) each year compared with 7.2 per 100,000 adults (179). In a 14-year study, pediatric GBMs accounted for only 3.1% of all GBM patients (180), and pediatric GBMs only constitute 8.8% of all childhood CNS tumours (181).

There are several genetic events and signaling pathways that are important to the initiation and progression of GBM. Frequently mutated genes in adult GBM include phosphatase and tensin homolog (PTEN), tumour protein 53 (TP53), epidermal growth factor receptor (EGFR), platelet-derived growth factor receptor-α (PDGFRA), neurofibromin 1 (NF1), and retinoblastoma protein 1 (RB1) (182). Also, two promoter mutations are frequently observed in GBM adult patients, telomerase reverse transcriptase (TERT) promoter and O^6-methylguanine methyltransferase (MGMT) promoter. Although pediatric GBMs show similar histological features as adult GBMs, the patterns of genetic alterations appear to be different. Most of the above mutations are uncommon in pediatric GBM, except for TP53 and PDGFRA. In fact, both TP53 and PDGFRA mutations are more common in pediatric GBM than adult GBM (183, 184). TP53 mutation is especially prevalent in patients younger than three years old (185). Another common feature in pediatric GBMs is mutation of the somatic histone H3. While histone H3 mutation only shows up in less than 3% of adult GBM patients, specific H3 mutations such as H3F3A K27M can be observed in up to 43% of pediatric GBM patients (183).

ATP-dependent helicase (ATRX), as a major histone H3 chaperone protein, is also commonly mutated in pediatric GBM (186).

Although impaired DNA repair pathways have been heavily associated with both adult and pediatric GBM (187), the link between PNKP and brain tumour is extremely limited. As mentioned above, the only reported linkage between *PNKP* mutation and cancer was observed in a German AOA4 patient, who was later diagnosed with a cerebellar pilocytic astrocytoma, a WHO grade I brain tumour (138). In 2016, a male MCSZ patient with GBM was identified, making it the first linkage between *PNKP* mutation in MCSZ and cancer, in particular childhood GBM. This clinical case forms the basis of one of the chapters in this thesis.

1.8 Mitochondria and neurological diseases

Besides DNA repair related malfunction, information from many sources strongly supports a linkage between mitochondria and neurological diseases. Mitochondria are the organelles responsible for producing and supplying ATP for various cellular activities, including the neurological system (188). Mitochondrial DNA (mtDNA) are circular genomes within the mitochondrial matrix that contain 16569 base pairs (189). Mammalian mtDNA lacks introns and is, therefore, more sensitive to mutagenesis than nuclear DNA (190). Although mtDNA only encodes 13 proteins, proteomic analysis revealed more than 3300 proteins in mitochondria and mitochondria-associated fractions (191). Most mitochondrial proteins are encoded by nuclear DNA, synthesized on cytosolic ribosomes,

and imported through the mitochondrial membrane (192). A large number of DNA repair proteins are also found in both locations (193), including PNKP (194). Although those proteins are common to both nuclei and mitochondria, their functions and contributions could be different. For example, the human DNA ligase III gene encodes both nuclear and mitochondrial proteins (195). By disruption and reintroduction of multiple ligase III variants, a study revealed that mitochondrial, but not nuclear ligase III, is required for cellular viability in mouse embryonic stem cells (196).

The potential involvement of mitochondria in Alzheimer's disease (AD) was proposed after the finding of reduced oxygen metabolism in AD patients (197). Altered mitochondrial morphology was also observed in AD patients: The shapes of most mitochondria are either small and rounded, or elongated, with disruption of the cristae, especially in neurons (198). Mitochondrial enzymes, such as cytochrome oxidase, were also found with greatly reduced activity in AD patients (199). The linkage between mitochondria and Parkinson's disease (PD) was discovered when a significant and specific reduction of mitochondrial complex I activity in the substantia nigra in PD patients was observed (200). The most crucial genetic evidence of the involvement of mitochondria in PD is *Parkin* (201) and *PINK1* (202), whose mutations are responsible for hereditary (autosomal recessive) early-onset PD. Down-regulation of both *Parkin* and *PINK1* in human neuroblastoma cells (SH-SY5Y) causes mitochondrial morphology changes such as mitochondrial fragmentation (203). Several other studies have shown a linkage between increased mtDNA mutations and PD (204, 205). However, controversial results have been reported as well. For example, analysis of mitochondrial DNA in

monozygotic twins found no significant differences between PD patients and non-affected siblings (206). Perhaps paradoxically, the cerebrospinal fluids of PD and AD patients have been shown to contain significantly less cell free circulating mtDNA (207, 208). The authors posited that the low level of circulating mtDNA reflected low neuronal mtDNA copy number in the neurons of these patients and further suggested that low circulating mtDNA in cerebrospinal fluid could be used as an early biomarker for AD and PD and perhaps other neurological diseases. In this regard, it would be interesting to determine if AOA4 shows the same mtDNA characteristics.

In addition to neurodegenerative diseases, mitochondrial involvement has also been associated with other neurological conditions. Epilepsy is a group of different neurological syndromes characterized by recurrent unprovoked seizures, which can be triggered by multiple factors (209). In addition to mitochondrial gene mutations linked with epilepsy (210), a large number of nuclear genes involved in mitochondrial function have also been found linked with epilepsy (211). Mitochondrial dysfunctions have been shown linked with brain tumours as well. Brain tumor initiating cells (BTICs) isolated from GBM patient-derived tumor cell populations displayed fragmented mitochondrial morphology compared to non-BTICs (212). The copy number of mtDNA was also found to increase in glioma patients, and patients with high mtDNA content had a significantly longer survival time than the patients with low mtDNA content (213).

1.9 Hypotheses and scope of the thesis

Due to the rarity of neurological diseases caused by PNKP mutation, it is still unclear how PNKP, a versatile DNA repair protein, can trigger different neurological consequences. As mentioned in **1.5.1** and **1.5.2**, MCSZ and AOA4 show apparent differences in mutation patterns. How the specific mutations in PNKP contribute to the development of different neurological diseases is also a mystery. In addition, the discovery of the first cancer patient with MCSZ indicates a possible linkage between the PNKP mutation and carcinogenesis. This primary aim of this thesis is to study the consequences of several specific PNKP mutations associated with MCSZ, AOA4, and GBM. We have used different approaches, including biochemical and cellular studies, to tackle the mystery behind those PNKP mutations.

The overarching hypothesis of this thesis is that selective PNKP mutations can disrupt the enzymatic and cellular functions of PNKP, which causes cells to malfunction or undergo transformation, thus leading to the development of neurological diseases and cancer. The specific hypotheses are as follows:

1) Specific mutations in PNKP will affect its DNA 3'-phosphatase and/or DNA 5'-kinase activities.

2) To fulfill the DNA repair process, PNKP must bind and interact with DNA substrates and other proteins. We hypothesize that the mutant PNKP will affect its binding affinity with DNA or other proteins.

3) Given the rarity of both MCSZ and pediatric GBM, we hypothesize that the specific PNKP mutations found in the patient under study can act as driver mutations leading to carcinogenesis.

4) Cells with mutant PNKP will be more sensitive to DNA damaging agents or neurotoxins.

In chapter 2, we focused on the MCSZ patient that developed GBM. We purified the recombinant mutant PNKP and performed a range of biochemical assays on the mutant protein. While these assays revealed several distinct features of the mutant PNKP protein, we also developed stable transfected cell lines harboring the mutant PNKP. The cellular experiments unveiled several unique features of the mutant cell lines, which matched our collaborators' clinical observations.

We expanded our study of mutant PNKP to AOA4 in chapter 3. We focused on the most frequent PNKP mutation found in AOA4. By approaching the case through biochemical and cellular studies, we observed several different characteristics of that mutant PNKP on its enzymatic, binding, and cellular functions.

The data we present in this thesis show that the mutant PNKPs found in the clinic feature several alterations in their protein and cellular functions. We also observed several features that have not been seen before in PNKP-related neurological diseases. Our study demonstrates the central role of mutant PNKP in causing different neurological diseases, expanded the spectrum of roles of PNKP in maintaining normal cellular function, and provided valuable insights in overcoming challenges in those diseases.

2 Chapter 2: Mutations of the DNA repair gene *PNKP* in a patient with Microcephaly, Seizures, and Developmental Delay (MCSZ) presenting with a high-grade brain tumor

Bingcheng Jiang[1], Cameron Murray[2], Bonnie L. Cole[3], J.N. Mark Glover[2], Gordon K. Chan[1], Jean Deschenes[4], Rajam S. Mani[1], Sudip Subedi[1], John D. Nerva[5], Anthony C. Wang[6], Christina M. Lockwood[7], Heather C. Mefford[8], Sarah E.S. Leary[9], Jeffery G. Ojemann[10], Michael Weinfeld[1*], Chibawanye I. Ene[11*]

[1] Department of Oncology, University of Alberta, Cross Cancer Institute, 11560 University Ave. Edmonton, Alberta, T6G 1Z2, Canada

[2] Department of Biochemistry, University of Alberta, Medical Sciences Building, Edmonton, Alberta, T6G 2H7, Canada

[3] Department of Pathology, University of Washington, Seattle, Washington, U.S.A.

[4] Department of Laboratory Medicine & Pathology, University of Alberta, Cross Cancer Institute, 11560 University Ave. Edmonton, Alberta, T6G 1Z2, Canada

[5] Department of Neurological Surgery, Tulane University, New Orleans, Louisiana, U.S.A.

[6] Department of Neurological Surgery, University of California Los Angeles, Los Angeles, California U.S.A.

[7] Department of Laboratory Medicine, University of Washington, Seattle, Washington, U.S.A.

[8] Division of Genetics Medicine, University of Washington, Seattle, Washington, U.S.A.

[9] Division of Pediatric Hematology/Oncology, Seattle Children's Hospital, Seattle Washington, U.S.A

[10] Department of Neurological Surgery, University of Washington, Seattle, Washington. U.S.A.

[11] Department of Neurological Surgery, MD Anderson Cancer Center, Houston Texas, U.S.A.

2.1 Introduction

Polynucleotide Kinase/Phosphatase (PNKP) is a bifunctional enzyme that possesses both DNA 3'-phosphatase and DNA 5'-kinase activities, which are required for processing termini of single- and double-strand breaks generated by reactive oxygen species (ROS), ionizing radiation and topoisomerase I poisons. (20, 95)The central nervous system (CNS) is particularly susceptible to defective enzymatic activity of PNKP, giving rise to neurological syndromes such as microcephaly, seizures and developmental delay (MSCZ) and Ataxia-ocular motor apraxia 4 (AOA4). Even though PNKP is central to DNA repair, there have been no reports linking *PNKP* mutations in an MSCZ patient to cancer. Here, we characterized the biochemical significance of 2 germ-line point mutations in the *PNKP* gene of a 3-year-old male with MSCZ who presented with a high-grade brain tumor (glioblastoma multiforme or GBM) within the cerebellum. A novel mutation at C302T, causes a proline to leucine change at position 101 (P101L) in the forkhead-associated domain, while the other previously described mutation C968T causes a threonine to methionine change at residue 323 (T323M) in the phosphatase domain of PNKP protein. Functional and biochemical studies demonstrated these *PNKP* mutations significantly diminished DNA kinase/phosphatase activities, altered its cellular distribution, caused defective repair of DNA single/double stranded breaks, and were associated with a higher propensity for oncogenic transformation. Our findings indicate that specific *PNKP* mutations may contribute to tumor initiation within susceptible cells in the CNS by limiting DNA damage repair and increasing rates of spontaneous mutations resulting in pediatric glioma associated driver mutations such as *ATRX* and *TP53*.

Mutations in *PNKP* have been found to be responsible for three different relatively rare neurological diseases: an autosomal recessive neurodegenerative disease Ataxia-ocular motor apraxia 4 (AOA4), (108, 136, 137, 139, 214, 215) a variant of the hereditary peripheral neuropathy Charcot-Marie-Tooth disease (CMT2B2)(109) and the autosomal recessive neurodevelopmental disorder Microcephaly, seizures, and developmental delay (MCSZ).(116, 118, 121, 215-217) To date MCSZ has been diagnosed in fewer than 30 families worldwide. It has the following clinical features: microcephaly, infantile-onset seizures, developmental delay and behavioral problems.(116, 118, 121, 215-217) Mutation sites of *PNKP* have been found in all three domains - FHA, phosphatase and kinase – in these cases of MCSZ. (116, 118, 121, 215-218) One patient with AOA4 was diagnosed with cerebellar pilocytic astrocytoma (low grade brain tumor) at the age of 23 years (214) and a second AOA4 patient developed a cerebellar hemangioblastoma resulting from a concurrent mutation in the *von Hippel-Lindau* gene (142), but until now no cancer has been reported in an MCSZ patient.

Here we report on a male MCSZ patient with glioblastoma multiforme (GBM) who was identified at the Seattle Children's Hospital. The patient had presented with MCSZ at birth. A cerebellar glioblastoma (GBM) was found when he was 3 years old. Genetic screening for mutations associated with his clinical features showed that he carried 2 newly discovered somatic *PNKP* point mutations. The two *PNKP* mutations found in the patient are C302T, which causes a proline to leucine change at position 101 (P101L) in the FHA domain and C968T, which causes a threonine to methionine change at position 323

(T323M) in the phosphatase domain of PNKP protein. While the latter mutation has recently been identified in a Dutch MCSZ patient (142), the other *PNKP* mutation has not been found in any reported MCSZ/AOA4/CMT2B2 patients before. Both mutations are found in highly conserved regions of *PNKP*. Furthermore, this is the first reported case of an MCSZ patient to develop cancer. The primary focus of our study was to determine the biochemical and cellular consequences of these *PNKP* mutations.

2.2 Material and methods

2.2.1 Tumor sample template preparation, gene capture and massively parallel sequencing

Tumor DNA sequencing was preformed using UW-OncoPlex version 5, a clinically validated method as previously reported.(219) Briefly, after DNA extraction, sequencing libraries were prepared using KAPA HyperPrep (Roche, Wilmington, MA) and hybridized to a custom set of complementary RNA (cRNA) biotinylated oligonucleotides targeting the exons of 262 genes and select intronic regions for a total of ~2Mb of targeted DNA sequenced. NGS was performed using a NextSeq500 sequencing system (Illumina, San Diego, CA) and data analysis was performed using custom bioinformatics developed by the UW NGS Analytics Laboratory.

Table 2.1 Primers for site mutagenesis

Primer name	Primer Sequence (5' to 3')
P101L Sense	5'-AATGGCCTCCACCTACTGACCCTGCGC-3'
P101L Antisense	5'-GCGCAGGGTCAGTAGGTGGAGGCCATT-3'
T323M Sense	5'-CCTGCCCTTCGCCATGCCTGAGGAG-3'
T323M Antisense	5'-CTCCTCAGGCATGGCGAAGGGCAGG-3'

Table 2.1. Primers for site mutagenesis. Primers for site-directed mutagenesis to generate desired single point mutants. The double mutant was generated by using T323M primers on the P101L plasmid.

2.2.2   Expression plasmids and site-directed mutagenesis

For the production and purification of PNKP protein, pET-16b (Novagen Inc., Madison, WI) bacterial expression plasmid harboring the full-length human *PNKP* cDNA was generated following previously reported procedures.(95, 220) To generate fluorescently tagged wild-type and mutant PNKP proteins in mammalian cells, the full-length cDNA was subcloned into the pCMV6-AC-mGFP (Origene, Rockville, MD) mammalian expression plasmid as described before.(221) To generate the desired *PNKP* single point mutants (C302T and C968T), the QuickChange II site-directed mutagenesis kit (Stratagene, La Jolla, CA) was used, following the manufacturer's protocol and using the mutagenic primers shown in **Table 2.1**. The *PNKP* double mutant (DM) was generated by using the C968T primers with the C302T-mutated cDNA in a similar procedure. Finally, the mutants were sequence validated by the Applied Genomics Core at the University of Alberta. Besides the site directed mutagenesis sites (C302T for P101L mutation; C968T for T323M mutation), the PNKP and GFP sequences among all constructs are full length and identical. However, we found a small difference in the linker that connects PNKP and GFP: the WT-PNKP codes for 4 more amino acids in the linker than P101L and T323M-PNKP constructs, the linkers between P101L and T323M PNKP are identical. This explains the slightly shorter size of the P101L and T323M proteins seen on western blots (Fig S2A). However, it is important to note that this change in the linker would not affect PNKP enzymatic activity or localization or change our interpretation of the results.

2.2.3 Expression and purification of mutant PNKPs

The PNKP wild-type and mutant bacterial expression plasmids were transfected into *E. coli* bacterial strain BL21 (DE3) (NEB). The bacteria were grown at 37°C in 4 L of lysogeny broth (LB) containing ampicillin (50 μg/mL) to reach an OD_{600} of 0.6. Protein expression was then induced by overnight incubation at 18°C in the presence of 100 μM isopropyl-β-D-1-thiogalactopyranoside (IPTG, Sigma, St. Louis, MO). After induction, the bacteria were harvested by centrifugation at 10000g for 10 min at 4°C and resuspended in 50 mL of lysis buffer (150 mM NaCl, 50 mM Tris-HCl, pH 8.0, 1 mM ethylenediaminetetraacetic acid (EDTA), 0.1 % β-mercaptoethanol, 0.5 mM phenylmethylsulfonyl fluoride (PMSF), 0.5 mg/mL lysozyme). After stirring on ice for 30 min, the bacteria were disrupted by sonication. The soluble fraction was separated by centrifugation at 15000g for 30 min at 4°C. To precipitate nucleic acids, 10% polyethyleneimine was added dropwise to the soluble fraction to a final concentration of 0.3 %, the sample was then stirred on ice for 20 min and centrifuged at 15000g for 20 min at 4°C. Protein in the supernatant was then precipitated by addition of ammonium sulfate to a final concentration of 50%, and then centrifuged at 15000g for 30 min at 4°C. The protein pellet was resuspended in solution and purified through a HiPrep 16/10 Butyl FF column (Amersham Pharmacia BioTech, Baie d'Urfe, PQ), SP Sepharose Fast Flow cation-exchange column (Amersham Pharmacia BioTech, Amersham, UK) and HiLoad 16/60 Superdex 75 gel filtration column (Amersham Pharmacia BioTech) as described before.(220) The purity and integrity of the protein were confirmed by gel electrophoresis and Coomassie Brilliant Blue staining (**Fig. 2.1**).

2.2.4   PNKP Kinase Assay

The 5'-kinase activities of wild-type and mutant PNKP proteins were measured by a kinase assay modified from procedures described before.(95) Briefly, PNKP (500 ng) was added to a reaction mixture (40 µL total volume) containing kinase buffer (80 mM succinic acid, 10 mM $MgCl_2$ and 1 mM Dithiothreitol (DTT), pH 5.5), 0.5 mM 24-mer oligonucleotide substrate (5'-GGCGCCCACCACCACTAGCTGGCC-3') with 5'-OH
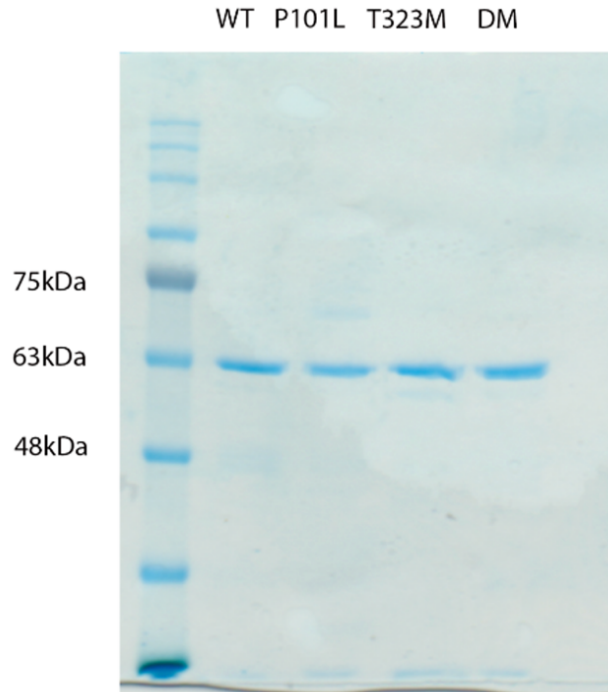
Figure 2.1 Coomassie blue stain of purified recombinant PNKP proteins.

From left to right lanes: wild-type (WT), P101L, T323M and double mutant (DM).

termini, 5 mM unlabeled ATP, and 5 µCi of [γ-^{32}P] ATP (3000 Ci/mmol, Amersham Pharmacia Biotech). The reaction mixture was incubated at 37°C for 0.5, 1, 2, 5, 10 and 20 min. 5 µL of the sample was mixed with 2.5 µL of 3 X sequencing gel loading dye (Fisher Scientific, Edmonton, AB), boiled for 10 min to stop the reactions then run on a 12% polyacrylamide gel containing 7 M urea at 200 V for 30 min. The gel was scanned on a Typhoon 9400 Variable mode imager (GE Healthcare Life Sciences, Mississauga, ON) and quantified using ImageQuant 5.2 (GE Healthcare Life Sciences). In the experiment to test the stability of the mutant proteins *in vitro*, all the purified wild-type/mutant PNKP proteins were pre-heated at 37°C for 10 minutes before being added into the reaction mixture.

2.2.5 PNKP Phosphatase Assay

The 3'-phosphatase activities of the wild-type and mutant PNKP proteins were measured by a phosphatase assay modified from previous studies.(100, 222) Briefly, PNKP (50 ng) was added to a reaction mixture (20 µL total volume) containing phosphatase buffer (70 mM Tris-HCl, 10 mM $MgCl_2$, 5 mM DTT, pH 7.6), 4 µM 24-mer oligonucleotide substrate (5'-GGCGCCCACCACCACTAGCTGGCC-3') bearing a ^{32}P-label at the 5'-terminus as well as a 3'-phosphate. The reaction was carried out at 37°C for 0.5, 1, 2, 5 and 10 min. 3 µL of the sample was mixed with 1.5 µL of 3 X sequencing gel loading dye, boiled for 10 min to stop the reaction then run on a 12% polyacrylamide gel containing 7 M urea at 1800 V for 3 hours. The gel was then scanned on a Typhoon 9400 Variable mode imager and quantified using ImageQuant 5.2.

2.2.6 Steady-state fluorescence spectra study

The affinity of mutant PNKP protein for DNA substrates was measured using steady-state fluorescence as previously described.(97, 220) Binding affinities (K_d) were obtained for double-stranded DNA substrates containing two different strand break termini (**Table 2.2**). The fluorescence titration with the Gap1 substrate was carried out at room temperature. The titration with Gap2 was performed at 5°C to avoid removal of the 3'-phosphate terminus.

2.2.7 Circular Dichroism Spectroscopy

Far-UV circular dichroism (CD) measurements were performed with an Olis DSM 17 CD spectropolarimeter (Bogart, GA, USA), calibrated with a 0.06% solution of ammonium *d*-camphor-10-sulfonate. The temperature in the sample chamber was maintained at 20°C. The CD spectra of wild-type and T323M-PNKP were measured as described previously (223) and the results were analyzed according to the method of Chen et al.(224)

2.2.8 Fluorescence polarization

For direct binding by fluorescence polarization (FP), 20 nM of fluorescent-labeled XRCC4 peptide (GGYDES-pT-DEESKK) was mixed with different concentrations of PNKP, 6.8 nM to 13.9 µM for P101L-PNKP and, 7.4 nM to 15.2 µM for wild-type PNKP, in a reaction

volume of 20 µL. The final buffer conditions were 22.5 mM Tris pH 8.0, 50 mM KCl, and 1 mM DTT. The fluorescence was recorded on a Perkin Elmer Envision plate reader (Waltham, MA, USA) at 538 nm with an excitation at 458 nm. The K_d values were determined using a plot of the polarization as a function of the log of protein concentration. Experiments were performed in duplicate or triplicate and plotted with error bars of one standard deviation.

2.2.9 Cell culture

Human HeLa cells were obtained from Dr. David Murray (University of Alberta) and validated by ATCC cell line authentication service using short tandem repeat (STR) analysis. Cells were cultured in Dulbecco's modified Eagle's medium (DMEM)-F12 media supplemented with 5% fetal calf serum and 2 mM L-glutamine, incubated at 37°C under 5% CO_2 in a humidified incubator. All culture supplies were purchased from Invitrogen/Thermo Fisher Scientific (Waltham, MA).

2.2.10 Quantitative real-time reverse transcription-polymerase chain reaction (qRT-PCR)

Whole RNA was extracted from the transient transfected cell lines (24 hours after transfection) using the RNeasy Plus Mini Kit (Qiagen, USA) following the manufacturer's protocol. Primers targeting the desired mRNA were designed through Primer-BLAST (NCBI).

GAPDH forward: 5'-GTCTCCTCTGACTTCAACAGCG-3',

reverse: 5'-ACCACCCTGTTGCTGTAGCCAA-3';

PNKP forward: 5'-ATCCCAGCCAGATACTCCGC-3',

reverse: 5'-CTGCGGTGAACACTAGCAACT-3'.

cDNA was reverse-transcribed with the High-Capacity cDNA Reverse Transcription kit (Applied Biosystems, USA). BrightGreen 2X qPCR MasterMix-Low ROX (Abm, Richmond, BC) was used to perform the quantitative PCR process on QuantStudio 6 Flex Real-Time PCR Systems (Thermo Fisher Scientific, USA). The $2^{-\Delta\Delta C_T}$ method (30) was applied by using GAPDH as the reference gene to calculate the PNKP mRNA level in all the transient transfected cell lines, compared with HeLa PNKP$^{-/-}$ + WT-PNKP.

2.2.11 Western blotting analysis

Western blotting was performed following a standard protocol with modifications (31). Antibodies used included PNKP antibody (sc-365724, Santa Cruz Biotech, USA), beta-actin antibody (sc-47778, Santa Cruz Biotech, USA), IR dye 800CW goat anti-mouse secondary antibody (926-32210, Li-COR Biosciences, USA). Results were visualized using an Odyssey Fc Imaging System (Li-Cor Biosciences, USA). Protein expression levels were calculated using beta-actin level as the reference protein.

2.2.12 Establishment of transiently- and stably-transfected cells

The generation of PNKP-knockout HeLa cells by CRISPR technology has been previously described.(225) HeLa PNKP$^{-/-}$ cells were plated in 60-mm dishes and transfected with plasmid constructs of interest using Turbofectin 8.0 following the manufacturer's protocol. Transfected cells were incubated at 37°C under 5% CO_2 in a humidified incubator. Transiently-transfected cells were established after 24 hours of transfection. Stably-transfected cells were established as follows: 24 hours after transfection, cells were trypsinized and passaged at a 1:10 dilution in selective medium containing 800 μg/ml G418 (Thermo Fisher Scientific). Cells were expanded in selective media and GFP-positive cells were selected by fluorescence-activated cell sorting (FACS) (BD BioSciences, USA). Single cells with high to medium GFP intensity were picked and seeded into 96-well plates. After expanding selected single cells in G418 selective medium for one week, a high-content automated microscopy imaging system (MetaXpress Micro XLS, software version 6, Molecular Devices, Sunnyvale, CA) was used to select GFP positive single colonies. Positive individual colonies were later expanded in selective medium containing 800 μg/ml G418.

2.2.13 Cellular localization of PNKP

For image acquisition, cells were plated on coverslips and fixed with 4% formaldehyde the next day. Immunofluorescence staining with tubulin antibody was performed to distinguish the cytoplasmic area. Nuclei were stained with DAPI. Cells were then placed on the stage of the Zeiss confocal LSM710 microscope. Images were acquired using 40X/1.3 NA oil immersion objective.

2.2.14 High-content screening

Widefield fluorescence images were taken with a high-content automated microscopy imaging system (MetaXpress Micro XLS, software version 6). Transient-transfected cells were plated in Greiner 96-well plates one day before imaging. Before acquiring images, cells were incubated with Hoechst 33258 (Sigma, cat. No. 94403) to a final concentration of 1 µg/ml for 20 min and then fed with fresh growth medium. At least 30 images (covering an area of ~2 mm^2/image) per group were taken with a 10X objective equipped with a siCMOS camera using bandpass filters (447-460 nm for Hoechst and 559-634 nm for GFP respectively). The images were analyzed with the MetaXpress Cell scoring module to compare each cell's ratio between the area of the GFP protein distribution and the area of the nucleus (Hoechst staining). Each group yielded 4000-6000 cells with both Hoechst and GFP positive signals.

2.2.15 Leptomycin B treatment

Stably-transfected HeLa PNKP$^{-/-}$ cells were seeded on coverslips 24 hours before treatment. In the leptomycin B treatment group, the growth medium of all cell lines was changed to medium containing 1 nM leptomycin B for 3 hours. Control groups were changed with regular growth medium. After 3 hours, the medium was removed and the cells washed with PBS 3 times. The cells were then fixed with 4% formaldehyde and

stained with DAPI. Images were acquired using a 40X/1.3 NA oil immersion objective on a Zeiss confocal LSM 710 microscope.

2.2.16 Crystal violet based viability assay

A crystal violet based assay was used for determining the viability of mutant cell lines after DNA damage as previously described (226) with minor modifications. Briefly, 1×10^4 cells were seeded in a 96-well plate and incubated for 24 hours to enable adhesion. Cells were then exposed to 5, 10 or 15 Gy γ radiation, incubated for 24 hours, washed with PBS, and stained with 0.5% crystal violet staining solution on a bench rocker. After 20 min, the plates were washed and air-dried. Methanol (200 µl) was added to each well and kept for 20 min at room temperature. The optical density of each well was measured at 570 nm (OD_{570}) using a FLUOstar Omega microplate reader (BMG Labtech, USA), setting the average OD_{570} of the wells without cells as background, which was subtracted from each well. The average OD_{570} from the unirradiated cells was set as 100%. Cells were treated in quintuplicate in each group in each experiment; the experiment was performed three times independently.

2.2.17 Alkaline single cell gel electrophoresis

Untransfected wild-type HeLa and HeLa PNKP$^{-/-}$ cells, and stably transfected HeLa PNKP$^{-/-}$ cells were exposed to 5 Gy γ radiation. 0, 1, 24 hours after irradiation, 1×10^5 cells were trypsinized and mixed with molten (37°C) Comet LMAgarose (Trevigen,

Gaithersburg, MD) at a volume ratio of 1:10. A 50-μl mixture was immediately pipetted onto comet slides (Trevigen). The slides were kept flat at 4°C in the dark to allow the mixture to solidify, and then immersed in a 4°C lysis solution (Trevigen) for 60 min. After that, the slides were immersed in a freshly made alkaline solution (300 mM NaOH, 1 mM EDTA) for 60 mins at 4°C. Slides were then placed in an electrophoresis apparatus filled with a freshly made alkaline solution before being subjected to electrophoresis at 1 V/cm and 300 mA for 40 min. The slides were then gently washed twice in distilled water for 5 min, immersed in 70% ethanol for 5 min and dried at 37°C for 15 min. The slides were stained with 20 μg/ml ethidium bromide for 5 min then washed in distilled water. Images were acquired using an AxioSkop 2 Upright Fluorescence Microscope (Zeiss). For each time point, a minimum of 300 random cells from each group was analyzed using Comet Score 2.0 (TriTek Corp, Sumerduck, VA).

2.2.18 Imaging of 53BP1 foci

Untransfected wild-type and PNKP$^{-/-}$ HeLa cells, as well as stably transfected HeLa PNKP$^{-/-}$ cells were exposed to 5 Gy γ radiation. 1, 6, 24 hours after irradiation, cells were fixed and underwent immunofluorescence staining with 53BP1 antibody (Santa Cruz #sc-517281). Z-stack images were acquired using a Zeiss confocal LSM710 microscope. For each time point, 120-200 cells from each group were analyzed using Imaris 9.5 software (Bitplane, Belfast, GB).

2.2.19 Soft agar colony-forming assay

The protocol used was based on a published procedure (227) with minor modifications. Briefly, the bottom layer added to wells in a 6-well plate consisted of melted 1% noble agar in pre-warmed 2X medium (1:1 v/v), which was then allowed to set. 10^4 untreated cells (un-transfected wild-type and PNKP$^{-/-}$ HeLa cells, and stably transfected HeLa PNKP-/- cells) were suspended in melted 0.6% agarose and pre-warmed 2X medium mixture (1: v/v) to form the upper layer. After 14 days, 1 ml of 0.02% crystal violet was added to each well to stain the colonies. Four independent experiments were performed with at least 3 replicates each time.

2.3 Results

2.3.1 Developmental history

The patient was a 3-year-old male with a history of known PNKP mutation resulting in medically intractable epilepsy, global developmental delay and microcephaly presenting with worsening seizures, difficulty feeding and failure to thrive. The patient was followed by the University of Washington genetics team since birth. Developmentally, at age 2, he had not yet crawled or pulled to a stand. He was able to sit independently and roll to get on his hands and knees. At 3 years, he had not yet spoken any words and did not understand any words spoken to him.

2.3.2 Initial imaging and treatment

A head computed tomography (CT) scan demonstrated a 2.5-cm hyper-dense lesion within the right cerebellum with evidence of obstructive hydrocephalus (**Fig. 2.2*a***). An MRI of the brain demonstrated a 3 x 2.4 cm contrast enhancing lesion within the right cerebellum with a large 3.3 x 2.7 cm peri-tumoral cyst (**Fig. 2.2*b***). Upon arrival to hospital, the patient received an external ventricular drain (EVD) for treatment of hydrocephalus. On hospital day 3, the patient was taken to the operating room for a near-total resection (NTR) of the cerebellar mass via a sub-occipital craniotomy (**Fig. 2.2*c-d***). The procedure went without any complications and he was admitted to the pediatric intensive care unit post-operatively.
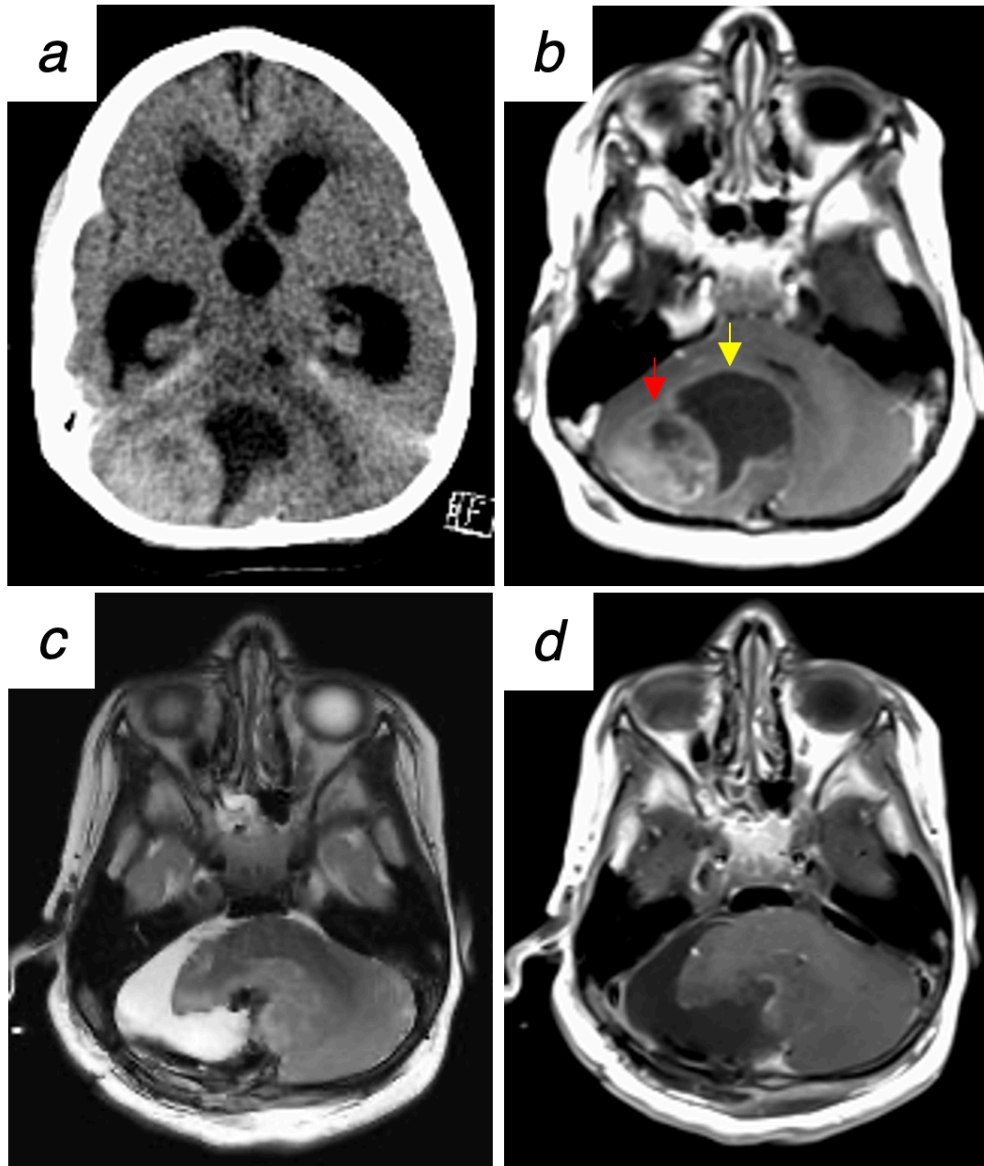
Figure 2.2 CT and MRI images of the patient.

(a) CT scan of the head demonstrating large cerebellar tumor causing obstructive hydrocephalus. (b) T1-weighted MRI scan of the brain with contrast showing a heterogenous lesion (red arrow) alongside large cyst (yellow arrow) within the cerebellum. (c-d) T2-weighted (c) and T1-contrast enhanced MRI scan (d) of the brain post-surgery showing near total resection of the tumor.
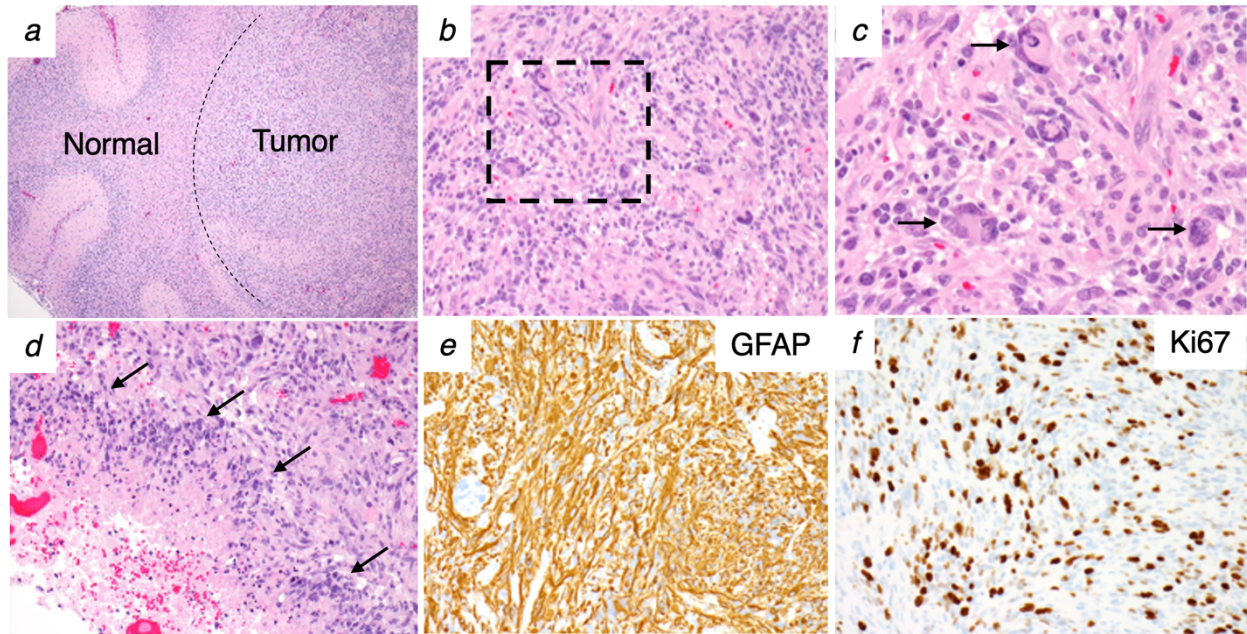
Figure 2.3 Tumor Histology images of the patient.

(a) Lower magnification hematoxylin and eosin (H&E) stain of tumor tissue showing expansion and infiltration of normal cerebellum (left) by tumor cells (right). (b) Higher magnification H&E stain of tumor demonstrating nuclear pleomorphism (aggressive tumor feature). (c) Higher magnification H&E stain (of dashed box in b) showing nuclear pleomorphism (black arrows). (d) The tumor also demonstrates pseudopallisading necrosis (black arrows), a histopathological feature of glioblastoma multiforme. (e-f) Immunohistochemistry showing glial origin for tumor based on glial fibrillary acid protein (GFAP) expression (i) and a highly proliferative lesion based on approximately >30-40% Ki-67 antigen expression in tumor cells imaged at medium power (j).

2.3.3 Pathology

Histological sections of the tumor tissue demonstrated a highly cellular neoplastic proliferation of intermediate to large sized pleomorphic cells (**Fig. 2.3*a-c***). There are also areas of pseudopallisading necrosis indicating the highest grade of glioma (**Fig. 2.3*d***). Immunohistochemistry demonstrated GFAP positivity suggesting glial tumor (**Fig. 2.3*e***) and a Ki67 proliferative index of 30-35% (**Fig. 2.3*f***). The final pathology was a glioblastoma multiforme (WHO Grade IV).

2.3.4 PNKP mutation analysis

Following institutional review board (IRB) approval and parental consent, we profiled blood samples from the patient and both parents. Using a sequencing panel for microcephaly, the blood-derived patient and parental DNA were sent for sequencing at the University of Chicago Genetic Services, Chicago, Illinois. The results revealed two changes in the PNKP gene. The first change, NM_007254.3:c.968C>T, abbreviated as 968C>T, converts a highly conserved threonine to methionine (T323M) in the functional domain of PNKP. The second change, NM_007254.3:c.302C>T, abbreviated 302C>T, converts a moderately conserved amino acid in the FHA domain (P101L) that has not been previously reported. Therefore, this mutation was of unknown significance. Mutational analysis of his parents, however, showed that they both carried the 302C>T

mutation. Further sequencing analysis of the tumor sample revealed deletions of ATRX, mutations in TP53 and NF1, copy loss of BRCA2 and RB1, and amplification of CDK4.

2.3.5 PNKP mutants have weaker DNA kinase and phosphatase activities

For analysis of the biochemical consequences of the *PNKP* mutations we expressed and purified the P101L and T323M proteins arising from the 302C>T and 968C>T mutated cDNA, respectively (**Fig. 2.4**). We also generated a double-mutant (PNKP-DM) containing both the P101L and T323M altered amino acids (**Fig. 2.4**).

The T323M mutant displayed a markedly reduced kinase activity, while the activity of the P101L mutant was only slightly lower than the wild-type protein (**Fig. 2.5**). In contrast, PNKP-DM completely lost activity. In the case of the T323M mutant, it was noticeable that although it exhibited significant activity at the start of the reaction, the activity plateaued after 10 min only achieving ~50% reaction (**Fig. 2.5*a***). One possibility for this is protein instability. This possibility was examined by pre-incubation of the protein at 37°C for 10 min prior to addition of the substrate and adenosine triphosphate (ATP; **Fig. 2.5*b***). Although the wild-type and P101L proteins retained residual activity, the T323M mutant exhibited almost complete heat inactivation. An examination of the phosphatase activity revealed that the P101L mutant retained significant activity albeit slower than the wild-type protein (**Fig. 2.5*c***). In contrast, the activity of the T323M protein was severely curtailed, while PNKP-DM exhibited almost no phosphatase activity (**Fig. 2.5*c***).
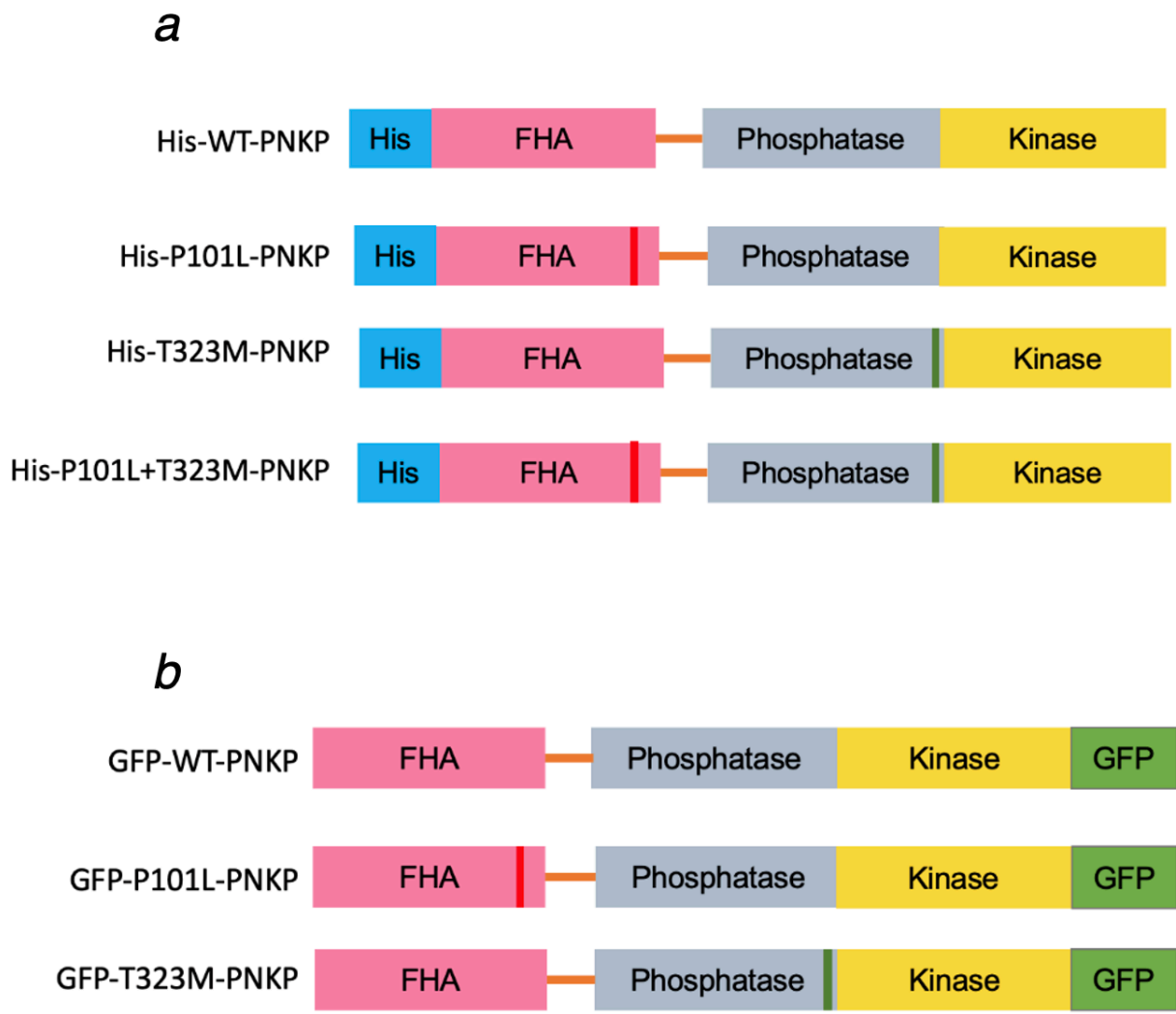
Figure 2.4 The structures of mutant PNKP constructs

The structures of mutant PNKP constructs designed to monitor the effects of the PNKP mutations found in the MCSZ patient. FHA represents the forkhead-associated domain of PNKP. His- indicated histidine tag (a) and GFP indicates the green fluorescent protein tag (b).
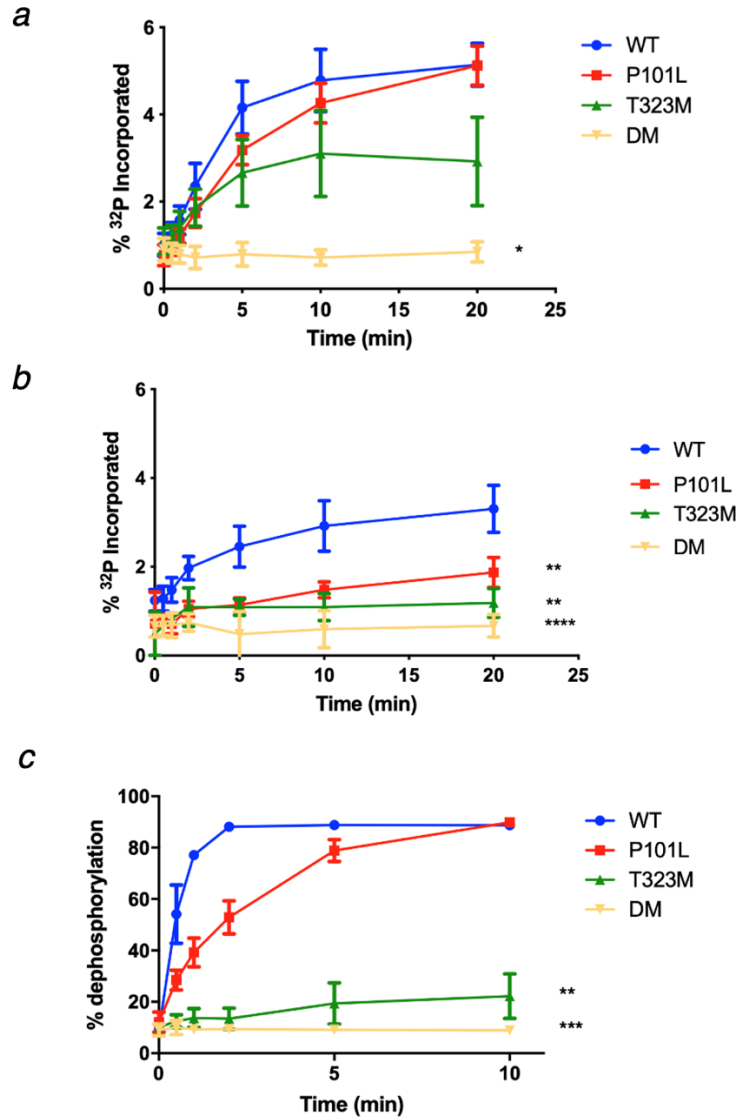
Figure 2.5 Measurement of enzymatic activities of wild-type and mutant PNKPs

Measurement of 5'-kinase and phosphatase activities of wild-type and mutant PNKPs (a) Kinase assay: a 24mer oligonucleotide bearing a 5'-hydroxyl terminus was incubated with wild-type or P101L, T323M, and the double mutant (DM) variant PNKP proteins in the presence of a 10-fold molar excess of radiolabelled ATP and then analyzed by gel electrophoresis. (b) To examine the temperature-dependent destabilization of wild-type and mutant forms of PNKP, the proteins were preincubated at 37ºC before carrying out the kinase assay. (c) Phosphatase assay: a 5'-labelled 24mer oligonucleotide bearing a 3'-phosphate group was incubated with wild-type or variant PNKP protein and then analyzed by gel electrophoresis.

2.3.6 Decreased binding affinity between mutant PNKP and DNA and XRCC4

To determine if reduced enzyme activity was due to lower substrate binding, we examined the affinities (K_d) of the mutant enzymes towards two double-stranded substrates containing a single-nucleotide gap with strand break termini reflecting the need for kinase (5'-OH) and both kinase and phosphatase (5'-OH and 3'-P) activity using steady-state fluorescence. The binding affinities between P101L PNKP and the DNA substrates does not differ markedly from those of the wild-type protein (**Table 2.2**). This is expected since P101L still retains relatively strong kinase and phosphatase activities. In contrast and consistent with their respective enzymatic activity, the T323M and PNKP-DM showed significantly reduced binding affinities (**Table 2.2**). Previous studies have indicated that the DNA-binding surfaces of PNKP reside in the catalytic domain.(226) It is therefore reasonable that the P101L mutation in the FHA domain would not substantially change the DNA binding affinity. The crystal structure of PNKP revealed that there is an intimate association between the phosphatase and kinase subdomains(97), therefore, it is not surprising that the T323M mutation, although located within the phosphatase domain, can reduce the binding affinity for the 5'-OH substrate (GAP1).

Analysis of the protein structure by circular dichroism, however, did not reveal a gross deformation caused by the T323M mutation (**Fig. 2.6***a* and **Table 2.3**). Since the P101L mutation lies in the FHA domain, which interacts with the phosphorylated scaffold proteins XRCC1 and XRCC4, we employed fluorescence polarization to examine the binding of the wild-type and mutant PNKP protein to a peptide sequence based on XRCC4 that

Table 2.2 PNKP DNA binding activity.

	GAP1[a]	GAP2 (5ºC)[b]
WT	200±10	300±10
P101L	230±10	400±20
T323M	330±20	750±30
DM	300±20	550±30

Table 2.2. Binding affinity (K_d value, nM) between wild-type (WT) and mutant PNKPs and DNA substrates. The binding affinities (K_d) values were obtained by steady-state fluorescence. The determination with the GAP1 substrate was carried out at room temperature while determination with the GAP2 substrate was carried out in 5ºC.

Substrate sequence:

5'-pATTACGAATGCCCACACCGC GGCGCCCACCACCACTAGCTGGCC-3'

3'-TAATGCTTACGGGTGTGGCGGCCGCGGGTGGTGGTGATCGACCGGp-5'

[a]GAP1 carried 3'- and 5'-OH termini at the gapped site.

[b]GAP2 carried 3'-phosphate and 5'-OH termini at the gapped site.

Table 2.3 Secondary structural analysis.

Sample	α-Helix (%)	β-Structure (%)	Random structure (%)
Wild type PNKP	39	31	30
T323M PNKP	37	33	30

Table 2.3. Secondary structural analysis of wild-type PNKP and T323M PNKP variant. The CD spectra of wild-type and T323M-PNKP were measured as described previously (223) and the results were analyzed according to the method of Chen et al.(224)
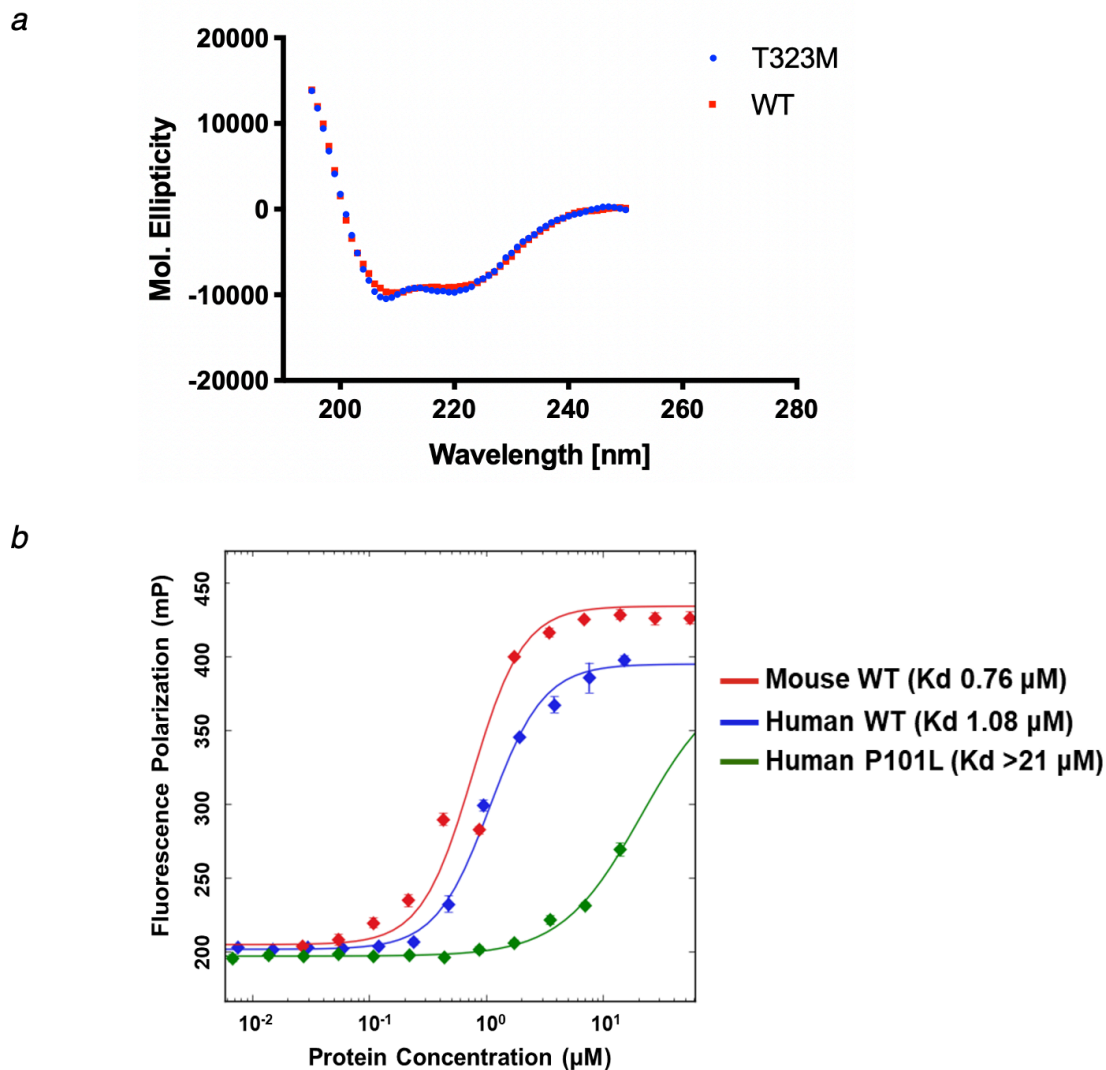
Figure 2.6 Structural analysis of mutant PNKP.

(a) Far-UV-CD spectra of wild-type (Wt) and T323M PNKP. The concentration of PNKP was 0.5 mg/ml dissolved in 50 mM Tris, pH 7.5, 100 mM NaCl and 1 mM DTT. (b) Interaction of wild-type and P101L PNKP with an XRCC4-based peptide. The interaction was monitored by fluorescence polarization of the fluorescent-dye labeled XRCC4-based phosphopeptide (GGYDES-pT-DEESKK) in the presence of increasing concentrations of wild-type murine and human wild-type or P101L PNKP. In each case the data represent the mean ± SEM of three independent experiments. Ordinary one-way ANOVA followed by Tukey's multiple comparisons test was performed using GraphPad Prism 7.0, GraphPad Software. *P<0.05, **P<0.01, ****P < 0.0001.

contains the key phospho-threonine residue (97). The results indicate that the P101L alteration causes a significantly reduced binding affinity to the phosphopeptide compared to the wild-type PNKP (**Fig. 2.6*b***).

2.3.7 Influence of PNKP mutation on cellular protein levels

Low cellular levels of PNKP appear to be a common feature of mutants associated with cases of MCSZ.(116, 217) Due to the unavailability of live cells from the patient, the influence of the P101L and T323M mutations was investigated at the cellular level using PNKP knock-out HeLa cells (HeLa PNKP$^{-/-}$) (225) transfected with vectors encoding either the wild-type or mutant GFP-tagged PNKP proteins. Western blot analysis following transient transfection revealed that the cellular levels of the mutant proteins were lower than those of the transfected wild-type PNKP, ~50% in the case of the P101L mutant and only ~10% for the T323M mutant (**Fig. 2.7*a and b***). We therefore asked if the reduced protein levels arose from reduced transcription or if the reduction was purely at the protein level. Transcription of the cDNAs with the 302C>T and 968C>T mutations was ~50% and ~60% lower, respectively, than the wild-type cDNA (**Fig. 2.7*c***). Thus, the lower level of the P101L protein could be accounted for by reduced transcription, but although there was a marked reduction in the transcription of the 968C>T cDNA, this cannot fully explain the low level of T323M-PNKP observed in the western blot, suggesting that either the translation process producing T323M-PNKP is less efficient, or that T323M-PNKP protein is less stable.
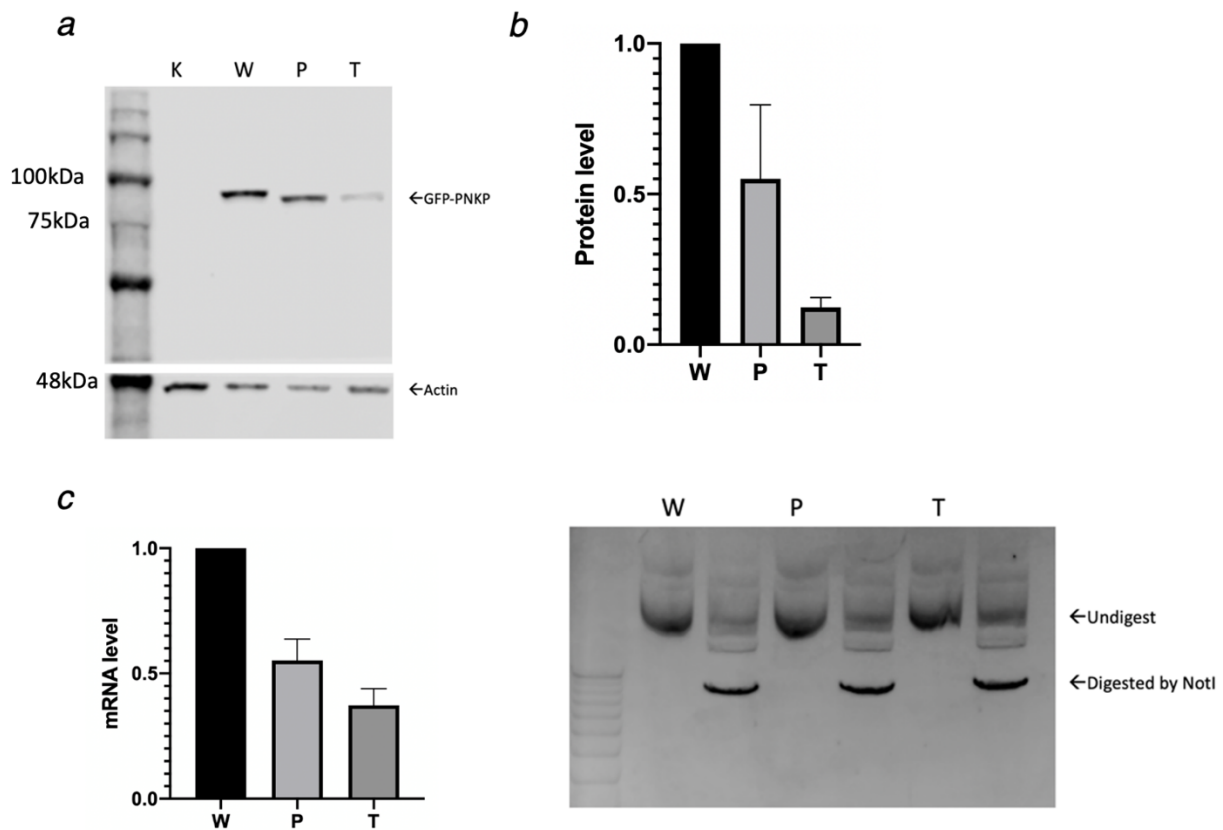
Figure 2.7 Protein and mRNA levels of PNKP in transiently transfected cells

(a) Western blot of transiently transfected cells, K - HeLa PNKP$^{-/-}$, W - HeLa PNKP$^{-/-}$ expressing wild-type PNKP, P - HeLa PNKP$^{-/-}$ expressing P101L PNKP, T - HeLa PNKP$^{-/-}$ expressing T323M PNKP. (b) Relative levels of PNKP in transiently transfected cell lines were determined using beta-actin as the reference protein and normalizing the level of the PNKP in the HeLa PNKP$^{-/-}$ cells expressing wild-type PNKP to 1. Data represent the mean ± SEM of three independent experiments. (c) Left: Relative PNKP mRNA levels in transiently transfected cell lines. mRNA levels were calculated using GAPDH level as the reference with the level of the PNKP mRNA in the HeLa PNKP$^{-/-}$ cells expressing wild-type PNKP normalized to 1. Data represent the mean ± SEM of three independent experiments. Right: DNA gel of the plasmid DNA (circular and linearized) used in the transfection showing equal quantities of the DNA constructs were used for the transfection.
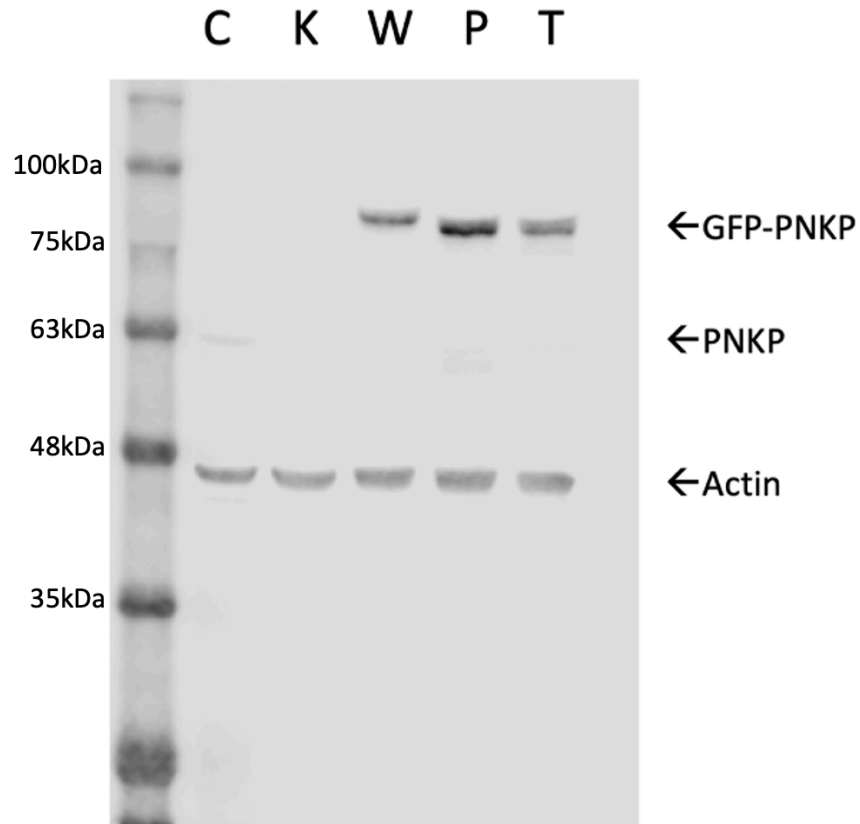
Figure 2.8 Western blot of stably transfected cells.

C: wild-type HeLa cells; K: HeLa PNKP$^{-/-}$ cells; W: HeLa PNKP$^{-/-}$ cells transfected with wild-type PNKP cDNA; P: HeLa PNKP$^{-/-}$ cells transfected with cDNA coding for P101L mutant PNKP; T: HeLa PNKP$^{-/-}$ cells transfected with cDNA coding for T323M mutant PNKP.

Therefore, to overcome the disparity of PNKP expression in transiently transfected cells, we established and utilized clonally-derived stably transfected cell lines expressing similar levels of wild-type and mutant PNKP (**Fig. 2.8**).

2.3.8 Influence of PNKP mutation on protein localization

Next, we examined the cellular localization of the mutant PNKP proteins following transfection of cDNA for GFP-tagged PNKP. The wild-type PNKP stably re-expressed in HeLa PNKP$^{-/-}$ cells predominantly localized to the nucleus (**Fig. 2.9*a***). Similarly, the T323M PNKP-GFP mutant localized to the nucleus, although these cells appeared to have a slightly higher cytoplasmic signal relative to wild-type PNKP (Fig. 9*a*). The P101L PNKP-GFP mutant, however, was predominantly cytoplasmic (**Fig. 2.9*a***). A western blot analysis verified that P101L PNKP-GFP maintained its full length with no degradation (**Fig. 2.8**), implying that the cytoplasmic signal arose from the PNKP-GFP full length protein rather than a GFP-tagged cleavage fragment. These localization patterns were observed in both transiently and stably transfected cells. To quantify the distribution pattern and exclude the possible bias from the selection of stably-transfected cell lines, we used high content screening to analyze over 2000 transiently-transfected cells in each group. The ratio between the area of the GFP signal and the area of the nucleus (Hoechst) within each cell was determined and it confirmed that the P101L mutation significantly changed the PNKP distribution pattern, with most cells having a GFP/Hoechst area ratio larger than 2 (**Fig. 2.10**). Similar to wild-type HeLa cells, wild-type PNKP is restricted to
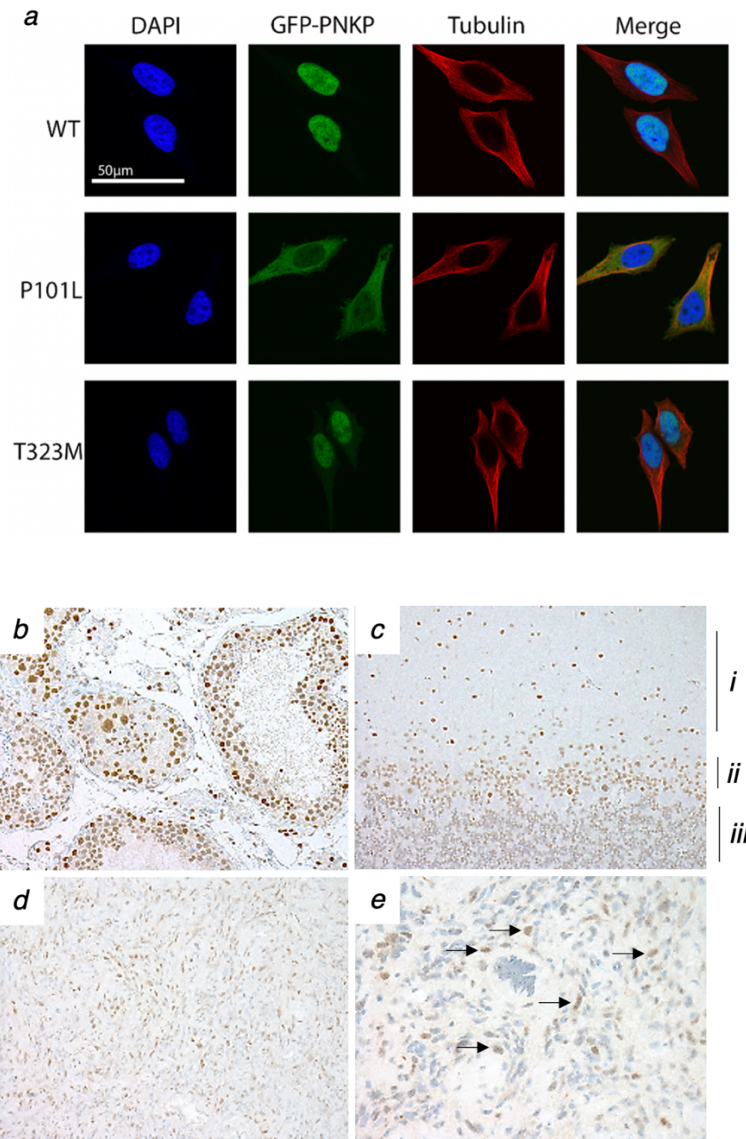
Figure 2.9 Cellular localization of PNKP

(a) HeLa PNKP^{-/-} cells were stably transfected with indicated GFP-tagged PNKP constructs (green), tubulin immunofluorescence (red) indicates the cytoplasmic area, Hoechst staining (blue) indicates the nuclear area. Images were captured using an LSM710 confocal microscope. (b-c) PNKP protein expression is restricted to the nucleus in normal tissue (b-Testes, c-Cerebellum. i-Molecular layer, ii-Purkinje layer, iii-granular layer). (d-e) PNKP expression in the patient derived tumor tissue is nuclear and cytoplasmic (higher magnification image with back arrows in e).
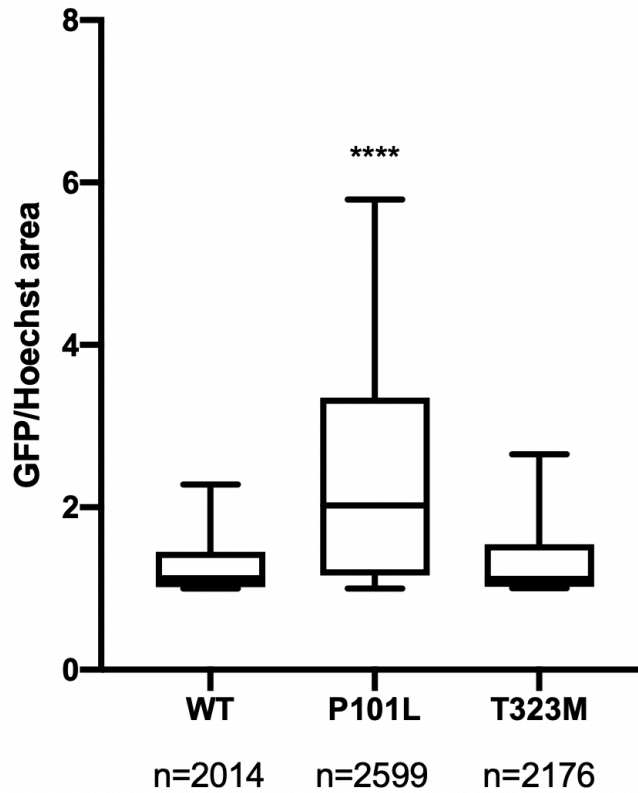
Figure 2.10 High content analysis of PNKP cellular localization.

(a) Nuclear vs cytoplasmic distribution of PNKP. The ratios were obtained by high-content analysis as described in Material and Methods. Whiskers indicate Min to Max ratio of GFP/Hoechst area in each group. 2% outliers were excluded by ROUT method, **** $P < 0.0001$.

the nucleus in normal human testes and cerebellum (**Fig. 2.9*b-c***). Consistent with the localization of mutant PNKP-GFP in the HeLa PNKP$^{-/-}$ cells, the patient's tumor showed both nuclear and aberrant cytoplasmic distribution of PNKP (**Fig. 2.9*d-e***).

The transportation of protein through the nuclear membrane is bi-directional. Previously our group discovered a bipartite nuclear localization signal (NLS) located in the flexible linker between the FHA domain and catalytic domain (K130, R131 + KKRMRK,137-142) (74), which has recently been confirmed by others (73). While the P101L may potentially impact the NLS, another possible reason for the altered localization pattern is that the mutation created a novel nuclear export signal (NES) in PNKP. The NES signal is a leucine-rich peptide region first discovered in cAMP-dependent protein kinase inhibitor (PKI) (228) and human immunodeficiency virus type 1 (HTV-1) Rev protein (69). Export protein exportin 1 (CRM1) has been identified as the export receptor for proteins that harbor an NES signal and transports them from the nucleus to the cytoplasm (69, 229-231). We used two different NES prediction software programs to analyze the wild-type and mutant PNKP protein sequence. Both NetNES (232) and LocNES (233) indicate the P101L mutation creates a new NES signal in the FHA domain while T323M does not create any NES signal (**Table 2.4**). To confirm this prediction, we monitored the influence of leptomycin B (LMB), an inhibitor of exportin 1(230, 234) on PNKP localization. The results showed LMB treatment significantly changed the localization pattern of P101L PNKP with nearly all PNKP-GFP being retained in the nucleus (**Fig. 2.11**).

Table 2.4 Identifying PNKP mutation induced novel nuclear export signals

a. Analysis of mutant PNKP by NetNES

Amino Acid and Location	ANN	HMM	NES
P101 (Wt)	0.132	0.002	0.000
L101 (Mut)	0.433	0.008	0.195
T323 (Wt)	0.073	0.002	0.000
M323 (Mut)	0.082	0.010	0.000

b. Analysis of mutant PNKP by LocNES

Position	Sequence	LocNES Score
88-102 (Wt)	GVGDTLYLVNGLH*P*L	0.500
90-104 (Wt)	GDTLYLVNGLH*P*LTL	0.650
87-101 (Mut)	LGVGDTLYLVNGLH*L*	0.663
88-102 (Mut)	GVGDTLYLVNGLH*L*L	0.628
90-104 (Mut)	GDTLYLVNGLH*L*LTL	0.768
315-329 (Wt)	LNLGLPFA*T*PEEFFL	0.008
309-323 (Mut)	ADRLFALNLGLPFA*M*	0.015
315-329 (Mut)	LNLGLPFA*M*PEEFFL	0.011

Table 2.4. Identifying PNKP mutation induced novel nuclear export signals (a). Individual scores of two mutation sites of PNKP by NetNES program (232). ANN: Artificial Neural Network; HMM: Hidden Markov Models; NES: NES scores based on ANN and HMM value. (b). Possible NES candidates around the mutation sites, calculated by LocNES program (233). P101L mutation increased the numbers of possible NES candidates from 2 to 3 with higher NES score; T323M mutation increased the numbers of possible NES candidates from 1 to 2 with similar low NES score.
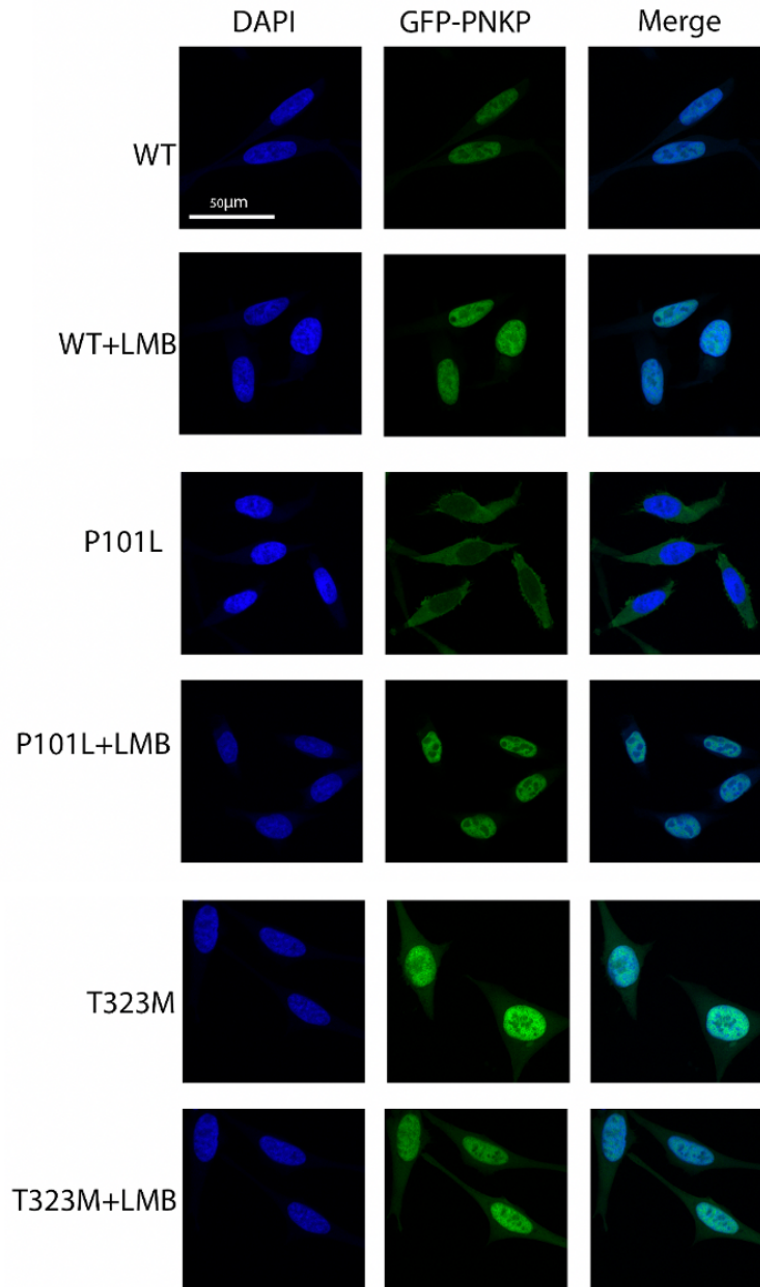
Figure 2.11 Inhibition of exportin 1 leads to nuclear retention of P101L PNKP.

Stably-transfected PNKP-knockout HeLa cells expressing GFP-tagged wild-type and mutant PNKP were treated with leptomycin B (LMB) for 3 hours and then stained with DAPI and imaged at 40x magnification.

2.3.9 Influence of PNKP mutations on radiation sensitivity

Hydroxyl radicals produced endogenously or by ionizing radiation generate strand break termini containing a high percentage of 3'-phosphate and to a lesser extent 5'-OH termini (235, 236). To carry out an examination of the influence of the PNKP mutations on cellular response to oxidative DNA damage and repair, the wild-type and stably transfected HeLa PNKP$^{-/-}$ cells were subjected to increasing doses of γ radiation. The un-transfected wild-type HeLa cells showed the most radiation-resistant phenotype, while the HeLa PNKP$^{-/-}$ cells displayed the greatest radio-sensitivity, similar to our previous observations(20) (**Fig. 2.12**). The re-expression of wild-type PNKP in HeLa PNKP$^{-/-}$ cells re-established resistance to radiation. The P101L mutant cells exhibited slightly increased radio-sensitivity, while the T323M mutant cells showed similar radio-sensitivity to the knockout cells (**Fig. 2.12**).

To further examine the relevance of mutant PNKP after radiation, we monitored the capacity of the cells to repair radiation-induced DNA damage. The alkaline single cell gel electrophoresis (comet) assay primarily detects DNA single-strand breaks and alkali-labile sites in the DNA. (223, 224) All cell lines repaired most of the DNA damage within 24 hours (**Fig. 2.13**). However, a significant difference was observed at early times (1 hour), with the HeLa wild-type cells and the HeLa PNKP$^{-/-}$ cells transfected with wild-type PNKP both displaying a rapid reduction in tail moment (indicating efficient repair), while HeLa PNKP$^{-/-}$ cells showed the slowest repair progress (**Fig. 2.13**). The two mutant cell lines displayed intermediate repair efficiency (**Fig. 2.13**).
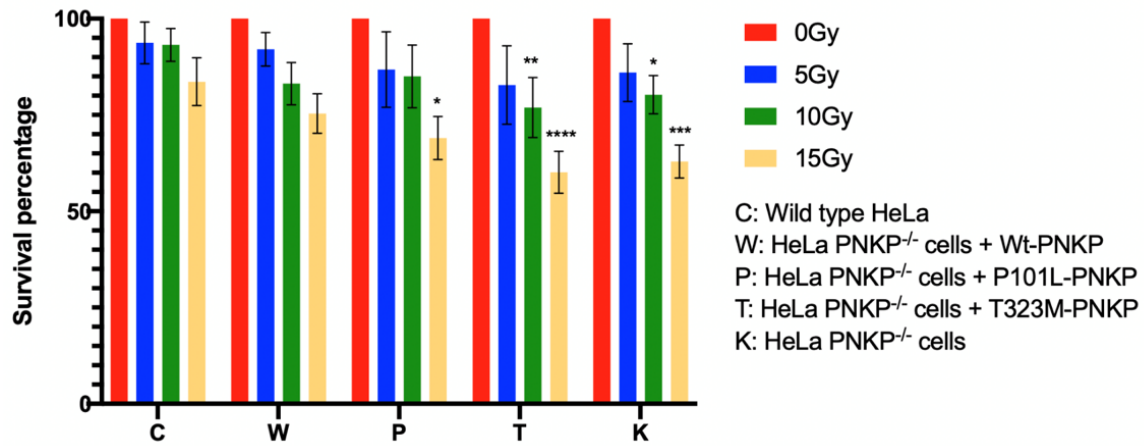
Figure 2.12 Viability of wild-type and mutant cell lines.

Viability of wild-type and mutant cell lines at different radiation dosages. Plots represent mean $\pm$SD. Ordinary one-way ANOVA was performed to compare each cell line with the wild-type HeLa at the same radiation dose using GraphPad Prism 7.0.
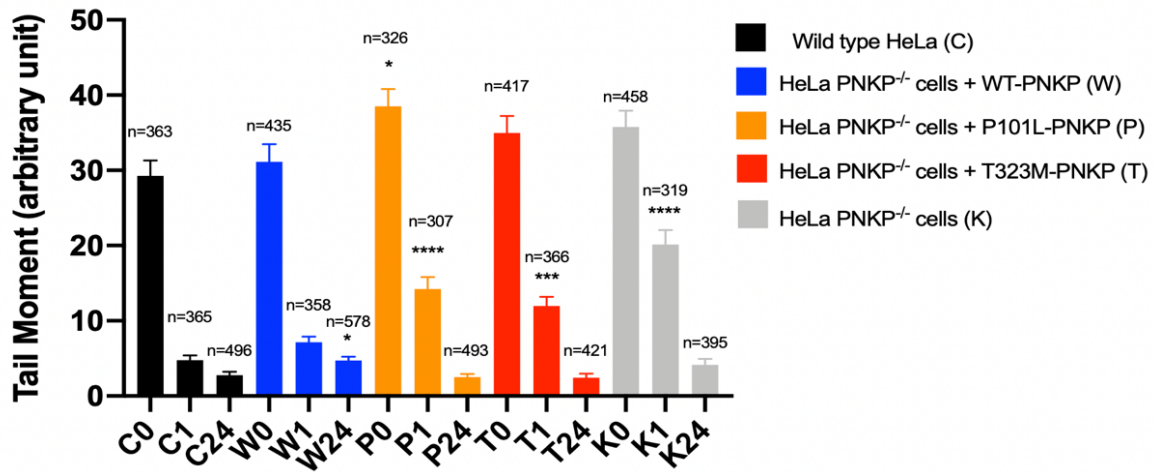
Figure 2.13 Single-strand break repair of wild-type and mutant cell lines.

Single-strand break repair measured by the single cell gel electrophoresis assay. DNA tail moments of cell lines were measured at 1 and 24 hrs after irradiation. Each column includes data from at least 300 cells. Plots represent mean ± SEM. At each time point, one-way ANOVA was performed to compare each group with the wild-type un-transfected HeLa cells at the same time point using GraphPad Prism 7.0.

PNKP participates in the non-homologous end joining pathway (NHEJ) but is not involved in the homologous recombination (HR) pathway(237), therefore to determine the influence of mutant PNKP in NHEJ repair we monitored the formation and disappearance of 53BP1 foci (238) following cell irradiation. HeLa PNKP$^{-/-}$ cell lines exhibited the highest number of foci at 1- and 4-hr post-radiation but returned to background levels by 24 hr (**Fig. 2.14**). This is similar to our previous observations monitoring the γH2AX signal (another marker of double-strand breaks) in PNKP knockdown A549 lung cancer cells. (222) A recent paper reported the existence of a yet unidentified alternative 3'-phosphatase that can act at DSB(234), which may explain the eventual repair of radiation-induced DSB in HeLa PNKP$^{-/-}$ cells. The cell lines complemented with wild-type and P101L mutant displayed similar foci levels at each time point, indicating that the P101L expressing cells repair double-strand breaks with near normal kinetics and that sufficient PNKP is retained in the nucleus to carry out the repair. In contrast, cells expressing the T323M PNKP failed to return to background level by 24 hr (**Fig. 2.14**). This suggests that mutant T323M PNKP is inefficient at repairing DSB, likely due to a combination of its intrinsically poor enzymatic capacity and by impeding access of the alternative, yet to be identified, backup repair enzyme(s) to the damaged termini.(225)
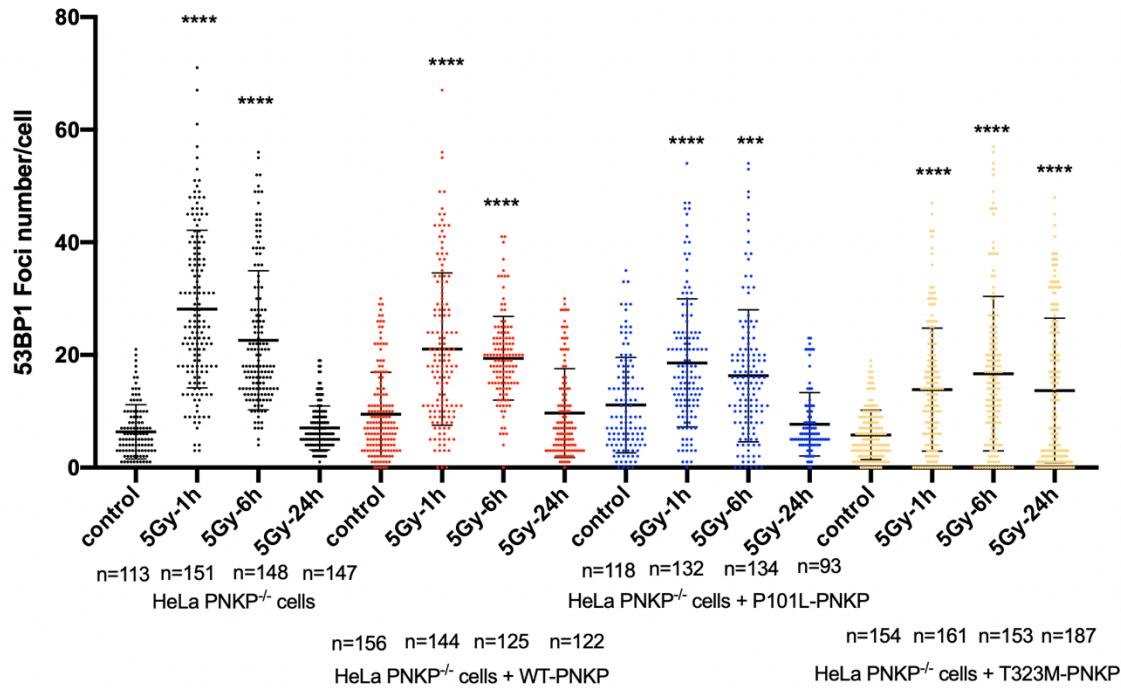
Figure 2.14 Repair of DNA double strand breaks by the NHEJ pathway.

Results are based on 53BP1 foci numbers observed in the wild-type and stably transfected cell lines at different times after irradiation, *n* indicates the measured cell numbers in each group. The plots represent mean ± SD. In each graph, one-way ANOVA was performed to compare 53BP1 foci at each time point with the number of foci in unirradiated cells using GraphPad Prism 7.0, GraphPad Software. P***<0.001, P****<0.0001.

2.3.10 Anchorage-independent growth raised in mutant cell lines

Anchorage-independent growth is frequently used as an indicator of pro-oncogenic transformation.(239) The soft agar colony formation assay is a well-established method for characterizing anchorage-independent growth capacity and is one of the most stringent tests for malignant transformation in cells.(240) The higher concentration of agar in the growth environment prevents cells from adhering yet allows transformed cells to form visible colonies.(227) HeLa PNKP$^{-/-}$ cells demonstrated increased transformation frequency approximately 4-fold over wild-type HeLa cells (**Fig. 2.15**). HeLa PNKP$^{-/-}$ cells transfected with wild-type PNKP reduced the number of transformants similar to the parental HeLa cell line. Expression of the P101L and T323M mutant PNKP in HeLa PNKP$^{-/-}$ cells, however, increased the transformation frequency 2-3 fold (**Fig. 2.15**).
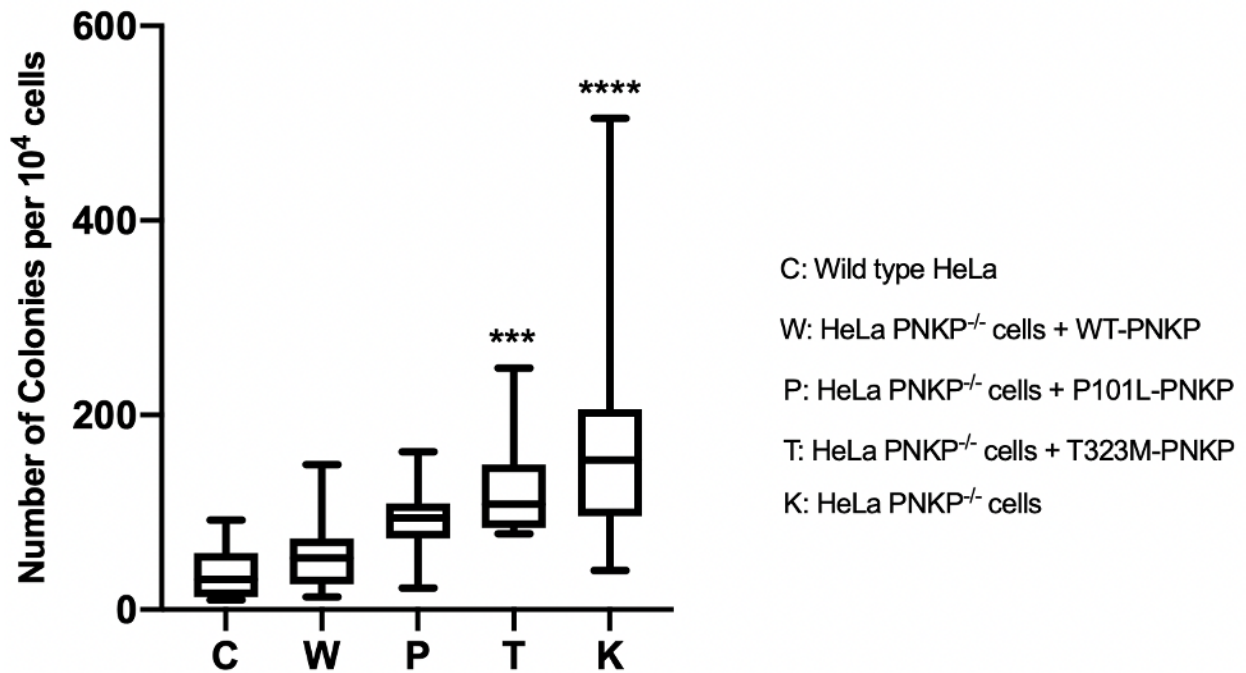
Figure 2.15 Influence of *PNKP* mutation on cell transformation.

The plot indicates the number of colonies generated by each cell type in soft agar two weeks after plating. Four independent experiments were performed with at least 3 replicates each time. Whiskers indicates Min to Max number of colonies per 10^4 cells. One-way ANOVA was performed to compare each outcome with the wild-type un-transfected HeLa cells using GraphPad Prism 7.0, GraphPad Software. P***<0.001, P****<0.0001.

2.4 Discussion

Several DNA repair disorders, such as Ataxia telangiectasia, are known to be associated with both neurological dysfunction and elevated cancer risk. MCSZ is an extremely rare autosomal recessive disorder and to date there has been no indication of elevated cancer risk associated with MCSZ, although one case of a lower-grade cerebellar pilocytic astrocytoma was diagnosed in a patient with AOA4.(214) The occurrence of primary CNS tumors in children in the US is ~5.3 cases per 100,000 children, of which the high-grade brain tumor, glioblastoma multiforme (GBM) accounts for 3-15% (241, 242). Although not definitive, these cases of relatively rare brain tumors in AOA4 and MCSZ strongly suggest a link between *PNKP* mutation and elevated cancer risk. However, since complete loss of PNKP is likely to be embryonic lethal (102), some residual activity is required for survival(243) and so it is important to characterize the mutant proteins in terms of their enzyme activity and cellular impact.

Based on the location of the mutation, the P101L alteration did not significantly affect either the phosphatase or kinase activities since the altered amino acid residue lies in the FHA domain rather than the catalytic domain. In contrast, the T323M alteration severely curtailed the PNKP kinase activity and to a lesser extent the phosphatase activity. Studies on the biochemical and cellular consequences of PNKP mutation causing MCSZ are limited. Understandably, substantial structure loss such as frameshifts, e.g. T424Gfs, could reduce protein stability and enzymatic activities. But it is interesting that single mutations, such as L176F, also showed reduced enzymatic activities (218). Both

mutations found in our patient are one amino acid replacements. The purified mutant PNKPs retained their full size and the circular dichroism analysis suggested that the structure of the more affected T323M mutant did not appear to be grossly altered by the change in amino acid despite the larger size of methionine compared to threonine. This is probably due to a pocket that the extended amino acid can fit into with relatively minor clashes predicted with Glu 326 and Arg 293. We show the structure for the highly conserved 300s loop within mouse PNKP (97) in which the equivalent amino acids are Glu 325 and Arg 292 (**Fig. 16*a-b***). However, the mutation to methionine does remove a hydrogen bond between the main chain nitrogen of Glu 326 and the hydroxyl of Thr 323. The clashes with Glu 326 and Arg 293, along with the missing hydrogen bond, could disrupt the loop between residues 291 and 307 (300s loop), which has been shown to be important in binding double stranded DNA substrates (226) which in turn may explain the reduced affinity of the T323M mutant for the double stranded DNA substrates (**Table 2.2**). The fact that this mutation appears minimally disruptive and yet causes such a pronounced phenotype speaks to the necessity and sensitivity of the PNKP phosphatase domain.

While the P101L mutation did not significantly affect its affinity for DNA substrates or its enzymatic activity, it did reduce its affinity for the XRCC4-based phosphopeptide. This reduction in affinity is likely due to conformational changes caused by the mutation and resulting clashes with Y94. A conformational change in the P101/ Y94 loop will likely affect the pThr binding interface through residues H100 and N97 (**Fig. 2.16*c***). However, the degree of reduced binding to the phosphopeptide may not entirely reflect reduced binding
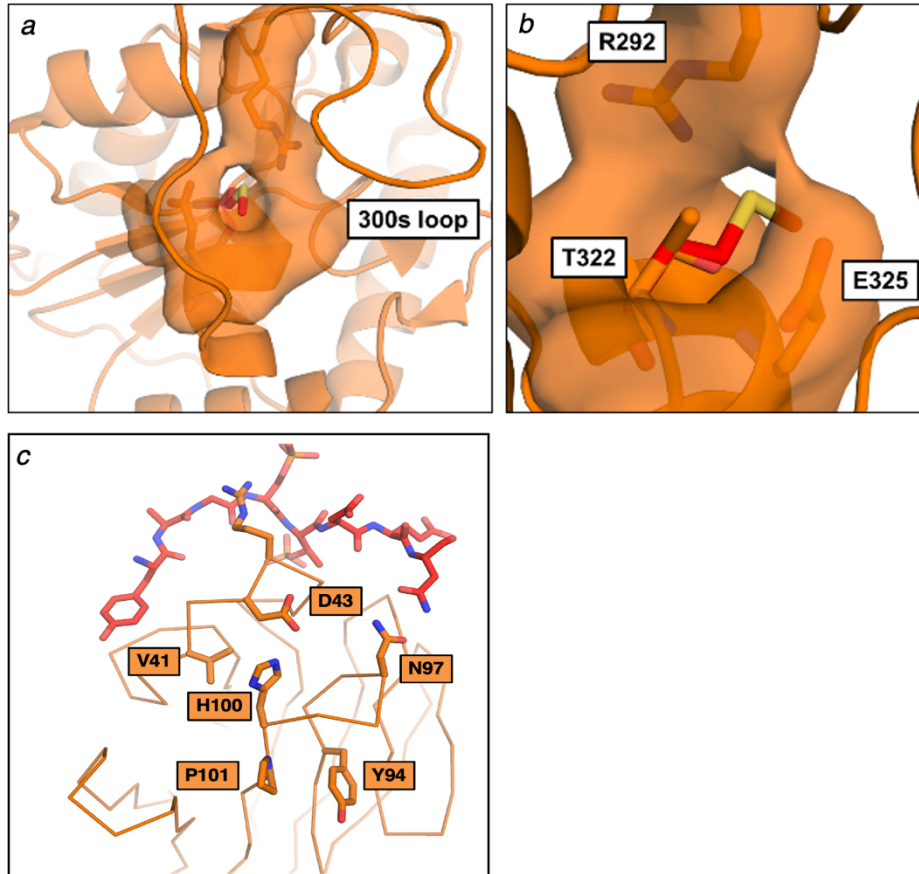
Figure 2.16 Local structures within PNKP at the sites of the amino acid changes.

(a-b) Images taken from murine PNKP surrounding T322 (T323 in human PNKP). The mutation T322M appears to be minimally disruptive despite the larger size of methionine, due to the presence of a pocket that can accommodate the extended amino acid. However, potential clashes can occur with Glu 325 and Arg 292 (Glu 326 and Arg 293 in human PNKP). (c) An alignment of the FHA domain of human PNKP with the phosphopeptide binding site of XRCC4. The PNKP FHA domain is shown in orange and the XRCC4 pThr/pSer peptide is shown in red (PDB: 2W3O). A disruption in the P101/Y94 loop that causes a conformational change will affect His 100 which would affect the pThr binding interface through packing with V41 and D43. Additional movement in the P101/Y94 loop would affect direct binding to the pThr peptide through N97's hydrogen bonds.

to full-length phosphorylated XRCC4 since other protein-protein interactions are involved in the binding between the two full-length proteins and there is also an interaction between the two proteins that is not dependent on XRCC4 phosphorylation (244). It is also noticeable that DSB repair, as judged by 53BP1 foci, was not significantly different in the cells expressing the P101L mutant protein compared to cells complemented with the wild-type protein. An unanticipated consequence, however, of the novel P101L mutation is the alteration of its cellular localization. To date there are no other PNKP mutations that have been reported to contribute to localization changes. Similar to the result we observed with the cells expressing mutant P101L PNKP-GFP, the IHC result of the patient showed cytoplasmic localization of PNKP. The NES analysis and LMB treatment indicate that the P101L mutation creates a new nuclear export signal that enables binding to exportin 1 and export into the cytoplasm. Although it is not uncommon for disease-associated mutations to alter the cellular localization of proteins, to our knowledge there is only one other report of a gain-of-function mutation that results in the formation of a new NES (245). In the latter case a mutation in the nucleophosmin gene, *NPM*, linked to acute myeloid leukemia was found to generate an additional NES responsible for relocalizing NPM to the cytoplasm. Interestingly, in our transfected cell lines (both transient and stable), the T323M mutant also displayed a low level of cytoplasmic localization. However, neither NetNES nor LocNES programs indicated the production of a novel NES signal. We and others (73) have previously identified a bipartite NLS signal in PNKP (K130, R131 + 137-142, KKRMRK). The T323M amino acid change is unlikely to interfere with this signal directly, so the cause for an increased presence of the T323M in the cytoplasm remains to be determined.

Expression of mutant PNKP proteins revealed several consequences that together raise the possibility that PNKP mutations could lead to tumorigenesis as well as MCSZ. As seen with other PNKP mutations, the level of the mutant proteins, particularly the T323M PNKP, was significantly depressed. Taking this into account together with its severely curtailed level of enzymatic activity would imply that this variant of the protein will provide extremely limited DNA repair capacity. Indeed, even in cells expressing artificially high levels of the T323M variant the repair of radiation-induced double-strand breaks is far from complete after 24hr (**Fig. 2.14**). Another important consequence of defective DNA repair is increased spontaneous mutation frequency. Spontaneous mutations continually arise from endogenous genotoxic agents in live cells such as ROS. (246) We have previously shown that shRNA-mediated knockdown of PNKP in human A549 lung cancer cells led to a 7-fold increase in the spontaneous mutation frequency.(222) Sequence analysis of the proband's tumor sample showed that it carried multiple molecular alterations in addition to the *PNKP* mutations, including deletion of *ATRX*, mutations with corresponding loss of heterozygosity in *TP53* and *NF1*, copy loss of *BRCA2* and *RB1*, and amplification of *CDK4*. *TP53* and *ATRX* mutations are commonly found in pediatric GBM (247), and a recent study revealed that inactive ATRX in Trp53 deficient murine neuroepithelial progenitors (mNPCs) altered the transcriptional patterns strongly correlated with several glioma signatures (248). Through the mutual exclusivity analysis of all listed studies on cBioPortal (including data from the cancer genome atlas; TCGA), all 6 genes mentioned above showed certain levels of co-occurrence tendency with *PNKP* mutations (**Table 2.5**). Since the entire genome of the patient was not sequenced, the

mutation time of different genes are difficult to determine. However, it is possible that in our patient, mutant PNKP induced impairment in DNA damage repair, preceded and synergized with pediatric glioma associated mutations such as ATRX and TP53 resulting in brain tumor initiation and progression.

In conclusion, although functional studies in a mouse model are needed to characterize the influence of both the novel P101L and previously described T323M PNKP alterations on brain tumor initiation, we speculate that mutant PNKP-driven impaired DNA damage response and higher spontaneous mutation rates contributed to the generation of pediatric glioma associated driver mutations such as TP53 and ATRX in the clinical case described.

Table 2.5 Analysis of PNKP's co mutated genes by cBioPortal

a. Mutual exclusivity between PNKP and candidate mutations in TCGA Pan Cancer Atlas studies

A	B	Neither	A Not B	B Not A	Both	Log2 Odds Ratio	p-Value	q-Value	Tendency
PNKP	BRCA2	9520	97	546	28	2.331	<0.001	<0.001	Co-occurrence
PNKP	ATRX	9394	101	672	24	1.732	<0.001	<0.001	Co-occurrence
PNKP	NF1	9274	102	792	23	1.401	<0.001	<0.001	Co-occurrence
PNKP	RB1	9320	103	746	22	1.416	<0.001	<0.001	Co-occurrence
PNKP	TP53	6258	63	3808	62	0.694	0.005	0.007	Co-occurrence
PNKP	CDK4	9787	120	279	5	0.548	0.269	0.283	Co-occurrence

b. Mutual exclusivity between candidate mutations in CNS/brain studies

A	B	Neither	A Not B	B Not A	Both	Log2 Odds Ratio	p-Value	q-Value	Tendency
ATRX	TP53	2692	92	734	822	>3	<0.001	<0.001	Co-occurrence
RB1	BRCA2	4054	272	71	33	2.792	<0.001	<0.001	Co-occurrence
TP53	RB1	2744	1381	98	207	2.069	<0.001	<0.001	Co-occurrence
TP53	BRCA2	2809	1517	33	71	1.994	<0.001	<0.001	Co-occurrence
ATRX	BRCA2	3375	864	51	50	1.937	<0.001	<0.001	Co-occurrence
NF1	RB1	3724	401	237	68	1.414	<0.001	<0.001	Co-occurrence
NF1	BRCA2	3881	445	80	24	1.388	<0.001	<0.001	Co-occurrence
TP53	CDK4	2619	1419	223	169	0.484	0.001	0.002	Co-occurrence
BRCA2	CDK4	3946	92	380	12	0.438	0.206	0.221	Co-occurrence
ATRX	RB1	3193	852	233	62	-0.004	0.527	0.527	Mutual exclusivity
TP53	NF1	2525	1436	317	152	-0.246	0.055	0.064	Mutual exclusivity
ATRX	NF1	3046	840	380	74	-0.502	0.004	0.005	Mutual exclusivity
ATRX	CDK4	3096	869	330	45	-1.041	<0.001	<0.001	Mutual exclusivity
NF1	CDK4	3586	452	375	17	-1.475	<0.001	<0.001	Mutual exclusivity
RB1	CDK4	3738	300	387	5	-2.635	<0.001	<0.001	Mutual exclusivity

Table 2.5. Mutual exclusivity analysis of PNKP and candidate mutations that were found in the patient's tumor sample. (a) Mutual exclusivity between PNKP and candidate mutations in TCGA PanCancer Atlas studies in cBioPortal. (b) Mutual exclusivity between candidate mutations in all CNS/brain studies in cBioPortal. Neither: Numbers of samples with alterations in neither A or B. A Not B/ B Not A: Numbers of samples with alterations in only gene A / B. Both: Numbers of samples with alterations in both gene A and B. Log2 Odds Ratio: Quantifies how strongly the presence or absence of alterations in A are associated with the presence or absence of alterations in B in the selected samples. Log2 Odds Ratio = (Neither * Both) / (A Not B * B Not A). Log2 odds ratio > 0: Tendency towards co-occurrence. Log2 odds ratio <= 0: Tendency towards mutual exclusivity. p-value: derived from one-side Fisher Exact Test. q-Value: derived from Benjamini-Hochberg FDR correction procedure.

3 Chapter 3: Mutation of PNKP in Ataxia with ocular motor apraxia type 4 (AOA4)

3.1 Introduction

In 1988, the first cases of Ataxia with ocular motor apraxia (AOA) were identified in 14 patients from 10 families (125). Signature symptoms of AOA include progressive ataxia, choreoathetosis, and ocular motor apraxia (125). The clinical features of AOA are similar to Ataxia-Telangiectasia (AT), i.e. progressive neurodegeneration and loss of Purkinje cells (126) but AOA patients do not have the additional AT neurological features such as telangiectasia, immunodeficiency, and susceptibility to malignancies (125, 127). So far, four subtypes of AOA have been identified, each associated with mutations in different genes. AOA1 is linked to mutations in Aprataxin (APTX) (128, 129), AOA2 is linked to mutations in Senataxin (SETX) (130), AOA3 is linked to mutations in Phosphoinostitide-3-kinase regulatory subunit 5 (PIK3R5) (131), and AOA4 is linked to mutations in the DNA repair protein Polynucleotide phosphatase/kinase (PNKP) (108).

As a bifunctional enzyme, PNKP possesses both DNA 3'-phosphatase and DNA 5'-kinase activities (94, 95). Human PNKP protein comprises of three domains, the N-terminal forkhead-associated (FHA) domain, phosphatase domain, and C-terminal kinase domain (249). Besides AOA4, mutations in PNKP have been found to be responsible for the autosomal recessive neurodevelopment disease Microcephaly, seizures, and developmental delay (MCSZ) (114-116, 118, 121, 215-217), and hereditary peripheral neuropathies Charcot-Marie-Tooth disease (CMT2B2) (109). While the mutations related to MCSZ are located in all three domains of PNKP, the mutations linked with AOA4 are almost all located in the kinase domain of PNKP (108, 135-139, 215) (108, 135-137, 139,

140, 214), except for one recently published report without signature AOA symptoms (154) as shown in **Fig. 3.1**.

Interestingly, most of the AOA4-associated mutations are compound heterozygous forms. The only mutation that has been found in both heterozygous and homozygous forms is G375W resulting from DNA point mutation G1123T. In addition, in the initial eight families identified with AOA4, the G375W mutation occurred with the highest frequency, in six out of eight families (108). Although additional PNKP mutations were found associated with AOA4 in later studies, no other mutation has shown up with such a high frequency.

To date, almost all the biochemical and cellular studies of PNKP mutations have focused on the MCSZ-associated mutations. The only AOA4 associated mutation that has been studied at the biochemical level is T424GfsX49, which is also observed in some MCSZ patients (116, 218). Considering its unique inheritance and high frequency (108, 140), we decided to examine the biochemical and cellular consequences of the G375W alteration to PNKP in order to gain more knowledge of the underlying causes of AOA4.
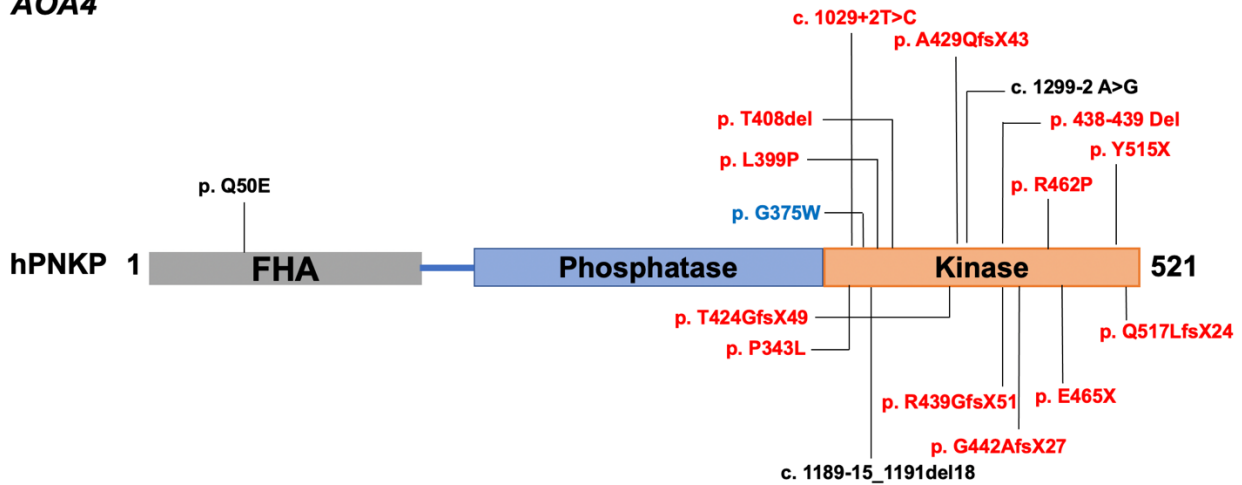
Figure 3.1 Mutations associated with AOA4.

Mutations marked in black have only been found in homozygous mutation format. Mutations marked in red have been found only in compound heterozygous mutation format. Mutations marked in blue have been found in both homozygous and heterozygous formats.

3.2 Material and methods

3.2.1 Expression plasmids and site-directed mutagenesis

To produce and purify the PNKP protein, pET-16b (Novagen Inc., Madison, WI) bacterial expression plasmid harboring the full-length human PNKP cDNA was generated following previously reported procedures (95, 220). To generate fluorescent-tagged versions of PNKPs in mammalian cells, the full-length human PNKP cDNA was subcloned into the pCMV6-AC-mGFP (Origene, Rockville, MD) mammalian expression plasmid as described before (221).

The desired PNKP single point mutant (PNKP G365W) was generated using the QuickChange II site-directed mutagenesis kit (Stratagene, La Jolla, CA) and following the manufacturer's protocol. The following mutagenic primers were used to generate the G375W plasmid:

Forward: 5'-GCAGTGGGATTCCCTTGGGCCGGG-3'

Reverse: 5'-CCCGGCCCAAGGGAATCCCACTGC-3'

Finally, the mutants were sequence validated in The Applied Genomics Core at the University of Alberta. The maps of mutant PNKP constructs are shown in **Fig. 3.2**.
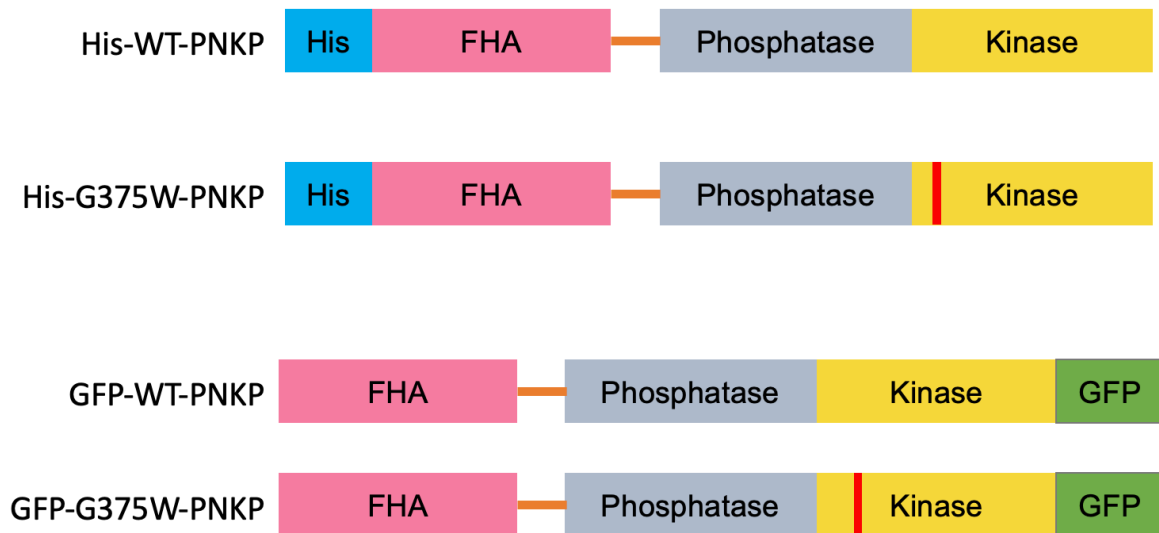
Figure 3.2 The structures of wild-type and mutant PNKP constructs.

All constructs are designed to monitor the effects of the G375W-PNKP mutations found in the AOA4 patients. FHA represents the forkhead-associated domain of PNKP, GFP represents the green fluorescent protein tag. The red line represents the location of the mutation site.

3.2.2 Expression and purification of mutant PNKPs

The PNKP wild-type and PNKP-G375W bacterial expression plasmids were transfected into *E. coli* bacterial strain BL21 (DE3) (NEB). The bacteria were grown at 37°C in 4 L of lysogeny broth (LB) medium containing ampicillin (50 µg/mL) to reach an OD_{600} of 0.6. Protein expression was then induced at 18°C with overnight incubation in the presence of 100 µM isopropyl-β-D-1-thiogalactopyranoside (IPTG, Sigma, St. Louis, MO). The bacteria were then harvested by centrifugation at 10000g for 10 min at 4°C and resuspended in 50 mL of lysis buffer (150 mM NaCl, 50 mM Tris-HCl, pH 8.0, 1 mM ethylenediaminetetraacetic acid (EDTA), 0.1 % β-mercaptoethanol, 0.5 mM phenylmethylsulfonyl fluoride (PMSF), 0.5mg/mL lysozyme. The bacteria were then disrupted by sonication after stirring on ice for 30 min. The soluble fraction was separated by centrifugation at 15000g for 30 min at 4°C.

The 10% polyethylenimine was added dropwise to the soluble fraction to a final concentration of 0.3 % to precipitate nucleic acids. The sample was then stirred on ice for 20 min and centrifuged at 15000g for 20 min at 4°C. Protein in the supernatant was precipitated by a final concentration of 50% ammonium sulfate and centrifuged at 15000g for 30 min at 4°C. The protein pellet was resuspended in solution and purified through three different columns as described before (220): HiPrep 16/10 Butyl FF column (Amersham Pharmacia BioTech, Baie d'Urfe, PQ), SP Sepharose Fast Flow cation-exchange column (Amersham Pharmacia BioTech) and HiLoad 16/60 Superdex 75 gel

filtration column (Amersham Pharmacia BioTech). The purity and integrity of the protein were confirmed by Coomassie Brilliant Blue staining (**Fig. 3.3**).

3.2.3 PNKP Kinase Assays

After obtaining the purified wild-type and mutant PNKPs, the 5'-kinase activities of the PNKP proteins were measured by a kinase assay modified from procedures described before (95). Briefly, PNKP (500 ng) was added to a reaction mixture (40 µL total volume) containing kinase buffer (80 mM succinic acid, 10 mM $MgCl_2$ and 1 mM DTT, pH5.5), 0.5 mM 24-mer oligonucleotide substrate (5'-GGCGCCCACCACCACTAGCTGGCC-3') with 5'-OH termini, 5 mM unlabeled ATP and 5 µCi of [γ-^{32}P] ATP (3000 Ci/mmol, Amersham Pharmacia Biotech). The reaction mixture was incubated at 37ºC for 0.5, 1, 2, 5, 10 and 20 min. 5 µL of the sample was mixed with 2.5 µL of 3 X sequencing gel loading dye (Fisher Scientific, MA, USA) and frozen immediately in dry ice to stop the reaction. The samples were then run on a 12% polyacrylamide gel containing 7 M urea at 200 V for 30 min. The gel was scanned on a Typhoon 9400 Variable mode imager (GE Healthcare Life Sciences, IL, USA) and quantified using ImageQuant 5.2 (GE Healthcare Life Sciences, IL, USA).

3.2.4 PNKP Phosphatase Assays

The 3'-phosphatase activities of PNKP proteins were measured by a phosphatase assay modified from previous studies (100, 222). Briefly, PNKP (50 ng) was added to a reaction mixture (20 µL of total volume) containing phosphatase buffer (70 mM Tris-HCl, 10 mM
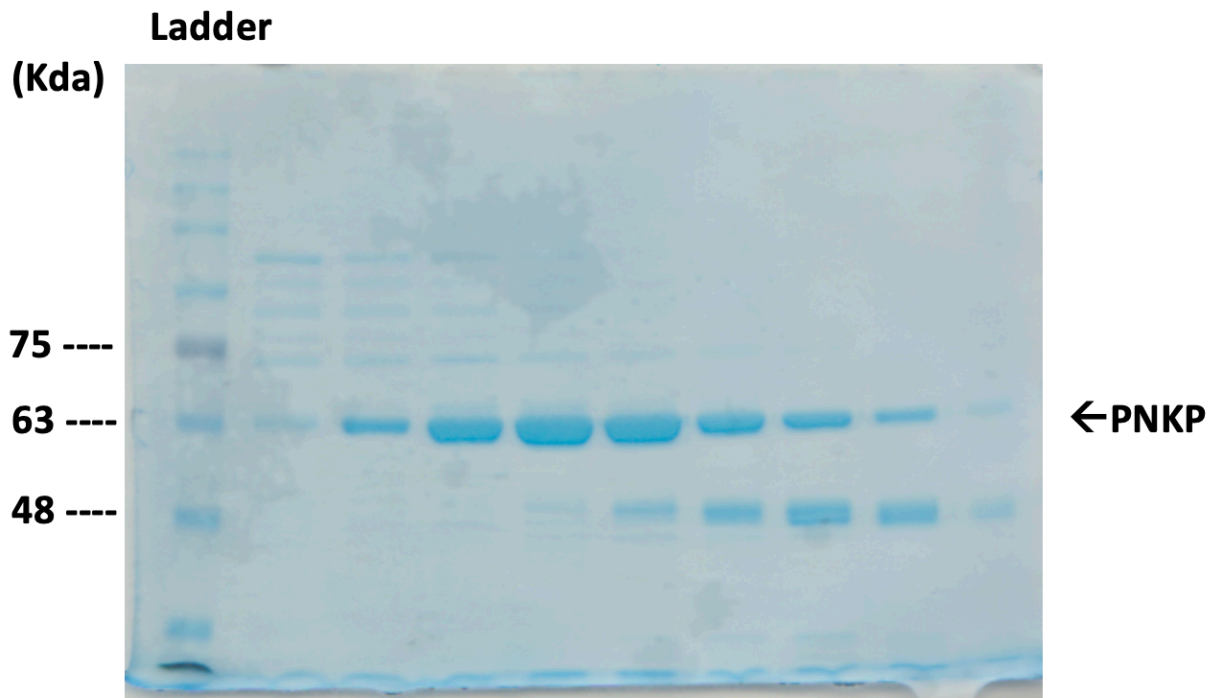
Figure 3.3 Coomassie Brilliant Blue staining of purified protein fractions post gel filtration.

The size of Purified PNKP is marked in the arrow.

MgCl$_2$, 5 mM DTT, pH 7.6), 4 µM 24-mer oligonucleotide substrate (5'-GGCGCCCACCACCACTAGCTGGCC-3') bearing a fluorescein moiety (FAM) at the 5'-terminus and a phosphate at the 3'-terminus (IDT, IA, USA). The reaction was carried out at 37ºC for 0.5, 1, 2, 5 and 10 min. 3 µL of the sample was mixed with 1.5 µL of 3 X sequencing gel loading dye, frozen on dry ice to stop the reaction, then run on a 12% polyacrylamide gel containing 7 M urea at 1800 V for 3 hours. The gel was then scanned on a Typhoon 9400 Variable mode imager and quantified using ImageQuant 5.2.

3.2.5 Steady state fluorescence spectra

Steady-state fluorescence spectra were measured at 25ºC on a PerkinElmer Life Sciences LS-55 spectrofluorometer with 5 nm spectral resolution for excitation and emission using purified wild-type PNKP and G375W-PNKP as described in our previous studies (250). Protein fluorescence was excited at 295 nm, and fluorescence emission spectra were recorded in the 300-400 nm range. To study the ATP binding affinity, 0.1 µM purified protein was monitored first in the buffer (50 mM Tris, pH 7.5, 100 mM NaCl, 5 mM MgCl$_2$, and 1 mM DTT), and ATP (Sigma, MO, USA) was then added into the reaction mixture at a 1:1 molar ratio. The fluorescence emission spectra were recorded in the 300-400nm range. Changes in fluorescence were usually monitored at the emission maximum (340nm). To study the ssDNA binding affinity, 0.4 µM purified protein was titrated against increasing concentrations of 20-mer oligonucleotide substrate (5'-ATTACGAATGCCCACACCGC-3') (IDT, IA, USA) in the buffer (50 mM Tris, pH 7.5, 100 mM NaCl, 5 mM MgCl$_2$, and 1 mM DTT). Fraction of bound (i.e., relative fluorescence

quenching) versus free oligonucleotide concentration was plotted, and the K_d value determined as previously described (220).

3.2.6 Circular Dichroism Spectroscopy

Far-UV circular dichroism (CD) measurements were performed with an Olis DSM 17 CD spectropolarimeter (Bogart, GA, USA), calibrated with a 0.06% solution of ammonium *d*-camphor-10-sulfonate. The temperature in the sample chamber was maintained at 20°C. The CD spectra of wild-type and G375W-PNKP were measured as described previously (223) and the results were analyzed according to the method of Chen et al.(224)

3.2.7 Cell culture

Human HeLa cells were obtained from Dr. David Murray (University of Alberta) and validated by ATCC cell line authentication service using short tandem repeat (STR) analysis. Cells were cultured in Dulbecco's modified Eagle's medium (DMEM)-F12 media supplemented with 5% fetal calf serum and 2 mM L-glutamine, incubated at 37ºC under 5% CO_2 in a humidified incubator. All culture supplies were purchased from Invitrogen/ThermoFisher Scientific, MA, USA.

3.2.8 Western-Blotting

Western blot was performed following a standard protocol with modifications (251). Antibodies used included PNKP antibody (sc-365724, Santa Cruz Biotech, TX, USA), GFP antibody (ab290, Abcam, UK), beta-actin antibody (sc-47778, Santa Cruz Biotech, TX, USA), IR dye 800CW goat anti-mouse secondary antibody (926-32210, Li-COR Biosciences, NE, USA) and IR dye 800CW goat anti-rabbit secondary antibody (926-32211, Li-COR Biosciences). Results were visualized using an Odyssey Fc Imaging System (Li-Cor Biosciences).

3.2.9 Stably transfected cells

To exclude the possible influence from endogenous wild-type PNKP in HeLa cells, CRISPR-Cas9-generated HeLa PNKP$^{-/-}$ cells (225) were complemented with the wild-type and mutant proteins. The HeLa PNKP$^{-/-}$ cells were plated in 60-mm dishes and transfected with the plasmid constructs carrying the cDNA for the wild-type and mutant proteins using Turbofectin 8.0 (OriGene, Rockville, MD) following the manufacturer's protocol. 24 hours after transfection, cells were trypsinized and passaged at a 1:10 dilution in selective medium containing 800 μg/ml G418 (Thermo Fisher Scientific, MA, USA). After expansion in the selective medium for one week, GFP-positive cells were selected through fluorescence-activated cell sorting (FACS) (BD BioSciences, NJ, USA). The positive cells were then expanded again in selective medium with 800 μg/ml G418.

3.2.10 Cellular localization of PNKP

For image acquisition, cells were plated on coverslips and fixed with 4% formaldehyde the next day. Immunofluorescence staining with Tubulin antibody (sc-53646, Santa Cruz Biotech, TX, USA) was performed to distinguish the cytoplasm. Nuclei were stained with DAPI (MilliporeSigma, MA, USA). Cells were then placed on the stage of a Zeiss confocal LSM 710 microscope (ZEISS, Germany). Images were acquired using 40X/1.3 NA oil immersion objective.

3.2.11 Cell viability measurement

Cell viability was measured by a crystal violet staining assay. The experiment was performed as described (252) with minor modifications. Briefly, 1×10^4 cells were seeded in a 96-well plate, and incubated for 24 hours to enable adhesion. For radiation treatment, cells were exposed to 5, 10, or 15 Gy γ radiation, and then incubated for 24 hours, washed and stained cells with 0.5% crystal violet staining solution on a bench rocker. After 20 min, the plates were washed and air-dried. Methanol (200 µl) was then added to each well and left for 20 min at room temperature before measuring the optical density of each well at 570 nm (OD_{570}) with a FLUOstar Omega microplate reader (BMG Labtech, Germany). The average OD_{570} of the wells without cells was set as background and subtracted from each well. The mean OD_{570} of unirradiated cells was normalized to 100% for comparison to the irradiated cells. Paraquat treatment was performed with a similar protocol employing paraquat doses based on previous publications (253, 254). Cells were treated with 100, 200, 400 µM paraquat dichloride for 24 hours before staining. In both radiation

and paraquat treatment, cells were treated in quintuplicate in each group in each experiment, and the experiment was performed three times independently.

3.2.12 Assessment of mitochondria morphology

Cells were plated in 35-mm glass-bottom dishes. After 24 hours, cells were treated with or without 400 µM paraquat dichloride for 12 hours. After the treatment, cells were washed with standard medium and stained with Mitotracker Red and Hoechst 33258 (Sigma, MO, USA) followed by the manufacturer's protocol. Cells were then placed on the stage of the Zeiss confocal LSM 710 microscope. Images were acquired using 40X/1.3 NA oil immersion objective. On the basis of previously published criteria (255), mitochondrial morphology was scored as either normal, i.e. longer than 5 µm, filamentous with network formation, or fragmented, i.e. shorter than 1 µm, rounded, without fusion to other mitochondria. At least 250 cells were counted in each group.

3.3 Results

3.3.1 The G375W PNKP mutant lacks kinase activity and has a weaker ATP binding affinity

As shown in **Fig. 3.4**, the G375W mutation effectively eliminates the PNKP kinase activity, but has only a marginal effect on the phosphatase activity compared to wild-type PNKP. Since G375 is a highly conserved residue within the ATP binding site of PNKP (249), we next examined the binding affinity between G375W-PNKP and ATP. Steady-state

Kinase Assay
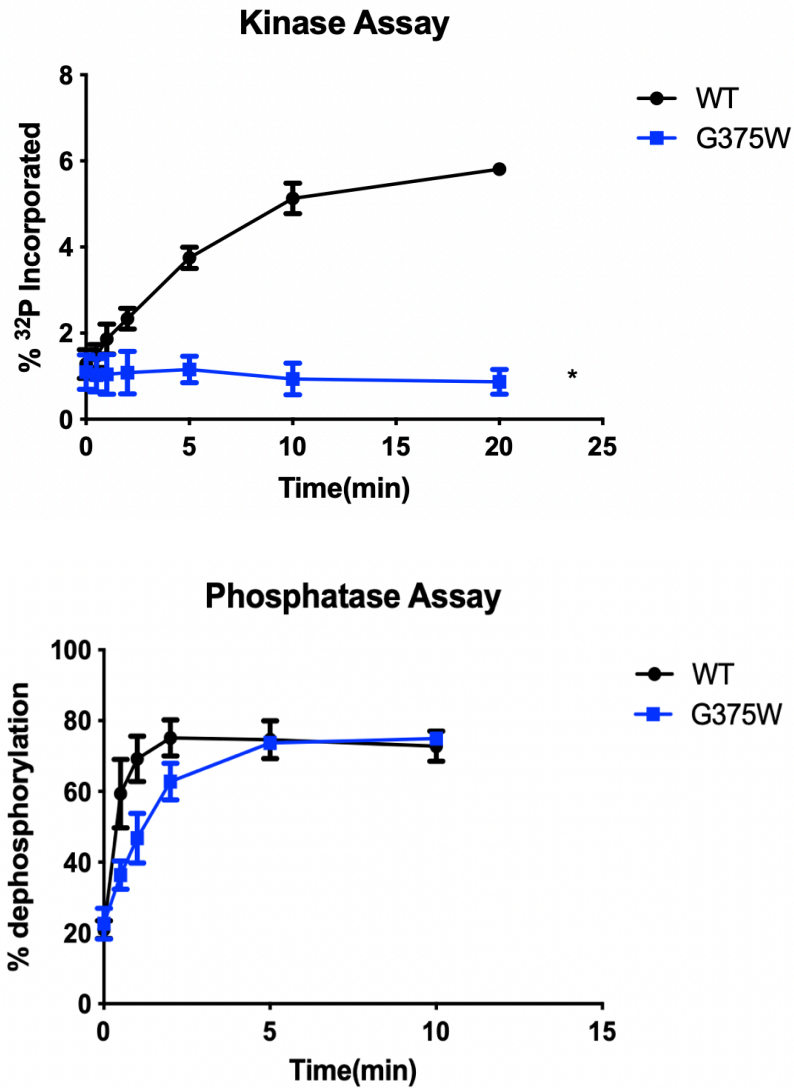
Phosphatase Assay

Figure 3.4 Enzymatic activities of wild-type and mutant PNKPs.

Measurement of 5'-kinase activities and 3'-phosphatase activities of wild-type and mutant PNKPs. Data are the mean $\pm$ SEM of three independent experiments. T tests were performed using GraphPad Prism 7.0, GraphPad Software. *$P<0.05$.

fluorescence was used to monitor quenching of intrinsic fluorescence of the protein (resulting from excitation of the tryptophan at 295 nm) in the presence of ATP (220). As shown in **Fig. 3.5**, in the absence of ATP, wild-type PNKP displayed an emission maximum around 340 nm, similar to what we observed before (220). When ATP was added into the mixture, the fluorescence was quenched due to a binding-induced conformational change. Although it contains an additional tryptophan residue, G375W-PNKP exhibits a similar emission spectrum with a maximum of around 340 nm. In contrast, adding ATP to G375W-PNKP did not change the spectrum significantly, indicating that the binding affinity between ATP and G375W-PNKP is greatly reduced compared to the affinity between ATP and wild-type PNKP.

3.3.2 G375W-PNKP did not affect the direct binding to oligonucleotide

To rule out the possibility that the loss of kinase activity was due to a failure of the G375W mutant to bind to the substrate, we examined the binding affinity between PNKP and a single-stranded nonphosphorylated oligonucleotide by steady state fluorescence. The maximum quenching of fluorescence intensity was taken as 1, and the observed quenching at different concentrations of the oligonucleotide was plotted as the fraction of bound versus ssDNA concentration. As shown in the **Fig. 3.6**, the fraction bound between ssDNA and PNKP is similar between the wild-type and G375W proteins. Nonlinear regression analysis of the binding data revealed a K_d value of 340 ± 10 nM for wild-type PNKP and 390 ± 10 nM for G375W-PNKP. In order to evaluate the protein structural changes, far-UV-CD spectra of wild-type and G375W PNKP were generated. However,
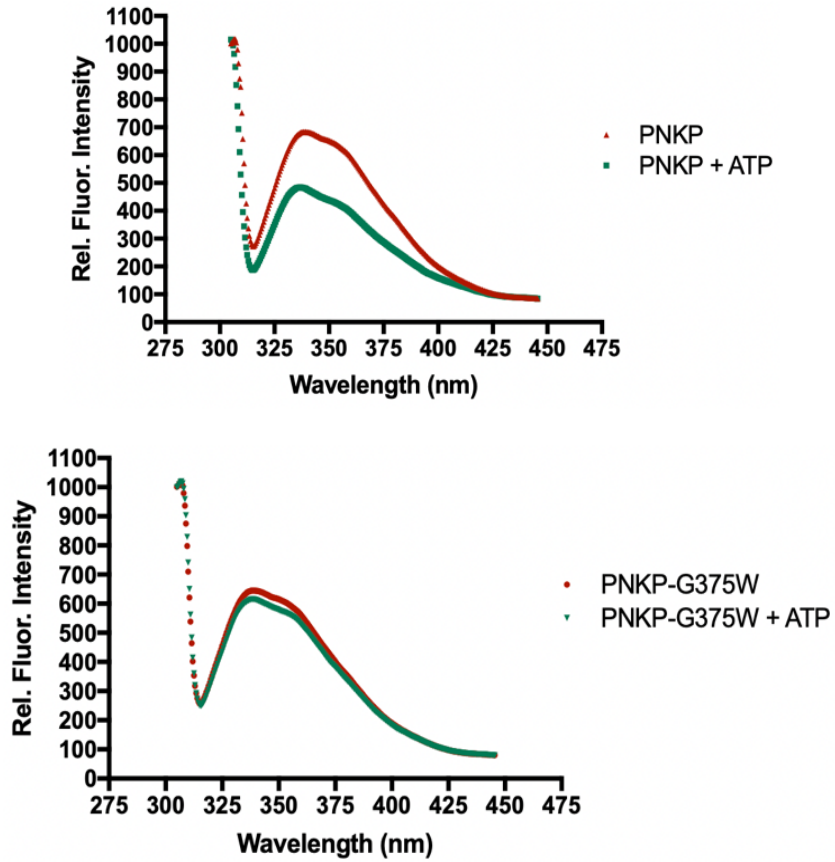
Figure 3.5 Fluorescence emission spectra.

The fluorescence emission spectra of ▲ wild-type PNKP ■ wild-type PNKP + ATP●G375W-PNKP ▼ G375W-PNKP + ATP. The excitation wavelength was 295nm.
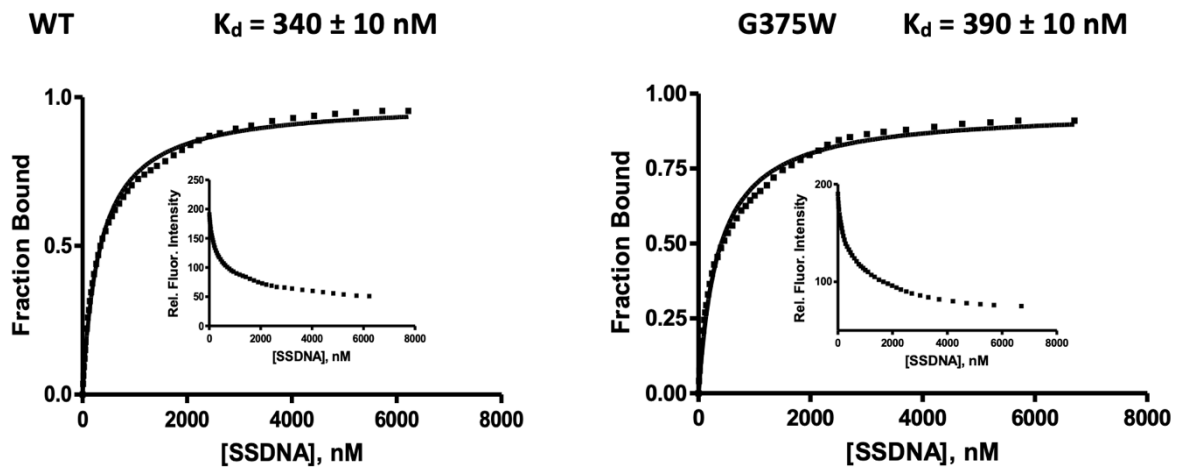
Figure 3.6 Fluorescence titration of PNKPs versus oligonucleotide.

The excitation wavelength of PNKPs was 295nm, intensities were monitored at 340nm.
The fraction bound versus ssDNA concentration is plotted.

circular dichroism did not reveal a gross deformation caused by the T323M mutation, as shown in **Fig. 3.7**.

3.3.3 G375W-PNKP has the same subcellular localization as the wild-type protein

After establishing the stably transfected cell lines, western blotting (**Fig. 3.8**) revealed the stable expression of GFP-tagged PNKP without significant degradation with similar expression levels between wild-type and G375W PNKP. Immunofluorescence also confirmed that both the GFP-tagged wild-type and G375W PNKP retained the same predominantly nuclear localization (**Fig. 3.8)**.

3.3.4 G375W-PNKP partially rescues radiation sensitivity but increases paraquat sensitivity

As shown in **Fig. 3.9**, compared to untransfected wild-type HeLa cells, the PNKP knockout cells showed elevated sensitivity to γ radiation, similar to previous reports with other cell lines with depleted levels of PNKP (222, 256). Complementation of the knockout cells with wild-type PNKP restored most of the resistance to the radiation. Interestingly, the G375W-PNKP transfected cells showed a similar response to the those complemented with the wild-type protein.

While ionizing radiation is deemed to exert its effects by damaging DNA in the nucleus, paraquat is considered to be more effective at targeting mitochondrial DNA through its
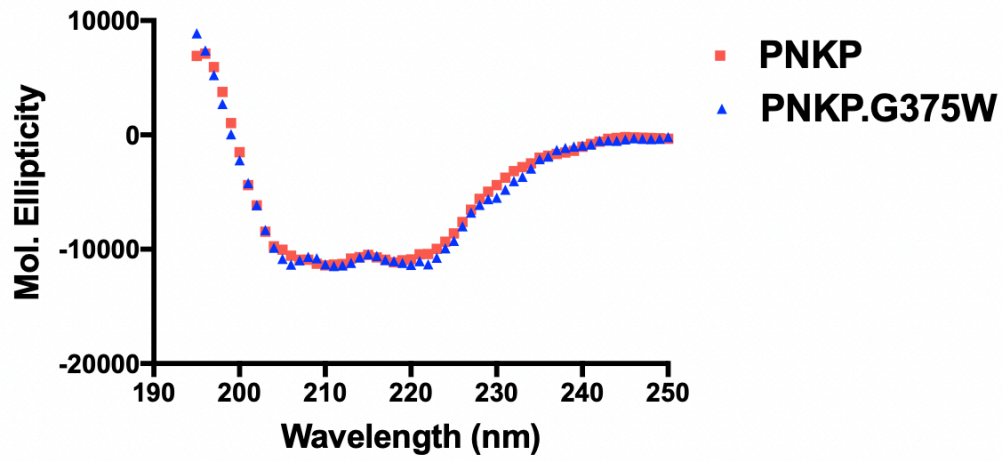
Figure 3.7 Far-UV-CD spectra of wild-type and G375W PNKP.

The concentration of PNKP was 0.5 mg/ml dissolved in 50 mM Tris, pH 7.5, 100 mM NaCl and 1 mM DTT.
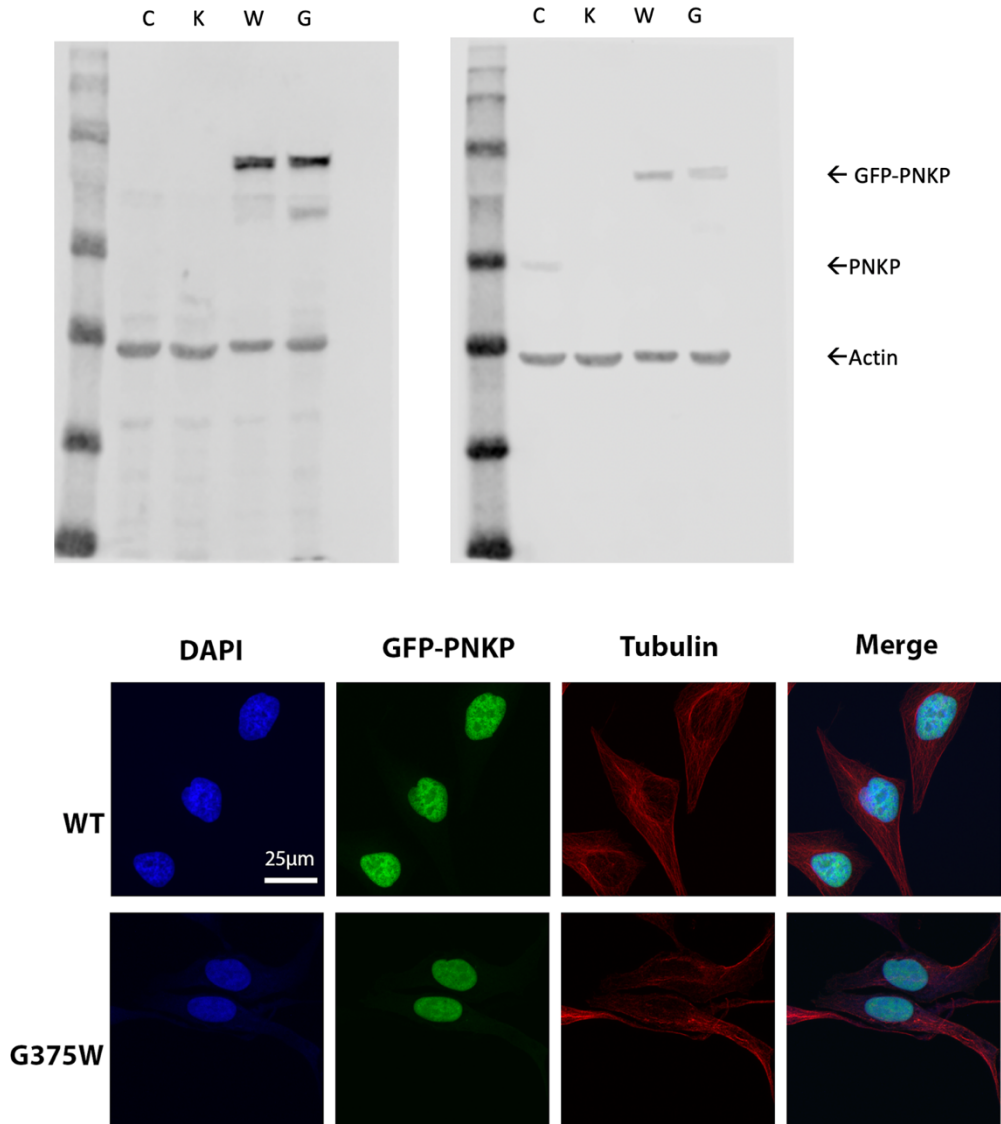
Figure 3.8 Cellular localization of mutant PNKP.

Top: Western blot of cell extract from HeLa wild-type cells (C), HeLa PNKP-/- cells (K), HeLa PNKP-/- cells re-expressing WT-PNKP (W) and HeLa PNKP-/- cells expressing G375W-PNKP (G). The blot top left was probed with PNKP antibody, while the blot top right was probed with GFP antibody. Bottom: Subcellular localization of PNKP in HeLa PNKP-/- cells stably expressing GFP-tagged wild-type (WT) or G375W protein. PNKP tagged constructs (green), tubulin immunofluorescence (red) indicates the cytoplasm, DAPI staining (blue) indicates the nuclei.
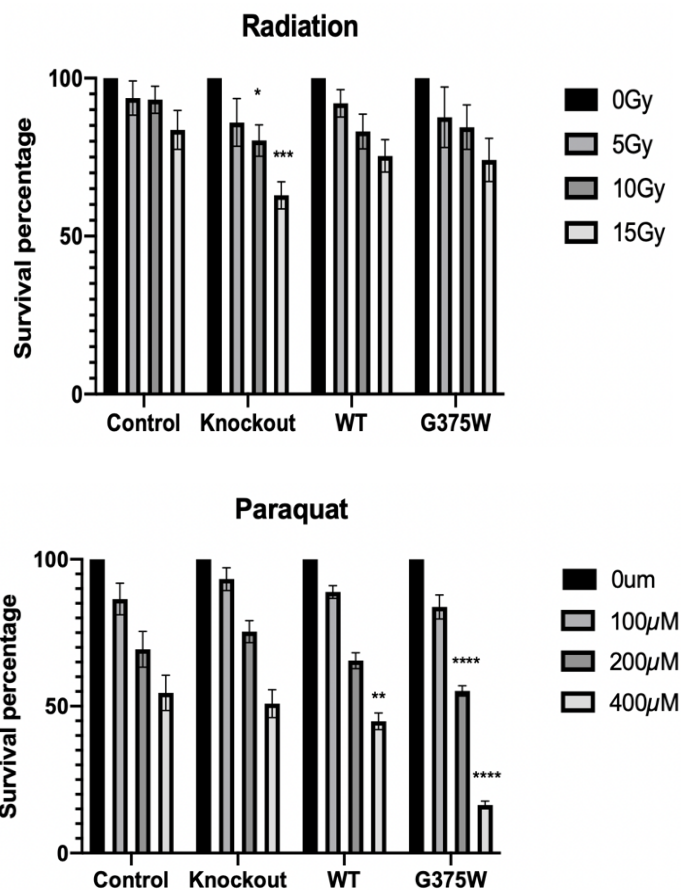
Figure 3.9 Viability assays of different cell lines.

Top: Viability measurement of cells after irradiation based on crystal violet staining assay. Bottom: Viability measurement of cells after treatment with paraquat. Control represents HeLa wild-type cells. Knockout represents HeLa PNKP-/- cells. WT represents HeLa PNKP-/- + WT-PNKP. G375W represents HeLa PNKP-/- + G375W-PNKP. Plots represent mean ± SD. Ordinary one-way ANOVA was performed to compare each cell line with the wild-type HeLa (Control) at the same treatment dosage by using GraphPad Prism 7.0, GraphPad Software. P*<0.05, P***<0.001.

stimulation of production of superoxide within mitochondria (257, 258). Since PNKP is localized in mitochondria as well as nuclei, we examined the influence of the G375W mutation in the response to cellular exposure to increasing concentrations of paraquat.

In contrast to the response seen following irradiation, the cells expressing G375W PNKP displayed a marked sensitivity to 24-hour exposure to paraquat (**Fig. 3.9**). Surprisingly, there was no significant difference in this short term assay between the wild-type and knockout cells over the concentration range analyzed.

3.3.5 Mitochondria are more sensitive to paraquat treatment in G375W cell lines

Paraquat has been shown to alter the mitochondrial membrane permeability inducing mitochondrial dysfunction (259). We, therefore, further examined the mitochondrial morphology in the mutant cells. As shown in **Fig. 3.10**, all untreated HeLa cells display typical mitochondrial filamentous networks, while paraquat treatment induces significant mitochondrial fragmentation in a subset of cells manifesting as small (≤ 1 μm) rounded independent bodies. Quantification of the data obtained from untreated cells and cells treated with 400 μM paraquat for 12 hours (**Table 3.1)**, indicated that with no treatment, all four cell lines, including those expressing G375W PNKP, showed similar mitochondrial morphology without fragmented mitochondria. However, after exposure to paraquat, significantly more cells expressing G375W PNKP showed increased fragmented mitochondria than cells expressing wild-type PNKP or the PNKP-knockout cells.
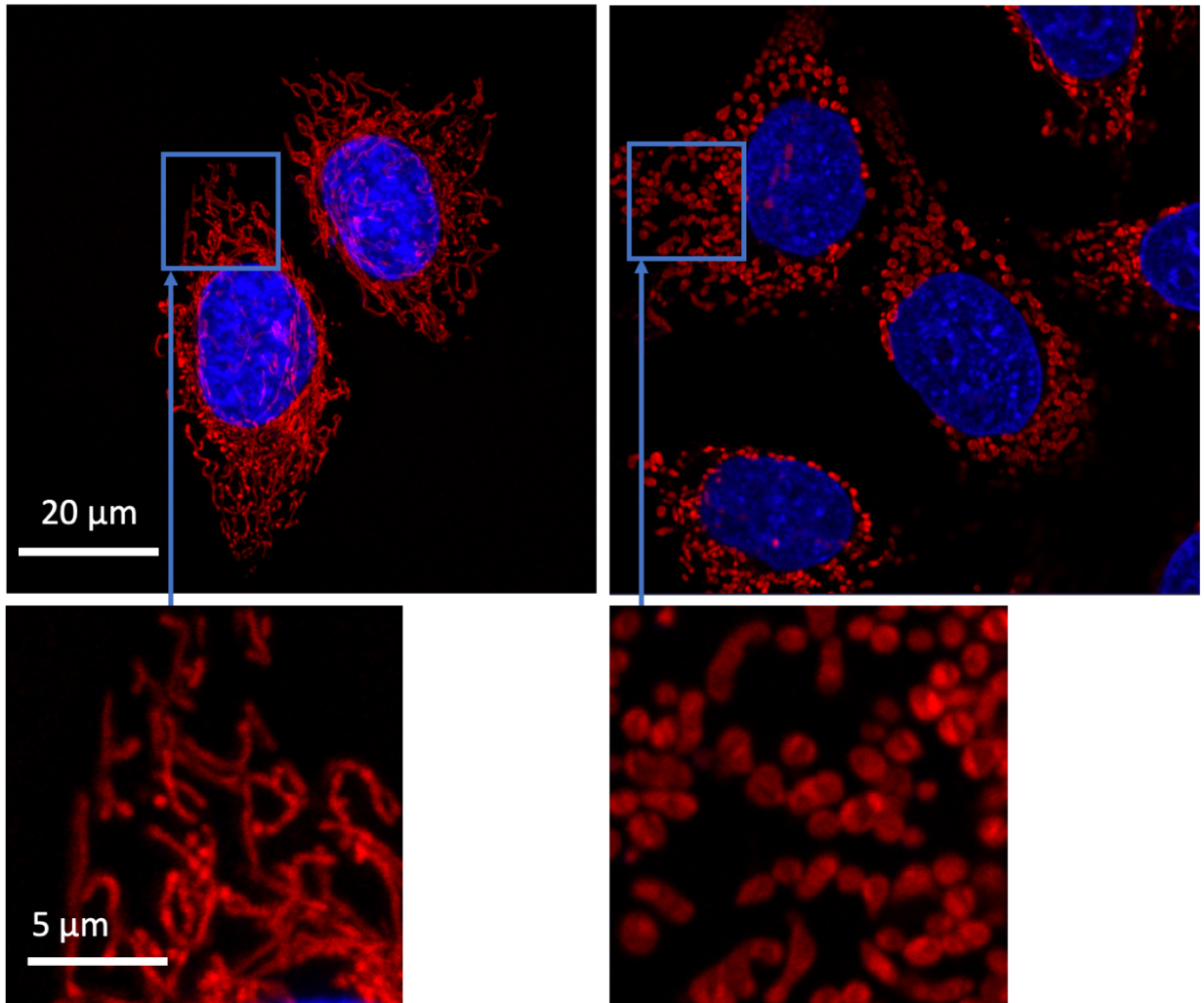
Figure 3.10 Abnormal mitochondria in mutant cell lines after paraquat treatment.
Left: HeLa cells with no treatment, mitochondria show normal morphology status. Right:
Paraquat-treated HeLa cells show fragmented mitochondria. Lower panel are magnified
area of blue box from Upper panel.

Table 3.1 Mitochondria morphology assessment.

	No treatment			PQ-400 µM-12h		
	Numbers of cells with Fragmented Mt	Total cell number	Mt Fragmentation %	Numbers of cells with Fragmented Mt	Total cell number	Mt Fragmentation %
HeLa Wild-type	0	398	0	10	528	1.89
HeLa PNKP-/-	0	416	0	9	316	2.85
HeLa PNKP-/- + WT-PNKP	0	281	0	3	279	1.08
HeLa PNKP-/- + G375W-PNKP	0	314	0	65	418	15.55

Table 3.1 Mitochondria morphology assessment. Mitochondria morphology assessment of cells with/without paraquat treatment. At least 250 cells were counted in each group. On the basis of previously published criteria (255), normal mitochondria are characterized as longer than 5 µm, filamentous with network formation, fragmented mitochondria are characterized as shorter than 1 µm, rounded, without fusion to other mitochondria.

3.4 Discussion

To date studies of the biochemical consequences of mutant PNKPs found in patients, including those with MCSZ, AOA4, and CMT2B2, have been limited. Two previously tested mutations in the PNKP kinase domain (T424GfsX48 and Exon 15 del) both showed near-normal phosphatase activities and significantly reduced kinase activities (218). Considering the dramatic structural changes caused by these frameshift and deletion mutations such results are not surprising. Our results, however, indicate that even a point mutation in a specific location could cause similar biochemical consequences.

Located at the C terminus of PNKP, the kinase domain consists of five β sheets, seven α helices, and one 3_{10} helix (249). The crystal structure of murine PNKP (249) revealed D396 (D397 in human PNKP) as the catalytic site of the kinase domain (F341 to E522 human PNKP). The ATP binding site is located around this catalytic site, containing the conserved Walker A motif (G372 to S379 in human PNKP) and Walker B motif (centered around D422 in human PNKP) (**Fig. 3.11**).

Any alterations in those conserved functional domains are likely to affect the kinase activity. G375 is located within the Walker A box, in particular the P loop nest in which it is the first glycine in the GAGK sequence. The nest forms a cavity that binds, via inward facing amino groups, to the β- and/or γ-phosphates of ATP (260). This cavity would clearly be disrupted by the exchange of glycine for a bulky tryptophan residue, and hence it is not surprising that binding of ATP and kinase activity is almost completely abolished in

```
H    341  FDPRTVSRSGPLCLPESRALLSASPEVVVAVGFPGAGKST  380
M    340  FDPRTISSAGPLYLPESSSLLSPNPEVVVAVGFPGAGKST  379

H    381  FLKKHLVSAGYVHVNRDTLGSWQRCVTTCETALKQGKRVA  420
M    380  FIQEHLVSAGYVHVNRDTLGSWQRCVSSCQAALRQGKRVV  419

H    421  IDNTNPDAASRARYVQCARAAGVPCRCFLFTATLEQARHN  460
M    420  IDNTNPDVPSRARYIQCAKDAGVPCRCFNFCATIEQARHN  459

H    461  NRFREMTDSSHIPVSDMVMYGYRKQFEAPTLAEGFSAILE  500
M    460  NRFREMTDPSHAPVSDMVMFSYRKQFEPPTLAEGFLEILE  499

H    501  IPFRL--WVEPRLGRLYCQFSEG  521
M    500  IPFRLQEHLDPALQRLYRQFSEG  522
```

Figure 3.11 Sequence comparison between human and mouse PNKP.

Sequence comparison of the kinase domain of human (H) PNKP and mouse (M) PNKP. The conserved region is marked in yellow. The catalytic site is marked with a red rectangle, ATP binding sites are marked with blue rectangles. Blue arrow points at G375.

the G375W mutant PNKP (**Fig. 3.4 and Fig. 3.5**). In contrast, the binding affinity between G375W-PNKP and DNA substrate is similar to wild-type (**Fig. 3.6**). PNKP contains a bipartite DNA-binding surface within its kinase domain: surface 1 (contains R396, R404, and R433) and surface 2 (R483 and K484) (261). Since the G375W mutation did not affect the binding to DNA, it suggests that this mutation does not cause a gross conformational change to the protein kinase domain, as confirmed by structural analysis (**Fig. 3.7**). The unchanged gross structure is also supported by the normal phosphatase activity displayed by the G375W mutant (**Fig. 3.4**), despite the fact that due to the intimate association between the kinase and phosphatase domains (249), mutations in either domain can sometimes affect the other domain (218, 262).

After exposure to γ radiation, the cells expressing the G375W-PNKP mutant exhibited a similar survival rate compared to the wild-type cells or wild-type PNKP transfected cells, while the survival rate of the PNKP knockout cells was significantly reduced. This speaks to the issue of the relative importance of the nature of the 5' and 3'-termini generated by ionizing radiation, as well as the possible existence of back up enzymes/pathways in the absence of PNKP enzymatic activity. It is clear that the vast majority of radiation-induced 3'-strand-break termini possess either phosphoglycolate and phosphate residues (236), which are removed by PNKP phosphatase activity, with or without the assistance of TDP1, respectively (105). In contrast, <15% percent of radiation-induced 5'-strand-break ends lack a 5'-phosphate group (263, 264) and so the requirement for a 5'-kinase is much more limited. A second possible explanation for the absence of a radiosensitive phenotype for the G375W- PNKP expressing cells could be the action of backup DNA kinases or an

alternative pathway. Two potential alternatives to PNKP have been reported. The first is a Polymin P-precipitable polynucleotide kinase that can phosphorylate DNA and RNA but lacks phosphatase activity (265), and the second is BCL-3-binding protein (B3BP) (266). An alternative pathway may require removal of the 5'-terminal nucleoside (or a short patch) followed by gap filling DNA synthesis after ligation.

The G375W mutation has only been associated with AOA4 and not the more serious MSCZ condition. Since the major defect in the mutated protein is the loss of kinase activity, our data support the proposal by Kalasova et al., based on a study of cells derived from patients with a 17 bp duplication in the kinase domain of PNKP (c.1250_1266dup), that AOA4 is primarily associated with loss of PNKP 5'-kinase rather than 3'-phosphatase activity (262). Also, in agreement with Kalasova et al. we did not observe that loss of 5'-kinase activity significantly increased the radiosensitivity of the cells.

There has been continuing debate concerning the role of mitochondrial dysfunction in neurological disorders. Indeed, Bermúdez-Guzmán and Leal recently speculated on a mitochondrial role for the PNKP-associated neurological diseases (267) because of PNKP's involvement in mitochondrial DNA repair. As a result, we wanted to assess the consequences of the G375W mutation in response to a neurotoxin that acts on the mitochondria and through the production of reactive oxygen species (268, 269). In recent years, paraquat has become a popular tool for studying neurodegenerative disorders such as Parkinson's disease (270, 271). Paraquat induced cell death has been reported in several studies and several mechanisms have been identified including increased ROS

production (272), decreased mitochondrial membrane potential, and release of cytochrome C (273), all of which are focused on the effects of mitochondrial functions. The dramatic structural changes of mitochondria from the typical tubular shape to spheroid shape have been observed under different circumstances, including exposure to osmotic stress reagents, such as the mitochondrial K^+/H^+ exchange inhibitor (274), and agents such as rotenone and antimycin that that interfere with the electron transport chain and stimulate ROS production (275). Paraquat has been shown to induce mitochondrial fragmentation, which could be relieved by antioxidants, indicating that oxidative stress triggers mitochondria fragmentation (276). Several recent studies have highlighted the fragmentation of mitochondria in neurodegenerative diseases. Electron microscopy analyses of patients with Alzheimer's disease have shown reduced sizes of mitochondria and disruption of the cristae (277, 278). A study of animal models of familial Alzheimer's disease and patients of Alzheimer's disease also noticed the transformation of mitochondrial morphology: The uniformly elongated mitochondria network changed into tear dropped mitochondria or tear dropped mitochondria connected by a thin double membrane (279). Silencing of Parkinson disease-related protein (PINK1) significantly increased the number of cells with truncated or fragmented mitochondrial morphology (280). Similar observations have also been reported in the studies of amyotrophic lateral sclerosis (281) and spinocerebellar ataxia type 3 (282).

We observed paraquat treatment to be more deleterious to the cells expressing the G375-PNKP mutant protein than to wild-type cells or knock-out cells expressing wild-type PNKP, both in terms of short term toxicity and mitochondrial fragmentation, suggesting that

AOA4 may be more susceptible to damage to mitochondrial DNA and loss of mitochondrial integrity. Unexpectedly, the PNKP-knockout cells exhibited a similar response to paraquat as the wild-type cells. One possible explanation is that in the complete absence of mitochondrial PNKP a back-up repair machinery can gain full access to the mitochondrial DNA. This back-up pathway may be prevented from gaining access to the damaged site by the presence of the mutant PNKP, which retains full capacity to bind to 5'-OH termini (**Fig. 3.6**). Such a situation would be further exacerbated in the mitochondria because of the absence of XRCC1 (283), which we have previously found can enhance the displacement of PNKP from DNA (250). In this regard, it is worth noting that a homozygous mutation of human tyrosyl-DNA phosphodiesterase 1 (TDP1) responsible for the related neurodegenerative syndrome, spinocerebellar ataxia with axonal neuropathy (SCAN1) causes the protein to be selectively trapped on mtDNA (284). Furthermore, mutated TDP1 linked to mitochondrial DNA termini that block repair of strand breaks may engender a vicious cycle in which blocking repair could lead to increased ROS production (285).

A further consideration is the potential role of protein-protein interactions involving PNKP. PNKP has been shown to interact with mitofilin, a transmembrane protein of the mitochondria inner membrane (194). One possible benefit from such interaction is bringing PNKP into the mitochondria similar to the interaction between PARP-1 and mitofilin (286). Mitofilin plays a vital role in maintaining mitochondria inner membrane organization and mitochondria protein biogenesis (287). Although the loss of mitofilin does not directly affect mitochondrial fusion and fission, it results in altered cristae

structure (288, 289). Thus, the mutant PNKP may affect the stability of the mitochondrial structure through its interaction with mitofilin or other mitochondrial proteins.

In summary, our data show that G375W, the most common point mutation associated with AOA4, lacks DNA 5'-kinase activity due to decreased ATP binding affinity. Furthermore, we have shown that this mutation renders cells sensitive to paraquat, which disrupts mitochondrial integrity, implicating mitochondrial dysfunction as a contributing factor to the pathology of AOA4.

4 Chapter 4: General Discussion and Future Direction

4.1 Overview

Based on the clinical case of MCSZ with GBM, we assessed two newly discovered PNKP mutations. The two point-mutations corrupt PNKP's function in different ways.

The P101L mutation showed almost normal enzymatic characteristics. However, since the mutation is located in the FHA domain, the binding affinity between PNKP and XRCC4 decreased. In addition, cellular transfection showed a different cellular localization pattern. Software analysis indicated that the cytoplasmic localization of the protein is due to a newly formed NES signal, which was confirmed by inhibition of exportin.

In contrast to P101L, enzymatic activities of T323M revealed a significant reduction in both kinase and phosphatase activities. The biochemical evaluation indicated that reduced activity is driven, at least in part, by decreased DNA substrate binding affinity. In addition, cellular transfection showed T323M increased anchorage-independent transformation.

Further studies of cell lines expressing the mutant *PNKP* cDNAs revealed that both of them displayed inefficient DNA repair. Our functional studies, combined with clinical observation such as the PNKP localization in the patient's sample and the identification of other mutations in the GBM sample, suggested that the combination of the two *PNKP* mutations will impair the DNA damage response and increase the frequency of spontaneous mutations including driver mutations that induce pediatric GBM.

We then broadened our investigation of *PNKP* mutations associated with neurological disorders to examine a frequently observed *PNKP* mutation found in individuals with AOA4, i.e. G375W.

In this case, the major biochemical deficiency was observed to be the loss of DNA kinase activity due to the inability of the protein to bind ATP. When the mutant was protein was expressed in cells, we observed an increased sensitivity towards the neurotoxin paraquat coupled with increased morphology changes to the mitochondria. These observations led us to propose that the G375 mutant PNKP has a deleterious effect on mitochondrial homeostasis.

Due to the rarity of PNKP related diseases, studies on functional analysis of mutant PNKP are limited. The functional studies of our study revealed different types of mechanisms and their consequences, as shown in **Figure 1**. Understanding the biochemical and cellular consequences of the mutations could lead to more targeted treatments in the future. Below I will discuss different aspects in the related areas.
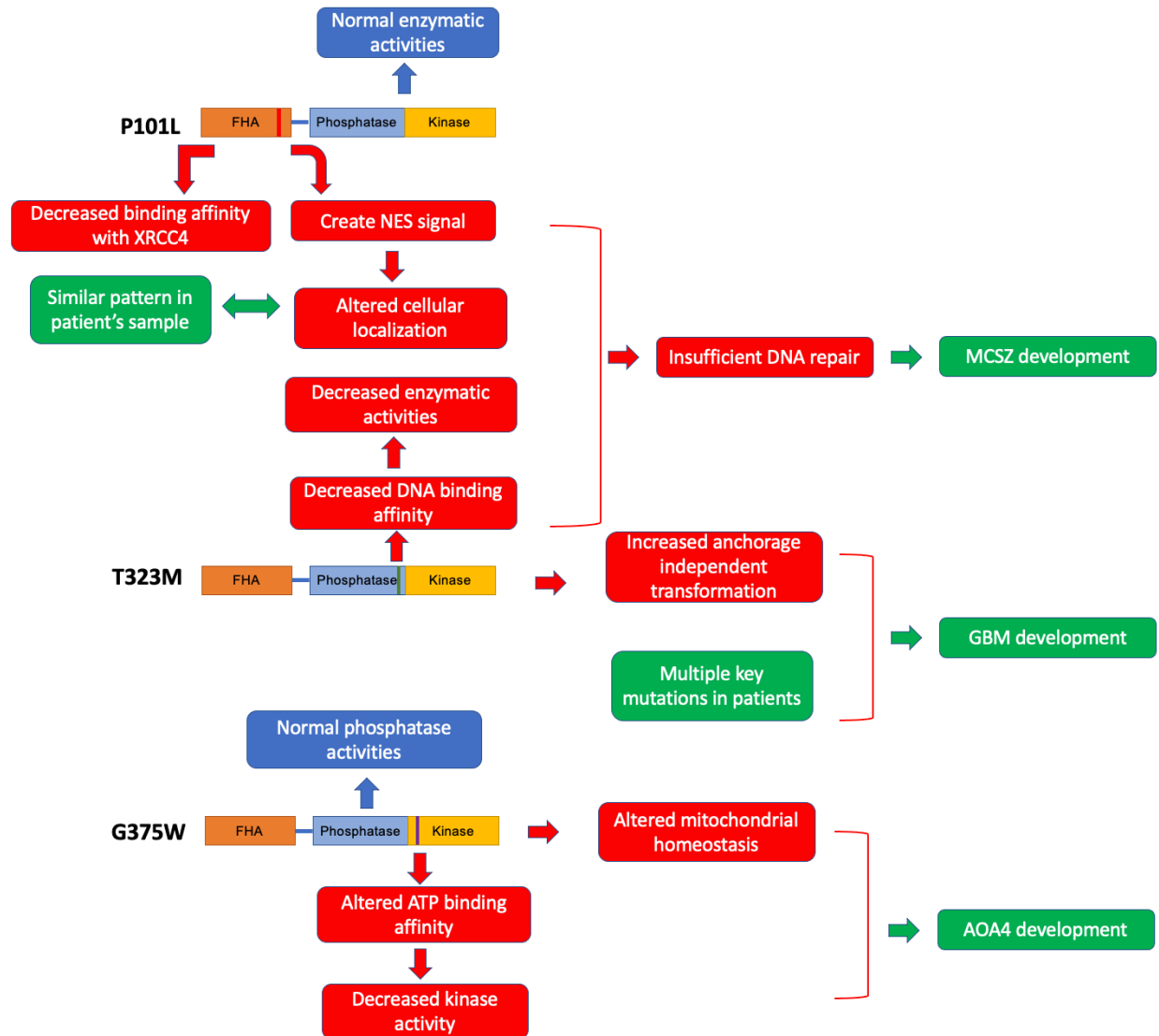
Figure 4.1 The overview of our study on MCSZ and AOA4 mutations.

Red indicates the altered functions, blue indicates the unchanged functions, green indicates clinical observations.

4.2 The complexity between PNKP mutation and phenotype

Single gene disorders such as MCSZ and AOA4 are defined as diseases caused by variants in one specific gene (290). However, it is not a new discovery that different mutations on the same gene could exhibit different phenotypes. Since a particular gene consists of thousands of base pairs that are potential targets for mutation, the phenotype of one single gene disorder could manifest great complexity such as different symptoms, severities, age of onset (291). This is not an uncommon feature of neurological diseases.

Huntington's disease (HD) is an autosomal dominant neurodegenerative disease caused by CAG repeat expansion in the *Huntingtin* (*HTT*) gene (161). Generally, the number of trinucleotide CAG repeats is linked with the severity of the disease. Increased CAG number indicates poor prognosis; while the normal range of CAG repeats is 26 or less (292) for individuals with >40 repeats the disease is fully penetrant (293),. In addition, there is also a strong correlation between age of onset and the length of CAG repeats: when repeats increase from 45 to 60, the age of onset is expected to decrease from 41 to 23 years old (294). Because trinucleotide repeats represent the major mutation form in *HTT*, the phenotype is easy to compare. Other neurological diseases arise from single gene mutations with less predictable phenotypes. For example, the classic form of Ataxia telangiectasia (AT) is induced by two truncating mutations in both alleles, leading to total loss of the ATM protein. However, missense mutations in *ATM* usually lead to milder symptoms as some residual activity of ATM is retained (295). Such complexity increases when more clinical cases and mutation types evolve. Cystic fibrosis (CF) is caused by

mutations in cystic fibrosis transmembrane conductance regulator (*CFTR*) (296). Over 2000 different mutations have been identified in *CFTR* with different disease severity. In order to gain a better understanding between the genotype and phenotype, and provide a better pharmacotherapy solution, the classification of these mutations is based on the consequences of the mutation, such as protein expression level, protein stability, protein interactions, etc. (297). Analysis of different *CFTR* mutations distinguishes them based on their molecular pathology and therefore provides possible drug combinations for treatment, an approach termed "theratyping" (298).

This complexity is pertinent to our study since the mutation map of *PNKP* is expanding with more clinical cases with different severity showing up. It is necessary to assess the mutations' functional and clinical consequences to reveal their therapeutic susceptibility. Although we have only explored a small part of the PNKP mutation map, alterations in protein structure, protein function, and cellular localization have all been observed. These multiple functional changes provide possible etiology for MCSZ and AOA4. A major question is why different PNKP mutants contribute to different symptoms, such as neurodevelopment related ones versus neurodegenerative related ones. One possible reason is related to the enzymatic activities of PNKP, while T323M (MCSZ) affects phosphatase activity more, and G375W (AOA4) only affects kinase activity. A recent study also indicates similar consequences while using MCSZ/AOA4/CMT2B2 patients-derived primary fibroblasts: The phosphatase activity of PNKP is lower in MCSZ cells while its kinase activity is lower in AOA4/CMT2B2 cells (262). To confirm such a theory, a complete enzymatic assessment of all diseases related to PNKP mutants is necessary.

Another raised question is whether there's an overlap between different PNKP related diseases. Indeed, there have been reports that patients displayed mild or unorthodox symptoms of MCSZ (121) or AOA4 (154). There are also cases that displayed both symptoms from MCSZ and AOA4 (120, 215). It is possible that different symptoms are related to different levels of protein functional changes. Our study did show MCSZ-related mutants exhibit more functional alterations than AOA4-related mutant. Other studies also indicate that milder phenotypes are related to less affected PNKP functions (267, 299). However, other possibilities are worthwhile to explore as well, such as changes of related proteins' interactions, or mitochondria functions. We did observe the binding affinity changes between P101L-PNKP and XRCC4 peptide and the altered mitochondria homeostasis in G375W cells. It is necessary to expand these studies to understand the full picture of different phenotypes.

4.3 PNKP mutation and cancer development

The frequency of germline mutations in humans is 1.2×10^{-8} mutations per base pair on average (300). In contrast to germline mutations, somatic mutations constantly accumulate throughout our lifetime. Exogenous factors such as UV light, ionizing radiation, and chemicals, endogenous factors such as reactive oxygen species, endogenous retrotransposons, DNA repair failure can all contribute to this process (1). The somatic mutation frequency is considerably greater than the germline mutation frequency (301). In fact, such differences are even evident in childhood. By using primary dermal

fibroblasts from a 6-year-old male human, the median somatic mutation frequency was found to be ~2.8 × 10^{-7} mutations per base pair (300).

Like all the cells in the human body, cancer cells are also the product of numerous cell divisions and genetic succession. Cancer cells gain their tumorigenic hallmarks through constant somatic mutation and selection (302). Although mutations presumably occur by the same processes, mutation frequencies differ among different cancer types. A study of 27 cancer types showed that the median frequency of mutations varied by more than 1000-fold across cancer types (303). Pediatric cancer types, such as pediatric GBM and medulloblastoma, are among those with the lowest somatic mutation frequency, which means they usually require fewer rounds of mutations to gain certain driver mutation advantages (304). DNA repair failure has been linked with increased mutation frequency (246), and such an observation has been previously found for loss of PNKP as well (222). In addition, PNKP plays a pivotal role in maintaining progenitor neural cells, differentiated neurons, and glial homeostasis (124, 305). It is therefore not surprising that the cancers identified to date in patients carrying *PNKP* mutations were cancers of the central nervous system including a pilocytic astrocytoma in an AOA4 patient (214).

All PNKP mutation-related patients are either homozygotes or compound heterozygotes (96, 109, 120). While both PNKP allele mutations inevitably lead to a more deleterious situation in patients, the risk to patients' parents, who are usually heterozygotes with one wild type PNKP (217), has not been discussed. In families with ataxia-telangiectasia (A-T), which is also an autosomal recessive neurological syndrome like the PNKP-related

diseases, A-T heterozygotes are predisposed to breast cancer (306). In addition, such predisposition to cancer in A-T heterozygotes seems to be site-specific, as the relative risk of other cancer types is not significantly increased (307). Studies also found increased skin cancer risks in heterozygotes of xeroderma pigmentosum families (308), increased melanoma, and other cancer types in heterozygotes of Nijmegen breakage syndrome families (309, 310), both of which are also autosomal recessive diseases. Due to the lack of symptoms, PNKP-heterozygotes (with one wild type allele) are often neglected while they are in fact, a much larger group. It may therefore be worthwhile to look for predisposition to cancer and neurological disorders in MCSZ/AOA4/CMT2B2 families in the future.

While we did observe the increased mutagenesis in T323M cells, it is still unknown what specific kind of mutations could be induced by PNKP mutation. It is worthwhile to assess the genetic background of MCSZ/AOA4/CMT2B2 patients to see if there are any hotspots related to PNKP mutation, and if specific PNKP mutations render a higher mutagenesis rate than other PNKP mutations. The expression of mutant PNKP in WT cells can also be assessed in the cellular transformation to explore the possible effects of PNKP mutations in the heterozygotes population.

4.4 Treatment for monogenic neurological disorders

So far, there is no cure for fetal microcephaly or ataxia with oculomotor apraxia (311, 312), only occupational therapy, cognitive-behavioral therapy, and pain relief to improve quality

of life. However, with the improvement of gene therapy technology, the treatment of monogenic neurological disorders has become possible.

To make the corrected or newly introduced gene continue working, the modified gene has to integrate into the patient's DNA. Right now, gene therapy can proceed via in vivo or ex vivo methods. In vivo gene therapy directly introduces a modified gene into the target region using vectors, while ex vivo gene therapy genetically modifies cells in vitro, which are then implanted into patients (313). One approach to alleviate the consequences of the mutant gene is reducing the mutant gene expression. An animal study on HD mice has shown that delivering shRNA targeting *HTT* mRNA can decrease mutant HTT expression and improve behavior deficits (314). Interestingly, we observed that cells expressing the G375W PNKP mutant found in AOA4 appeared to be more sensitive to paraquat than the knockout cells, i.e. the mutant PNKP was more deleterious than no PNKP. If the response to short term paraquat treatment is reflective of long term oxidative damage (to mitochondria) it suggests that reducing the level of mutant *PNKP* mRNA may hold a potential benefit. Directly targeting the mutant protein is another approach. Mutated cellular surface protein gene, amyloid-beta precursor protein (*APP*) gene increases the production of amyloid beta (Aβ) 42, which contributes to early onset familial AD (315). A study showed that by using an adeno-associated virus (AAV) vaccine that targets Aβ42, the cognitive behavior in APP transgenic mice improved significantly (316). Targeting proteins that interact with the mutant protein could be effective too. Brain-derived neurotrophic factor (BDNF) interacts with HTT, and mutant HTT decreases BDNF

production. A study showed that overexpression of BDNF attenuates the behavioral impairment in toxin-induced HD rats (317).

Although developing rapidly and promisingly, there are still many challenges for gene therapy targeting monogenic neurological disorders. Potential toxic effects related to gene modification, the uncertainty of immune response and durability, accurate delivery, and controlled expression all need to be addressed in future studies (313, 318). Furthermore, since the development of many neurological disorders can take place over decades, the correct time point to intervene also needs to be carefully considered (318).

Instead of targeting the genetic mutation itself, targeting the consequences of mutations could be another beneficial approach to alleviate the symptoms. Vitamin E, as an antioxidant (319) and regulator of mitochondrial superoxide generation (320), has shown protective effects for Parkinson's disease (321). Mitochondrial-targeted antioxidants, such as MitoQ, have also shown neuroprotective effects in a mouse model of traumatic brain injury (322).

4.5 Future directions

Most studies on monogenic neurological disorders have focused on the clinical and hereditary aspects. To date, there are very few publications examining the biochemistry and cellular consequences of *PNKP* mutations (116, 124, 218, 262). Our study expands

the spectrum of MCSZ and AOA4 related *PNKP* mutations and provides possible mechanisms related to enzymatic, structural, and cellular functions.

Previous biochemical studies of PNKP mutations have primarily examined the protein's enzymatic activity (116, 218), but the underlying mechanisms for the reduced enzymatic activity require further exploration. We have addressed this issue in our study, by examining the effects of the mutations on protein structure and interactions with DNA, ATP, and partner proteins. The alterations in the binding affinity between mutant PNKP (T323M) and DNA, mutant PNKP (G375W) and ATP, or mutant PNKP (P101L) and XRCC4 provide possible mechanisms for such enzymatic changes. However, as recent studies of other neurological disorders have pointed out, PNKP's interaction network is much more complicated. For example, Gao et al. (158) found that in Spinocerebellar ataxia type 3 (SCA3) wild type PNKP interacts with mutant ATXN3, resulting in inefficient DNA repair and neuronal death. A similar interaction has also been observed between wild type PNKP and wild type/mutant HTT which promotes the progress of HD (162). To gain a better understanding of mutant *PNKP's* role in neuro-homeostasis and neurotoxicity, we need to establish a complete protein interaction map for PNKP generated by a combination of mass spectrometry and computer-based modeling.

There are also gaps in our study that would benefit from further investigation. For example, cells transiently expressing either of the mutations found in the MCSZ patient displayed lower levels of the protein, particularly the T323M mutant. This is a common feature found with MCSZ-associated PNKP mutations (116, 217), however, the mechanism(s)

responsible for the low levels of PNKP protein remains to be elucidated. Part of the reason could be sensitivity to heat and reduced protein stability, as we observed in the enzymatic assay. However, we did not observe gross conformation changes in the CD study of the protein itself. Parsons et al. (323) have shown that PNKP undergoes proteasomal degradation catalyzed by Cul4A-DDB1 ubiquitin ligase, but ubiquitination can be blocked by ATM-mediated phosphorylation of PNKP at serines 114 and 126 following oxidative DNA damage. It would therefore be interesting to test if proteasomal inhibitors, such MG132, can extend the lifetime of wild-type and mutant PNKP proteins and if the mutant PNKP proteins fail to undergo ATM-dependent phosphorylation.

Although the most profound effect of the P101L mutation is the generation of a novel NES signal and the consequent cytoplasmic localization of the protein observed both in our mutant-expressing cells and in the patient's tumour tissue, a recent study (released as a preprint in MedRxiv) based on computer modeling indicated that the P101L mutation would decrease the flexibility of the protein in this region. Further studies would be needed to show if this affects interactions of the FHA domain with other proteins (e.g. full-length XRCC1 and XRCC4) as we observed with the XRCC4-derived phosphopeptide, or the linker region (e.g. phosphorylation by ATM). In addition, the GFP signal in our overexpressed cell model still indicates there is a small fraction of P101L-PNKP located in the nucleus. Whether these nuclei located proteins are enough to perform a normal function needs to be assessed in the future.

Our findings related to the G375W mutant raise two important issues. First of all, is the loss of the 5-kinase activity of PNKP sufficient to cause AOA4? Similar to what we found out, a recent study by Kalasova et al. (262) also implicated loss of PNKP kinase activity to be causal for the neurodegenerative disorders, i.e. AOA4, and CMT, while loss of phosphatase activity correlated with MCSZ. However, more PNKP mutations need to be assessed to confirm such hypothesis. Secondly, what role does mitochondrial PNKP play in the disorder? The potential involvement of mitochondrial PNKP requires further confirmation but may imply that there is a backup kinase activity in the nucleus but not in mitochondria. A potential role for mitochondria has also been reported for SCAN1, where the authors noted that a mutation in *TDP1* resulted in the trapping of the mutant protein on mitochondrial DNA thereby promoting mtDNA damage and mitochondrial fission (284). Another study on HD pointed out that mutant HTT, which has been found to interact with mutant PNKP (162), interacts with the mitochondrial inner membrane and disrupts the mitochondria proteome (324). More studies on the mtDNA damage and mitochondrial protein/DNA interaction need to be carried out to provide explanations for our observations. First of all, whether G375W-PNKP is located in mitochondria needs to be confirmed. Secondly, we need to assess if the mutant PNKP is trapped in the mtDNA or mitochondria protein complex. In addition, we could also assess the mtDNA damage level or mitochondrial functionality such as membrane potential and superoxide production to assess the influence of mutant PNKP on mitochondria.

It is also interesting that in the G375W study, mutant cells exhibit worse reactions than the knockout cells during paraquat treatment. This brings up another question of whether

certain mutant PNKP will render dominant effects on the cells. It will be worthwhile to express the mutant PNKP in wild type cells and subsequent assessment of cellular function and transformation. It will also be necessary to perform the PNKP activity assay with increasing levels of mutant PNKP present. Such dominant effects could be linked to specific mutations since we only observed in G375W, it will be interesting to explore the other PNKP mutations and their consequences, such as DNA damage sensitivity or cellular transformation, and whether the dominant effects of PNKP mutations can be a common feature.

Another issue that needs to be addressed is that since we don't have access to patient's cells, we were using cancer cells that are highly modified. It will be more suitable to use patient derived cells such as primary fibroblasts or primary neuronal cells in future studies. In order to solve the mystery between genetic mutation and disease development, especially the tumorigenesis observed in our patient, animal model-based studies need to be performed in the future. Although embryonic lethality and premature death are induced by PNKP modification (124), tamoxifen-induced PNKP deletion in all tissues in young mice was shown not to be lethal (305). In addition, CRISPR-engineered neurological disease animal modeling can also be used (325). The recent improvement in reducing off-target effects and tissue specific editing by the Cas9 system (326, 327) makes such an approach more feasible.

5 Bibliography

1.   Hoeijmakers JH. Genome maintenance mechanisms for preventing cancer. Nature. 2001;411(6835):366-74.

2.   Cooke MS, Evans MD, Dizdaroglu M, Lunec J. Oxidative DNA damage: mechanisms, mutation, and disease. FASEB J. 2003;17(10):1195-214.

3.   Halliwell B. Why and how should we measure oxidative DNA damage in nutritional studies? How far have we come? Am J Clin Nutr. 2000;72(5):1082-7.

4.   Holliday R, Ho T. Gene silencing and endogenous DNA methylation in mammalian cells. Mutat Res. 1998;400(1-2):361-8.

5.   Rydberg B, Lindahl T. Nonenzymatic methylation of DNA by the intracellular methyl group donor S-adenosyl-L-methionine is a potentially mutagenic reaction. EMBO J. 1982;1(2):211-6.

6.   Lindahl T. Instability and decay of the primary structure of DNA. Nature. 1993;362(6422):709-15.

7.   Jacobs AL, Schar P. DNA glycosylases: in DNA repair and beyond. Chromosoma. 2012;121(1):1-20.

8.   Dianov GL, Hubscher U. Mammalian base excision repair: the forgotten archangel. Nucleic Acids Res. 2013;41(6):3483-90.

9.   Mol CD, Izumi T, Mitra S, Tainer JA. DNA-bound structures and mutants reveal abasic DNA binding by APE1 and DNA repair coordination [corrected]. Nature. 2000;403(6768):451-6.

10.   Wiederhold L, Leppard JB, Kedar P, Karimi-Busheri F, Rasouli-Nia A, Weinfeld M, et al. AP endonuclease-independent DNA base excision repair in human cells. Mol Cell. 2004;15(2):209-20.

11.   Eustermann S, Wu WF, Langelier MF, Yang JC, Easton LE, Riccio AA, et al. Structural Basis of Detection and Signaling of DNA Single-Strand Breaks by Human PARP-1. Mol Cell. 2015;60(5):742-54.

12.   Messner S, Altmeyer M, Zhao H, Pozivil A, Roschitzki B, Gehrig P, et al. PARP1 ADP-ribosylates lysine residues of the core histone tails. Nucleic Acids Res. 2010;38(19):6350-62.

13.   Das SK, Rehman I, Ghosh A, Sengupta S, Majumdar P, Jana B, et al. Poly(ADP-ribose) polymers regulate DNA topoisomerase I (Top1) nuclear dynamics and camptothecin sensitivity in living cells. Nucleic Acids Res. 2016;44(17):8363-75.

14.   Rouleau M, Patel A, Hendzel MJ, Kaufmann SH, Poirier GG. PARP inhibition: PARP1 and beyond. Nat Rev Cancer. 2010;10(4):293-301.

15.   Krishnakumar R, Kraus WL. PARP-1 regulates chromatin structure and transcription through a KDM5B-dependent pathway. Mol Cell. 2010;39(5):736-49.

16.   Masson M, Niedergang C, Schreiber V, Muller S, Menissier-de Murcia J, de Murcia G. XRCC1 is specifically associated with poly(ADP-ribose) polymerase and negatively regulates its activity following DNA damage. Mol Cell Biol. 1998;18(6):3563-71.

17.	Whitehouse CJ, Taylor RM, Thistlethwaite A, Zhang H, Karimi-Busheri F, Lasko DD, et al. XRCC1 stimulates human polynucleotide kinase activity at damaged DNA termini and accelerates DNA single-strand break repair. Cell. 2001;104(1):107-17.

18.	Kubota Y, Nash RA, Klungland A, Schar P, Barnes DE, Lindahl T. Reconstitution of DNA base excision-repair with purified human proteins: interaction between DNA polymerase beta and the XRCC1 protein. EMBO J. 1996;15(23):6662-70.

19.	Caldecott KW, McKeown CK, Tucker JD, Ljungquist S, Thompson LH. An interaction between the mammalian DNA repair protein XRCC1 and DNA ligase III. Mol Cell Biol. 1994;14(1):68-76.

20.	Weinfeld M, Mani RS, Abdou I, Aceytuno RD, Glover JN. Tidying up loose ends: the role of polynucleotide kinase/phosphatase in DNA strand break repair. Trends Biochem Sci. 2011;36(5):262-71.

21.	Allinson SL, Dianova, II, Dianov GL. DNA polymerase beta is the major dRP lyase involved in repair of oxidative base lesions in DNA by mammalian cell extracts. EMBO J. 2001;20(23):6919-26.

22.	Beard WA, Prasad R, Wilson SH. Activities and mechanism of DNA polymerase beta. Methods Enzymol. 2006;408:91-107.

23.	Cappelli E, Taylor R, Cevasco M, Abbondandolo A, Caldecott K, Frosina G. Involvement of XRCC1 and DNA ligase III gene products in DNA base excision repair. J Biol Chem. 1997;272(38):23970-5.

24.	Kim YJ, Wilson DM, 3rd. Overview of base excision repair biochemistry. Curr Mol Pharmacol. 2012;5(1):3-13.

25.	Storici F, Henneke G, Ferrari E, Gordenin DA, Hubscher U, Resnick MA. The flexible loop of human FEN1 endonuclease is required for flap cleavage during DNA replication and repair. EMBO J. 2002;21(21):5930-42.

26.	Levin DS, McKenna AE, Motycka TA, Matsumoto Y, Tomkinson AE. Interaction between PCNA and DNA ligase I is critical for joining of Okazaki fragments and long-patch base-excision repair. Curr Biol. 2000;10(15):919-22.

27.	Sung JS, Demple B. Roles of base excision repair subpathways in correcting oxidized abasic sites in DNA. FEBS J. 2006;273(8):1620-9.

28.	Petermann E, Ziegler M, Oei SL. ATP-dependent selection between single nucleotide and long patch base excision repair. DNA Repair (Amst). 2003;2(10):1101-14.

29.	Fortini P, Dogliotti E. Base damage and single-strand break repair: mechanisms and functional significance of short- and long-patch repair subpathways. DNA Repair (Amst). 2007;6(4):398-409.

30.	Van Der Schans GP. Gamma-ray induced double-strand breaks in DNA resulting from randomly-inflicted single-strand breaks: temporal local denaturation, a new radiation phenomenon? Int J Radiat Biol Relat Stud Phys Chem Med. 1978;33(2):105-20.

31.	Shibata A. Regulation of repair pathway choice at two-ended DNA double-strand breaks. Mutat Res. 2017;803-805:51-5.

32.	Mao Z, Bozzella M, Seluanov A, Gorbunova V. Comparison of nonhomologous end joining and homologous recombination in human cells. DNA Repair (Amst). 2008;7(10):1765-71.

33.   Aravind L, Koonin EV. Prokaryotic homologs of the eukaryotic DNA-end-binding protein Ku, novel domains in the Ku protein and prediction of a prokaryotic double-strand break repair system. Genome Res. 2001;11(8):1365-74.

34.   Smith GC, Jackson SP. The DNA-dependent protein kinase. Genes Dev. 1999;13(8):916-34.

35.   Yoo S, Dynan WS. Geometry of a complex formed by double strand break repair proteins at a single DNA end: recruitment of DNA-PKcs induces inward translocation of Ku protein. Nucleic Acids Res. 1999;27(24):4679-86.

36.   Neal JA, Meek K. Choosing the right path: does DNA-PK help make the decision? Mutat Res. 2011;711(1-2):73-86.

37.   Koch CA, Agyei R, Galicia S, Metalnikov P, O'Donnell P, Starostine A, et al. Xrcc4 physically links DNA end processing by polynucleotide kinase to DNA ligation by DNA ligase IV. EMBO J. 2004;23(19):3874-85.

38.   Chappell C, Hanakahi LA, Karimi-Busheri F, Weinfeld M, West SC. Involvement of human polynucleotide kinase in double-strand break repair by non-homologous end joining. EMBO J. 2002;21(11):2827-32.

39.   Ma Y, Pannicke U, Schwarz K, Lieber MR. Hairpin opening and overhang processing by an Artemis/DNA-dependent protein kinase complex in nonhomologous end joining and V(D)J recombination. Cell. 2002;108(6):781-94.

40.   Kurosawa A, Adachi N. Functions and regulation of Artemis: a goddess in the maintenance of genome integrity. J Radiat Res. 2010;51(5):503-9.

41.   Bebenek K, Pedersen LC, Kunkel TA. Structure-function studies of DNA polymerase lambda. Biochemistry. 2014;53(17):2781-92.

42.   Nick McElhinny SA, Ramsden DA. Polymerase mu is a DNA-directed DNA/RNA polymerase. Mol Cell Biol. 2003;23(7):2309-15.

43.   Bryans M, Valenzano MC, Stamato TD. Absence of DNA ligase IV protein in XR-1 cells: evidence for stabilization by XRCC4. Mutat Res. 1999;433(1):53-8.

44.   Grawunder U, Wilm M, Wu X, Kulesza P, Wilson TE, Mann M, et al. Activity of DNA ligase IV stimulated by complex formation with XRCC4 protein in mammalian cells. Nature. 1997;388(6641):492-5.

45.   Andres SN, Vergnes A, Ristic D, Wyman C, Modesti M, Junop M. A human XRCC4-XLF complex bridges DNA. Nucleic Acids Res. 2012;40(4):1868-78.

46.   Akopiants K, Zhou RZ, Mohapatra S, Valerie K, Lees-Miller SP, Lee KJ, et al. Requirement for XLF/Cernunnos in alignment-based gap filling by DNA polymerases lambda and mu for nonhomologous end joining in human whole-cell extracts. Nucleic Acids Res. 2009;37(12):4055-62.

47.   Chakraborty A, Tapryal N, Venkova T, Horikoshi N, Pandita RK, Sarker AH, et al. Classical non-homologous end-joining pathway utilizes nascent RNA for error-free double-strand break repair of transcribed genes. Nat Commun. 2016;7:13049.

48.   Heyer WD, Ehmsen KT, Liu J. Regulation of homologous recombination in eukaryotes. Annu Rev Genet. 2010;44:113-39.

49.   Moreno-Herrero F, de Jager M, Dekker NH, Kanaar R, Wyman C, Dekker C. Mesoscale conformational changes in the DNA-repair complex Rad50/Mre11/Nbs1 upon binding DNA. Nature. 2005;437(7057):440-3.

50.   Shibata A, Moiani D, Arvai AS, Perry J, Harding SM, Genois MM, et al. DNA double-strand break repair pathway choice is directed by distinct MRE11 nuclease activities. Mol Cell. 2014;53(1):7-18.

51.   Garcia V, Phelps SE, Gray S, Neale MJ. Bidirectional resection of DNA double-strand breaks by Mre11 and Exo1. Nature. 2011;479(7372):241-4.

52.   Uziel T, Lerenthal Y, Moyal L, Andegeko Y, Mittelman L, Shiloh Y. Requirement of the MRN complex for ATM activation by DNA damage. EMBO J. 2003;22(20):5612-21.

53.   Kijas AW, Lim YC, Bolderson E, Cerosaletti K, Gatei M, Jakob B, et al. ATM-dependent phosphorylation of MRE11 controls extent of resection during homology directed repair by signalling through Exonuclease 1. Nucleic Acids Res. 2015;43(17):8352-67.

54.   Zou Y, Liu Y, Wu X, Shell SM. Functions of human replication protein A (RPA): from DNA replication to DNA damage and stress responses. J Cell Physiol. 2006;208(2):267-73.

55.   Gibb B, Ye LF, Kwon Y, Niu H, Sung P, Greene EC. Protein dynamics during presynaptic-complex assembly on individual single-stranded DNA molecules. Nat Struct Mol Biol. 2014;21(10):893-900.

56.   McIlwraith MJ, Vaisman A, Liu Y, Fanning E, Woodgate R, West SC. Human DNA polymerase eta promotes DNA synthesis from strand invasion intermediates of homologous recombination. Mol Cell. 2005;20(5):783-92.

57.   Sung P, Klein H. Mechanism of homologous recombination: mediators and helicases take on regulatory functions. Nat Rev Mol Cell Biol. 2006;7(10):739-50.

58.   Ferguson DO, Holloman WK. Recombinational repair of gaps in DNA is asymmetric in Ustilago maydis and can be explained by a migrating D-loop model. Proc Natl Acad Sci U S A. 1996;93(11):5419-24.

59.   Ira G, Malkova A, Liberi G, Foiani M, Haber JE. Srs2 and Sgs1-Top3 suppress crossovers during double-strand break repair in yeast. Cell. 2003;115(4):401-11.

60.   Wu L, Hickson ID. The Bloom's syndrome helicase suppresses crossing over during homologous recombination. Nature. 2003;426(6968):870-4.

61.   Vasu SK, Forbes DJ. Nuclear pores and nuclear assembly. Curr Opin Cell Biol. 2001;13(3):363-75.

62.   Fried H, Kutay U. Nucleocytoplasmic transport: taking an inventory. Cell Mol Life Sci. 2003;60(8):1659-88.

63.   Macara IG. Transport into and out of the nucleus. Microbiol Mol Biol Rev. 2001;65(4):570-94, table of contents.

64.   Mosammaparast N, Pemberton LF. Karyopherins: from nuclear-transport mediators to nuclear-function regulators. Trends Cell Biol. 2004;14(10):547-56.

65.   Pemberton LF, Paschal BM. Mechanisms of receptor-mediated nuclear import and nuclear export. Traffic. 2005;6(3):187-98.

66.   Kalderon D, Richardson WD, Markham AF, Smith AE. Sequence requirements for nuclear location of simian virus 40 large-T antigen. Nature. 1984;311(5981):33-8.

67.   Robbins J, Dilworth SM, Laskey RA, Dingwall C. Two interdependent basic domains in nucleoplasmin nuclear targeting sequence: identification of a class of bipartite nuclear targeting sequence. Cell. 1991;64(3):615-23.

68.   Chook YM, Blobel G. Karyopherins and nuclear import. Curr Opin Struct Biol. 2001;11(6):703-15.

69.   Fischer U, Huber J, Boelens WC, Mattaj IW, Luhrmann R. The HIV-1 Rev activation domain is a nuclear export signal that accesses an export pathway used by specific cellular RNAs. Cell. 1995;82(3):475-83.

70.   Fornerod M, Ohno M, Yoshida M, Mattaj IW. CRM1 is an export receptor for leucine-rich nuclear export signals. Cell. 1997;90(6):1051-60.

71.   Fagotto F, Gluck U, Gumbiner BM. Nuclear localization signal-independent and importin/karyopherin-independent nuclear import of beta-catenin. Curr Biol. 1998;8(4):181-90.

72.   Kirby TW, Gassman NR, Smith CE, Pedersen LC, Gabel SA, Sobhany M, et al. Nuclear Localization of the DNA Repair Scaffold XRCC1: Uncovering the Functional Role of a Bipartite NLS. Sci Rep. 2015;5:13405.

73.   Tsukada K, Matsumoto Y, Shimada M. Linker region is required for efficient nuclear localization of polynucleotide kinase phosphatase. PLoS One. 2020;15(9):e0239404.

74.   Subedi S. Role of human polynucleotide kinase/phophatase (PNKP) in nuclear and mitochondrial DNA repair: University of Alberta; 2015.

75.   Fukuchi M, Wanotayan R, Liu S, Imamichi S, Sharma MK, Matsumoto Y. Lysine 271 but not lysine 210 of XRCC4 is required for the nuclear localization of XRCC4 and DNA ligase IV. Biochem Biophys Res Commun. 2015;461(4):687-94.

76.   Knudsen NO, Nielsen FC, Vinther L, Bertelsen R, Holten-Andersen S, Liberti SE, et al. Nuclear localization of human DNA mismatch repair protein exonuclease 1 (hEXO1). Nucleic Acids Res. 2007;35(8):2609-19.

77.   Santagati F, Botta E, Stefanini M, Pedrini AM. Different dynamics in nuclear entry of subunits of the repair/transcription factor TFIIH. Nucleic Acids Res. 2001;29(7):1574-81.

78.   McKinnon PJ. Genome integrity and disease prevention in the nervous system. Genes Dev. 2017;31(12):1180-94.

79.   Suberbielle E, Sanchez PE, Kravitz AV, Wang X, Ho K, Eilertson K, et al. Physiologic brain activity causes DNA double-strand breaks in neurons, with exacerbation by amyloid-beta. Nat Neurosci. 2013;16(5):613-21.

80.   Lu T, Pan Y, Kao SY, Li C, Kohane I, Chan J, et al. Gene regulation and DNA damage in the ageing human brain. Nature. 2004;429(6994):883-91.

81.   Parenti I, Rabaneda LG, Schoen H, Novarino G. Neurodevelopmental Disorders: From Genetics to Functional Pathways. Trends Neurosci. 2020;43(8):608-21.

82.   Weemaes CM, Hustinx TW, Scheres JM, van Munster PJ, Bakkeren JA, Taalman RD. A new chromosomal instability disorder: the Nijmegen breakage syndrome. Acta Paediatr Scand. 1981;70(4):557-64.

83.   Varon R, Vissinga C, Platzer M, Cerosaletti KM, Chrzanowska KH, Saar K, et al. Nibrin, a novel DNA double-strand break repair protein, is mutated in Nijmegen breakage syndrome. Cell. 1998;93(3):467-76.

84.   Zhang Y, Zhou J, Lim CU. The role of NBS1 in DNA double strand break repair, telomere stability, and cell cycle checkpoint control. Cell Res. 2006;16(1):45-54.

85.   Zou L, Elledge SJ. Sensing DNA damage through ATRIP recognition of RPA-ssDNA complexes. Science. 2003;300(5625):1542-8.

86.   O'Driscoll M, Ruiz-Perez VL, Woods CG, Jeggo PA, Goodship JA. A splicing mutation affecting expression of ataxia-telangiectasia and Rad3-related protein (ATR) results in Seckel syndrome. Nature genetics. 2003;33(4):497-501.

87.	Coppede F, Migliore L. DNA damage in neurodegenerative diseases. Mutat Res. 2015;776:84-97.

88.	Boder E, Sedgwick RP. Ataxia-telangiectasia; a familial syndrome of progressive cerebellar ataxia, oculocutaneous telangiectasia and frequent pulmonary infection. Pediatrics. 1958;21(4):526-54.

89.	Savitsky K, Bar-Shira A, Gilad S, Rotman G, Ziv Y, Vanagaite L, et al. A single ataxia telangiectasia gene with a product similar to PI-3 kinase. Science. 1995;268(5218):1749-53.

90.	Takashima H, Boerkoel CF, John J, Saifi GM, Salih MA, Armstrong D, et al. Mutation of TDP1, encoding a topoisomerase I-dependent DNA damage repair enzyme, in spinocerebellar ataxia with axonal neuropathy. Nature genetics. 2002;32(2):267-72.

91.	Yang SW, Burgin AB, Jr., Huizenga BN, Robertson CA, Yao KC, Nash HA. A eukaryotic enzyme that can disjoin dead-end covalent complexes between DNA and type I topoisomerases. Proc Natl Acad Sci U S A. 1996;93(21):11534-9.

92.	Interthal H, Chen HJ, Champoux JJ. Human Tdp1 cleaves a broad spectrum of substrates, including phosphoamide linkages. J Biol Chem. 2005;280(43):36518-28.

93.	Pheiffer BH, Zimmerman SB. 3'-Phosphatase activity of the DNA kinase from rat liver. Biochem Biophys Res Commun. 1982;109(4):1297-302.

94.	Jilani A, Ramotar D, Slack C, Ong C, Yang XM, Scherer SW, et al. Molecular cloning of the human gene, PNKP, encoding a polynucleotide kinase 3'-phosphatase and evidence for its role in repair of DNA strand breaks caused by oxidative damage. J Biol Chem. 1999;274(34):24176-86.

95.	Karimi-Busheri F, Daly G, Robins P, Canas B, Pappin DJ, Sgouros J, et al. Molecular characterization of a human DNA kinase. The Journal of biological chemistry. 1999;274(34):24187-94.

96.	Jiang B, Glover JN, Weinfeld M. Neurological disorders associated with DNA strand-break processing enzymes. Mech Ageing Dev. 2017;161(Pt A):130-40.

97.	Bernstein NK, Williams RS, Rakovszky ML, Cui D, Green R, Karimi-Busheri F, et al. The molecular architecture of the mammalian DNA repair enzyme, polynucleotide kinase. Molecular cell. 2005;17(5):657-70.

98.	Loizou JI, El-Khamisy SF, Zlatanou A, Moore DJ, Chan DW, Qin J, et al. The protein kinase CK2 facilitates repair of chromosomal DNA single-strand breaks. Cell. 2004;117(1):17-28.

99.	Dobson CJ, Allinson SL. The phosphatase activity of mammalian polynucleotide kinase takes precedence over its kinase activity in repair of single strand breaks. Nucleic acids research. 2006;34(8):2230-7.

100.	Karimi-Busheri F, Lee J, Tomkinson AE, Weinfeld M. Repair of DNA strand gaps and nicks containing 3'-phosphate and 5'-hydroxyl termini by purified mammalian enzymes. Nucleic Acids Res. 1998;26(19):4395-400.

101.	Karimi-Busheri F, Rasouli-Nia A, Allalunis-Turner J, Weinfeld M. Human polynucleotide kinase participates in repair of DNA double-strand breaks by nonhomologous end joining but not homologous recombination. Cancer Res. 2007;67(14):6619-25.

102.	Shimada M, Dumitrache LC, Russell HR, McKinnon PJ. Polynucleotide kinase-phosphatase enables neurogenesis via multiple DNA repair pathways to maintain genome stability. EMBO J. 2015;34(19):2465-80.

103.   Henner WD, Grunberg SM, Haseltine WA. Enzyme action at 3' termini of ionizing radiation-induced DNA strand breaks. The Journal of biological chemistry. 1983;258(24):15198-205.

104.   Dedon PC. The chemical toxicology of 2-deoxyribose oxidation in DNA. Chemical research in toxicology. 2008;21(1):206-19.

105.   Inamdar KV, Pouliot JJ, Zhou T, Lees-Miller SP, Rasouli-Nia A, Povirk LF. Conversion of phosphoglycolate to phosphate termini on 3' overhangs of DNA double strand breaks by the human tyrosyl-DNA phosphodiesterase hTdp1. J Biol Chem. 2002;277(30):27162-8.

106.   Zhou T, Akopiants K, Mohapatra S, Lin PS, Valerie K, Ramsden DA, et al. Tyrosyl-DNA phosphodiesterase and the repair of 3'-phosphoglycolate-terminated DNA double-strand breaks. DNA Repair (Amst). 2009;8(8):901-11.

107.   Shen J, Gilmore EC, Marshall CA, Haddadin M, Reynolds JJ, Eyaid W, et al. Mutations in PNKP cause microcephaly, seizures and defects in DNA repair. Nature genetics. 2010;42(3):245-9.

108.   Bras J, Alonso I, Barbot C, Costa MM, Darwent L, Orme T, et al. Mutations in PNKP Cause Recessive Ataxia with Oculomotor Apraxia Type 4. American Journal of Human Genetics. 2015;96(3):474-9.

109.   Leal A, Bogantes-Ledezma S, Ekici AB, Uebe S, Thiel CT, Sticht H, et al. The polynucleotide kinase 3'-phosphatase gene (PNKP) is involved in Charcot-Marie-Tooth disease (CMT2B2) previously related to MED25. Neurogenetics. 2018;19(4):215-25.

110.   Cox J, Jackson AP, Bond J, Woods CG. What primary microcephaly can tell us about brain growth. Trends Mol Med. 2006;12(8):358-66.

111.   Thornton GK, Woods CG. Primary microcephaly: do all roads lead to Rome? Trends Genet. 2009;25(11):501-10.

112.   Alter BP, Rosenberg PS, Brody LC. Clinical and molecular features associated with biallelic mutations in FANCD1/BRCA2. J Med Genet. 2007;44(1):1-9.

113.   O'Driscoll M, Cerosaletti KM, Girard PM, Dai Y, Stumm M, Kysela B, et al. DNA ligase IV mutations identified in patients exhibiting developmental delay and immunodeficiency. Mol Cell. 2001;8(6):1175-85.

114.   Bitarafan F, Khodaeian M, Almadani N, Kalhor A, Sardehaei EA, Garshasbi M. Compound Heterozygous Mutations in PNKP Gene in an Iranian Child with Microcephaly, Seizures, and Developmental Delay. Fetal Pediatr Pathol. 2019:1-7.

115.   Entezam M, Razipour M, Talebi S, Beiraghi Toosi M, Keramatipour M. Multi affected pedigree with congenital microcephaly: WES revealed PNKP gene mutation. Brain Dev. 2019;41(2):182-6.

116.   Kalasova I, Hanzlikova H, Gupta N, Li Y, Altmuller J, Reynolds JJ, et al. Novel PNKP mutations causing defective DNA strand break repair and PARP1 hyperactivity in MCSZ. Neurol Genet. 2019;5(2):e320.

117.   Nakashima M, Takano K, Osaka H, Aida N, Tsurusaki Y, Miyake N, et al. Causative novel PNKP mutations and concomitant PCDH15 mutations in a patient with microcephaly with early-onset seizures and developmental delay syndrome and hearing loss. J Hum Genet. 2014;59(8):471-4.

118.   Poulton C, Oegema R, Heijsman D, Hoogeboom J, Schot R, Stroink H, et al. Progressive cerebellar atrophy and polyneuropathy: expanding the spectrum of PNKP mutations. Neurogenetics. 2013;14(1):43-51.

119.   Nair P, Hamzeh AR, Mohamed M, Saif F, Tawfiq N, El Halik M, et al. Microcephalic primordial dwarfism in an Emirati patient with PNKP mutation. Am J Med Genet A. 2016;170(8):2127-32.

120.   Gatti M, Magri S, Nanetti L, Sarto E, Di Bella D, Salsano E, et al. From congenital microcephaly to adult onset cerebellar ataxia: Distinct and overlapping phenotypes in patients with PNKP gene mutations. Am J Med Genet A. 2019;179(11):2277-83.

121.   Carvill GL, Heavin SB, Yendle SC, McMahon JM, O'Roak BJ, Cook J, et al. Targeted resequencing in epileptic encephalopathies identifies de novo mutations in CHD2 and SYNGAP1. Nature genetics. 2013;45(7):825-30.

122.   Reynolds JJ, Walker AK, Gilmore EC, Walsh CA, Caldecott KW. Impact of PNKP mutations associated with microcephaly, seizures and developmental delay on enzyme activity and DNA strand break repair. Nucleic Acids Res. 2012;40(14):6608-19.

123.   Tebbs RS, Flannery ML, Meneses JJ, Hartmann A, Tucker JD, Thompson LH, et al. Requirement for the Xrcc1 DNA base excision repair gene during early mouse development. Dev Biol. 1999;208(2):513-29.

124.   Shimada M, Dumitrache LC, Russell HR, McKinnon PJ. Polynucleotide kinase-phosphatase enables neurogenesis via multiple DNA repair pathways to maintain genome stability. The EMBO journal. 2015;34(19):2465-80.

125.   Aicardi J, Barbosa C, Andermann E, Andermann F, Morcos R, Ghanem Q, et al. Ataxia-ocular motor apraxia: a syndrome mimicking ataxia-telangiectasia. Ann Neurol. 1988;24(4):497-502.

126.   Sekijima Y, Ohara S, Nakagawa S, Tabata K, Yoshida K, Ishigame H, et al. Hereditary motor and sensory neuropathy associated with cerebellar atrophy (HMSNCA): clinical and neuropathological features of a Japanese family. J Neurol Sci. 1998;158(1):30-7.

127.   Gueven N, Becherel OJ, Kijas AW, Chen P, Howe O, Rudolph JH, et al. Aprataxin, a novel protein that protects against genotoxic stress. Hum Mol Genet. 2004;13(10):1081-93.

128.   Date H, Onodera O, Tanaka H, Iwabuchi K, Uekawa K, Igarashi S, et al. Early-onset ataxia with ocular motor apraxia and hypoalbuminemia is caused by mutations in a new HIT superfamily gene. Nature genetics. 2001;29(2):184-8.

129.   Moreira MC, Barbot C, Tachi N, Kozuka N, Uchida E, Gibson T, et al. The gene mutated in ataxia-ocular apraxia 1 encodes the new HIT/Zn-finger protein aprataxin. Nature genetics. 2001;29(2):189-93.

130.   Moreira MC, Klur S, Watanabe M, Nemeth AH, Le Ber I, Moniz JC, et al. Senataxin, the ortholog of a yeast RNA helicase, is mutant in ataxia-ocular apraxia 2. Nature genetics. 2004;36(3):225-7.

131.   Al Tassan N, Khalil D, Shinwari J, Al Sharif L, Bavi P, Abduljaleel Z, et al. A missense mutation in PIK3R5 gene in a family with ataxia and oculomotor apraxia. Hum Mutat. 2012;33(2):351-4.

132.   Tarsy D, Simon DK. Dystonia. N Engl J Med. 2006;355(8):818-29.

133.   Schmahmann JD. Disorders of the cerebellum: ataxia, dysmetria of thought, and the cerebellar cognitive affective syndrome. J Neuropsychiatry Clin Neurosci. 2004;16(3):367-78.

134.   Cogan DG. A type of congenital ocular motor apraxia presenting jerky head movements. Trans Am Acad Ophthalmol Otolaryngol. 1952;56(6):853-62.

135.   Caputi C, Tolve M, Galosi S, Inghilleri M, Carducci C, Angeloni A, et al. PNKP deficiency mimicking a benign hereditary chorea: The misleading presentation of a neurodegenerative disorder. Parkinsonism Relat Disord. 2019;64:342-5.

136.   Paucar M, Malmgren H, Taylor M, Reynolds JJ, Svenningsson P, Press R, et al. Expanding the ataxia with oculomotor apraxia type 4 phenotype. Neurol Genet. 2016;2(1):e49.

137.   Schiess N, Zee DS, Siddiqui KA, Szolics M, El-Hattab AW. Novel PNKP mutation in siblings with ataxia-oculomotor apraxia type 4. J Neurogenet. 2017;31(1-2):23-5.

138.   Scholz C, Golas MM, Weber RG, Hartmann C, Lehmann U, Sahm F, et al. Rare compound heterozygous variants in PNKP identified by whole exome sequencing in a German patient with ataxia-oculomotor apraxia 4 and pilocytic astrocytoma. Clin Genet. 2018;94(1):185-6.

139.   Tzoulis C, Sztromwasser P, Johansson S, Gjerde IO, Knappskog P, Bindoff LA. PNKP Mutations Identified by Whole-Exome Sequencing in a Norwegian Patient with Sporadic Ataxia and Edema. Cerebellum. 2017;16(1):272-5.

140.   Rudenskaya GE, Marakhonov AV, Shchagina OA, Lozier ER, Dadali EL, Akimova IA, et al. Ataxia with Oculomotor Apraxia Type 4 with PNKP Common "Portuguese" and Novel Mutations in Two Belarusian Families. J Pediatr Genet. 2019;8(2):58-62.

141.   Freitas E, Costa O, Rocha S. A New Phenotype of Ataxia With Oculomotor Apraxia Type 4. Cureus. 2021;13(2):e13601.

142.   Garrelfs MR, Takada S, Kamsteeg EJ, Pegge S, Mancini G, Engelen M, et al. The Phenotypic Spectrum of PNKP-Associated Disease and the Absence of Immunodeficiency and Cancer Predisposition in a Dutch Cohort. Pediatr Neurol. 2020;113:26-32.

143.   Skre H. Genetic and clinical aspects of Charcot-Marie-Tooth's disease. Clin Genet. 1974;6(2):98-118.

144.   Harding AE, Thomas PK. The clinical features of hereditary motor and sensory neuropathy types I and II. Brain. 1980;103(2):259-80.

145.   Lupski JR, de Oca-Luna RM, Slaugenhaupt S, Pentao L, Guzzetta V, Trask BJ, et al. DNA duplication associated with Charcot-Marie-Tooth disease type 1A. Cell. 1991;66(2):219-32.

146.   Raeymaekers P, Timmerman V, Nelis E, De Jonghe P, Hoogendijk JE, Baas F, et al. Duplication in chromosome 17p11.2 in Charcot-Marie-Tooth neuropathy type 1a (CMT 1a). The HMSN Collaborative Research Group. Neuromuscul Disord. 1991;1(2):93-7.

147.   Reilly MM, Murphy SM, Laura M. Charcot-Marie-Tooth disease. J Peripher Nerv Syst. 2011;16(1):1-14.

148.   Dematteis M, Pepin JL, Jeanmart M, Deschaux C, Labarre-Vila A, Levy P. Charcot-Marie-Tooth disease and sleep apnoea syndrome: a family study. Lancet. 2001;357(9252):267-72.

149.   Bienfait HM, Verhamme C, van Schaik IN, Koelman JH, de Visser BW, de Haan RJ, et al. Comparison of CMT1A and CMT2: similarities and differences. J Neurol. 2006;253(12):1572-80.

150.   Bird TD. Charcot-Marie-Tooth (CMT) Hereditary Neuropathy Overview. In: Adam MP, Ardinger HH, Pagon RA, Wallace SE, Bean LJH, Stephens K, et al., editors. GeneReviews((R)). Seattle (WA)1993.

151.   Leal A, Morera B, Del Valle G, Heuss D, Kayser C, Berghoff M, et al. A second locus for an axonal form of autosomal recessive Charcot-Marie-Tooth disease maps to chromosome 19q13.3. Am J Hum Genet. 2001;68(1):269-74.

152.   Leal A, Huehne K, Bauer F, Sticht H, Berger P, Suter U, et al. Identification of the variant Ala335Val of MED25 as responsible for CMT2B2: molecular data, functional studies of the SH3 recognition motif and correlation between wild-type MED25 and PMP22 RNA levels in CMT1A animal models. Neurogenetics. 2009;10(4):375-6.

153.   Pedroso JL, Rocha CR, Macedo-Souza LI, De Mario V, Marques W, Jr., Barsottini OG, et al. Mutation in PNKP presenting initially as axonal Charcot-Marie-Tooth disease. Neurol Genet. 2015;1(4):e30.

154.   Campopiano R, Ferese R, Buttari F, Femiano C, Centonze D, Fornai F, et al. A Novel Homozygous Variant in the Fork-Head-Associated Domain of Polynucleotide Kinase Phosphatase in a Patient Affected by Late-Onset Ataxia With Oculomotor Apraxia Type 4. Front Neurol. 2019;10:1331.

155.   Kawaguchi Y, Okamoto T, Taniwaki M, Aizawa M, Inoue M, Katayama S, et al. CAG expansions in a novel gene for Machado-Joseph disease at chromosome 14q32.1. Nature genetics. 1994;8(3):221-8.

156.   Schmitt I, Linden M, Khazneh H, Evert BO, Breuer P, Klockgether T, et al. Inactivation of the mouse Atxn3 (ataxin-3) gene increases protein ubiquitination. Biochem Biophys Res Commun. 2007;362(3):734-9.

157.   Costa Mdo C, Paulson HL. Toward understanding Machado-Joseph disease. Prog Neurobiol. 2012;97(2):239-57.

158.   Gao R, Liu Y, Silva-Fernandes A, Fang X, Paulucci-Holthauzen A, Chatterjee A, et al. Inactivation of PNKP by mutant ATXN3 triggers apoptosis by activating the DNA damage-response pathway in SCA3. PLoS Genet. 2015;11(1):e1004834.

159.   Chatterjee A, Saha S, Chakraborty A, Silva-Fernandes A, Mandal SM, Neves-Carvalho A, et al. The role of the mammalian DNA end-processing enzyme polynucleotide kinase 3'-phosphatase in spinocerebellar ataxia type 3 pathogenesis. PLoS Genet. 2015;11(1):e1004749.

160.   Chakraborty A, Tapryal N, Venkova T, Mitra J, Vasquez V, Sarker AH, et al. Deficiency in classical nonhomologous end-joining-mediated repair of transcribed genes is linked to SCA3 pathogenesis. Proc Natl Acad Sci U S A. 2020;117(14):8154-65.

161.   MacDonald ME, Ambrose CM, Duyao MP, Myers RH, Lin C, Srinidhi L, et al. A novel gene containing a trinucleotide repeat that is expanded and unstable on Huntington's disease chromosomes. Cell. 1993;72(6):971-83.

162.   Gao R, Chakraborty A, Geater C, Pradhan S, Gordon KL, Snowden J, et al. Mutant huntingtin impairs PNKP and ATXN3, disrupting DNA repair and transcription. Elife. 2019;8.

163.   Stratton MR, Campbell PJ, Futreal PA. The cancer genome. Nature. 2009;458(7239):719-24.

164.   Kiwerska K, Szyfter K. DNA repair in cancer initiation, progression, and therapy-a double-edged sword. J Appl Genet. 2019;60(3-4):329-34.

165.   Jeggo PA, Pearl LH, Carr AM. DNA repair, genome stability and cancer: a historical perspective. Nat Rev Cancer. 2016;16(1):35-42.

166.   Cleaver JE. Xeroderma pigmentosum: a human disease in which an initial stage of DNA repair is defective. Proc Natl Acad Sci U S A. 1969;63(2):428-35.

167.   Lehmann AR, McGibbon D, Stefanini M. Xeroderma pigmentosum. Orphanet J Rare Dis. 2011;6:70.

168.   Fishel R, Lescoe MK, Rao MR, Copeland NG, Jenkins NA, Garber J, et al. The human mutator gene homolog MSH2 and its association with hereditary nonpolyposis colon cancer. Cell. 1993;75(5):1027-38.

169.   Bronner CE, Baker SM, Morrison PT, Warren G, Smith LG, Lescoe MK, et al. Mutation in the DNA mismatch repair gene homologue hMLH1 is associated with hereditary non-polyposis colon cancer. Nature. 1994;368(6468):258-61.

170.   Kastrinos F, Mukherjee B, Tayob N, Wang F, Sparr J, Raymond VM, et al. Risk of pancreatic cancer in families with Lynch syndrome. JAMA. 2009;302(16):1790-5.

171.   Moldovan GL, D'Andrea AD. How the fanconi anemia pathway guards the genome. Annu Rev Genet. 2009;43:223-49.

172.   Digweed M, Sperling K. Nijmegen breakage syndrome: clinical manifestation of defective response to DNA double-strand breaks. DNA Repair (Amst). 2004;3(8-9):1207-17.

173.   Reiman A, Srinivasan V, Barone G, Last JI, Wootton LL, Davies EG, et al. Lymphoid tumours and breast cancer in ataxia telangiectasia; substantial protective effect of residual ATM kinase activity against childhood tumours. Br J Cancer. 2011;105(4):586-91.

174.   Louis DN, Ohgaki H, Wiestler OD, Cavenee WK, Burger PC, Jouvet A, et al. The 2007 WHO classification of tumours of the central nervous system. Acta Neuropathol. 2007;114(2):97-109.

175.   Adamson C, Kanu OO, Mehta AI, Di C, Lin N, Mattox AK, et al. Glioblastoma multiforme: a review of where we have been and where we are going. Expert Opin Investig Drugs. 2009;18(8):1061-83.

176.   Ohgaki H, Kleihues P. Genetic pathways to primary and secondary glioblastoma. Am J Pathol. 2007;170(5):1445-53.

177.   Ohgaki H, Dessen P, Jourde B, Horstmann S, Nishikawa T, Di Patre PL, et al. Genetic pathways to glioblastoma: a population-based study. Cancer Res. 2004;64(19):6892-9.

178.   Ohgaki H, Kleihues P. Population-based studies on incidence, survival rates, and genetic alterations in astrocytic and oligodendroglial gliomas. J Neuropathol Exp Neurol. 2005;64(6):479-89.

179.   Dolecek TA, Propp JM, Stroup NE, Kruchko C. CBTRUS statistical report: primary brain and central nervous system tumors diagnosed in the United States in 2005-2009. Neuro Oncol. 2012;14 Suppl 5:v1-49.

180.   Mahvash M, Hugo HH, Maslehaty H, Mehdorn HM, Stark AM. Glioblastoma multiforme in children: report of 13 cases and review of the literature. Pediatr Neurol. 2011;45(3):178-80.

181.   Dohrmann GJ, Farwell JR, Flannery JT. Glioblastoma multiforme in children. J Neurosurg. 1976;44(4):442-8.

182.   Brennan CW, Verhaak RG, McKenna A, Campos B, Noushmehr H, Salama SR, et al. The somatic genomic landscape of glioblastoma. Cell. 2013;155(2):462-77.

183.   Sturm D, Bender S, Jones DT, Lichter P, Grill J, Becher O, et al. Paediatric and adult glioblastoma: multiform (epi)genomic culprits emerge. Nat Rev Cancer. 2014;14(2):92-107.

184.   Paugh BS, Qu C, Jones C, Liu Z, Adamowicz-Brice M, Zhang J, et al. Integrated molecular genetic profiling of pediatric high-grade gliomas reveals key differences with the adult disease. J Clin Oncol. 2010;28(18):3061-8.

185.   Das KK, Kumar R. Pediatric Glioblastoma. In: De Vleeschouwer S, editor. Glioblastoma. Brisbane (AU)2017.

186.   Haase S, Garcia-Fabiani MB, Carney S, Altshuler D, Nunez FJ, Mendez FM, et al. Mutant ATRX: uncovering a new therapeutic target for glioma. Expert Opin Ther Targets. 2018;22(7):599-613.

187.   Erasimus H, Gobin M, Niclou S, Van Dyck E. DNA repair mechanisms and their clinical impact in glioblastoma. Mutat Res Rev Mutat Res. 2016;769:19-35.

188.   Annesley SJ, Fisher PR. Mitochondria in Health and Disease. Cells. 2019;8(7).

189.   Taylor RW, Turnbull DM. Mitochondrial DNA mutations in human disease. Nat Rev Genet. 2005;6(5):389-402.

190.   Taanman JW. The mitochondrial genome: structure, transcription, translation and replication. Biochimica et biophysica acta. 1999;1410(2):103-23.

191.   Morgenstern M, Stiller SB, Lubbert P, Peikert CD, Dannenmaier S, Drepper F, et al. Definition of a High-Confidence Mitochondrial Proteome at Quantitative Scale. Cell Rep. 2017;19(13):2836-52.

192.   Schmidt O, Pfanner N, Meisinger C. Mitochondrial protein import: from proteomics to functional mechanisms. Nat Rev Mol Cell Biol. 2010;11(9):655-67.

193.   Wisnovsky S, Jean SR, Kelley SO. Mitochondrial DNA repair and replication proteins revealed by targeted chemical probes. Nat Chem Biol. 2016;12(7):567-73.

194.   Tahbaz N, Subedi S, Weinfeld M. Role of polynucleotide kinase/phosphatase in mitochondrial DNA repair. Nucleic Acids Res. 2012;40(8):3484-95.

195.   Lakshmipathy U, Campbell C. The human DNA ligase III gene encodes nuclear and mitochondrial proteins. Mol Cell Biol. 1999;19(5):3869-76.

196.   Simsek D, Furda A, Gao Y, Artus J, Brunet E, Hadjantonakis AK, et al. Crucial role for DNA ligase III in mitochondria but not in Xrcc1-dependent repair. Nature. 2011;471(7337):245-8.

197.   Ishii K, Kitagaki H, Kono M, Mori E. Decreased medial temporal oxygen metabolism in Alzheimer's disease shown by PET. J Nucl Med. 1996;37(7):1159-65.

198.   Baloyannis SJ, Costa V, Michmizos D. Mitochondrial alterations in Alzheimer's disease. Am J Alzheimers Dis Other Demen. 2004;19(2):89-93.

199.   Parker WD, Jr., Filley CM, Parks JK. Cytochrome oxidase deficiency in Alzheimer's disease. Neurology. 1990;40(8):1302-3.

200.   Schapira AH, Cooper JM, Dexter D, Clark JB, Jenner P, Marsden CD. Mitochondrial complex I deficiency in Parkinson's disease. J Neurochem. 1990;54(3):823-7.

201.   Kitada T, Asakawa S, Hattori N, Matsumine H, Yamamura Y, Minoshima S, et al. Mutations in the parkin gene cause autosomal recessive juvenile parkinsonism. Nature. 1998;392(6676):605-8.

202.   Valente EM, Abou-Sleiman PM, Caputo V, Muqit MM, Harvey K, Gispert S, et al. Hereditary early-onset Parkinson's disease caused by mutations in PINK1. Science. 2004;304(5674):1158-60.

203.   Lutz AK, Exner N, Fett ME, Schlehe JS, Kloos K, Lammermann K, et al. Loss of parkin or PINK1 function increases Drp1-dependent mitochondrial fragmentation. J Biol Chem. 2009;284(34):22938-51.

204.   Ikebe S, Tanaka M, Ozawa T. Point mutations of mitochondrial genome in Parkinson's disease. Brain Res Mol Brain Res. 1995;28(2):281-95.

205.   Kapsa RM, Jean-Francois MJ, Lertrit P, Weng S, Siregar N, Ojaimi J, et al. Mitochondrial DNA polymorphism in substantia nigra. J Neurol Sci. 1996;144(1-2):204-11.

206.   Kosel S, Grasbon-Frodl EM, Hagenah JM, Graeber MB, Vieregge P. Parkinson disease: analysis of mitochondrial DNA in monozygotic twins. Neurogenetics. 2000;2(4):227-30.

207.   Pyle A, Brennan R, Kurzawa-Akanbi M, Yarnall A, Thouin A, Mollenhauer B, et al. Reduced cerebrospinal fluid mitochondrial DNA is a biomarker for early-stage Parkinson's disease. Ann Neurol. 2015;78(6):1000-4.

208.   Podlesniy P, Figueiro-Silva J, Llado A, Antonell A, Sanchez-Valle R, Alcolea D, et al. Low cerebrospinal fluid concentration of mitochondrial DNA in preclinical Alzheimer disease. Ann Neurol. 2013;74(5):655-68.

209.   Chang BS, Lowenstein DH. Epilepsy. N Engl J Med. 2003;349(13):1257-66.

210.   Debray FG, Lambert M, Chevalier I, Robitaille Y, Decarie JC, Shoubridge EA, et al. Long-term outcome and clinical spectrum of 73 pediatric patients with mitochondrial diseases. Pediatrics. 2007;119(4):722-33.

211.   Zhou Z, Austin GL, Young LEA, Johnson LA, Sun R. Mitochondrial Metabolism in Major Neurological Diseases. Cells. 2018;7(12).

212.   Xie Q, Wu Q, Horbinski CM, Flavahan WA, Yang K, Zhou W, et al. Mitochondrial control by DRP1 in brain tumor initiating cells. Nat Neurosci. 2015;18(4):501-10.

213.   Zhang Y, Qu Y, Gao K, Yang Q, Shi B, Hou P, et al. High copy number of mitochondrial DNA (mtDNA) predicts good prognosis in glioma patients. Am J Cancer Res. 2015;5(3):1207-16.

214.   Scholz C, Golas MM, Weber RG, Hartmann C, Lehmann U, Sahm F, et al. Rare compound heterozygous variants in PNKP identified by whole exome sequencing in a German patient with ataxia-oculomotor apraxia 4 and pilocytic astrocytoma. Clin Genet. 2018.

215.   Taniguchi-Ikeda M, Morisada N, Inagaki H, Ouchi Y, Takami Y, Tachikawa M, et al. Two patients with PNKP mutations presenting with microcephaly, seizure, and oculomotor apraxia. Clin Genet. 2018;93(4):931-3.

216.   Nakashima M, Takano K, Osaka H, Aida N, Tsurusaki Y, Miyake N, et al. Causative novel PNKP mutations and concomitant PCDH15 mutations in a patient with microcephaly with early-onset seizures and developmental delay syndrome and hearing loss. Journal of human genetics. 2014;59(8):471-4.

217.   Shen J, Gilmore EC, Marshall CA, Haddadin M, Reynolds JJ, Eyaid W, et al. Mutations in PNKP cause microcephaly, seizures and defects in DNA repair. Nature genetics. 2010;42(3):245-9.

218.   Reynolds JJ, Walker AK, Gilmore EC, Walsh CA, Caldecott KW. Impact of PNKP mutations associated with microcephaly, seizures and developmental delay on enzyme activity and DNA strand break repair. Nucleic acids research. 2012;40(14):6608-19.

219.   Kuo AJ, Paulson VA, Hempelmann JA, Beightol M, Todhunter S, Colbert BG, et al. Validation and implementation of a modular targeted capture assay for the detection of clinically significant molecular oncology alterations. Pract Lab Med. 2020;19:e00153.

220.   Mani RS, Karimi-Busheri F, Fanta M, Cass CE, Weinfeld M. Spectroscopic studies of DNA and ATP binding to human polynucleotide kinase: evidence for a ternary complex. Biochemistry. 2003;42(41):12077-84.

221.   Abdou I, Poirier GG, Hendzel MJ, Weinfeld M. DNA ligase III acts as a DNA strand break sensor in the cellular orchestration of DNA strand break repair. Nucleic Acids Res. 2015;43(2):875-92.

222.   Rasouli-Nia A, Karimi-Busheri F, Weinfeld M. Stable down-regulation of human polynucleotide kinase enhances spontaneous mutation frequency and sensitizes cells to genotoxic agents. Proc Natl Acad Sci U S A. 2004;101(18):6905-10.

223.   Mani RS, Karimi-Busheri F, Fanta M, Caldecott KW, Cass CE, Weinfeld M. Biophysical characterization of human XRCC1 and its binding to damaged and undamaged DNA. Biochemistry. 2004;43(51):16505-14.

224.   Chen YH, Yang JT, Chau KH. Determination of the helix and beta form of proteins in aqueous solution by circular dichroism. Biochemistry. 1974;13(16):3350-9.

225.   Chalasani SL, Kawale AS, Akopiants K, Yu Y, Fanta M, Weinfeld M, et al. Persistent 3'-phosphate termini and increased cytotoxicity of radiomimetic DNA double-strand breaks in cells lacking polynucleotide kinase/phosphatase despite presence of an alternative 3'-phosphatase. DNA Repair (Amst). 2018;68:12-24.

226.   Coquelle N, Havali-Shahriari Z, Bernstein N, Green R, Glover JN. Structural basis for the phosphatase activity of polynucleotide kinase/phosphatase on single- and double-stranded DNA substrates. Proc Natl Acad Sci U S A. 2011;108(52):21022-7.

227.   Borowicz S, Van Scoyk M, Avasarala S, Karuppusamy Rathinam MK, Tauler J, Bikkavilli RK, et al. The soft agar colony formation assay. J Vis Exp. 2014(92):e51998.

228.   Wen W, Meinkoth JL, Tsien RY, Taylor SS. Identification of a signal for rapid export of proteins from the nucleus. Cell. 1995;82(3):463-73.

229.   Fukuda M, Asano S, Nakamura T, Adachi M, Yoshida M, Yanagida M, et al. CRM1 is responsible for intracellular transport mediated by the nuclear export signal. Nature. 1997;390(6657):308-11.

230.   Ossareh-Nazari B, Bachelerie F, Dargemont C. Evidence for a role of CRM1 in signal-mediated nuclear protein export. Science. 1997;278(5335):141-4.

231.   Stade K, Ford CS, Guthrie C, Weis K. Exportin 1 (Crm1p) is an essential nuclear export factor. Cell. 1997;90(6):1041-50.

232.   la Cour T, Kiemer L, Molgaard A, Gupta R, Skriver K, Brunak S. Analysis and prediction of leucine-rich nuclear export signals. Protein Eng Des Sel. 2004;17(6):527-36.

233.   Xu D, Marquis K, Pei J, Fu SC, Cagatay T, Grishin NV, et al. LocNES: a computational tool for locating classical NESs in CRM1 cargo proteins. Bioinformatics. 2015;31(9):1357-65.

234.   Kudo N, Wolff B, Sekimoto T, Schreiner EP, Yoneda Y, Yanagida M, et al. Leptomycin B inhibition of signal-mediated nuclear export by direct binding to CRM1. Exp Cell Res. 1998;242(2):540-7.

235.   Coquerelle T, Bopp A, Kessler B, Hagen U. Strand breaks and 5' end-groups in DNA of irradiated thymocytes. Int J Radiat Biol Relat Stud Phys Chem Med. 1973;24(4):397-404.

236.   Henner WD, Rodriguez LO, Hecht SM, Haseltine WA. gamma Ray induced deoxyribonucleic acid strand breaks. 3' Glycolate termini. J Biol Chem. 1983;258(2):711-3.

237.   Livak KJ, Schmittgen TD. Analysis of relative gene expression data using real-time quantitative PCR and the 2(-Delta Delta C(T)) Method. Methods. 2001;25(4):402-8.

238.   Hu Y, Wang C, Huang K, Xia F, Parvin JD, Mondal N. Regulation of 53BP1 protein stability by RNF8 and RNF168 is important for efficient DNA double-strand break repair. PLoS One. 2014;9(10):e110522.

239.   Thullberg M, Stromblad S. Anchorage-independent cytokinesis as part of oncogenic transformation? Cell Cycle. 2008;7(8):984-8.

240.   Galick HA, Marsden CG, Kathe S, Dragon JA, Volk L, Nemec AA, et al. The NEIL1 G83D germline DNA glycosylase variant induces genomic instability and cellular transformation. Oncotarget. 2017;8(49):85883-95.

241.   Johnson KJ, Cullen J, Barnholtz-Sloan JS, Ostrom QT, Langer CE, Turner MC, et al. Childhood brain tumor epidemiology: a brain tumor epidemiology consortium review. Cancer Epidemiol Biomarkers Prev. 2014;23(12):2716-36.

242.   Ostrom QT, Gittleman H, Liao P, Rouse C, Chen Y, Dowling J, et al. CBTRUS statistical report: primary brain and central nervous system tumors diagnosed in the United States in 2007-2011. Neuro Oncol. 2014;16 Suppl 4:iv1-63.

243.   Bermudez-Guzman L, Jimenez-Huezo G, Arguedas A, Leal A. Mutational survivorship bias: The case of PNKP. PLoS One. 2020;15(12):e0237682.

244.   Mani RS, Yu Y, Fang S, Lu M, Fanta M, Zolner AE, et al. Dual modes of interaction between XRCC4 and polynucleotide kinase/phosphatase: implications for nonhomologous end joining. J Biol Chem. 2010;285(48):37619-29.

245.   Mariano AR, Colombo E, Luzi L, Martinelli P, Volorio S, Bernard L, et al. Cytoplasmic localization of NPM in myeloid leukemias is dictated by gain-of-function mutations that create a functional nuclear export signal. Oncogene. 2006;25(31):4376-80.

246.   Sakai A, Nakanishi M, Yoshiyama K, Maki H. Impact of reactive oxygen species on spontaneous mutagenesis in Escherichia coli. Genes Cells. 2006;11(7):767-78.

247.   Schwartzentruber J, Korshunov A, Liu XY, Jones DT, Pfaff E, Jacob K, et al. Driver mutations in histone H3.3 and chromatin remodelling genes in paediatric glioblastoma. Nature. 2012;482(7384):226-31.

248.   Danussi C, Bose P, Parthasarathy PT, Silberman PC, Van Arnam JS, Vitucci M, et al. Atrx inactivation drives disease-defining phenotypes in glioma cells of origin through global epigenomic remodeling. Nat Commun. 2018;9(1):1057.

249.   Bernstein NK, Williams RS, Rakovszky ML, Cui D, Green R, Karimi-Busheri F, et al. The molecular architecture of the mammalian DNA repair enzyme, polynucleotide kinase. Mol Cell. 2005;17(5):657-70.

250.   Mani RS, Fanta M, Karimi-Busheri F, Silver E, Virgen CA, Caldecott KW, et al. XRCC1 stimulates polynucleotide kinase by enhancing its damage discrimination and displacement from DNA repair intermediates. J Biol Chem. 2007;282(38):28004-13.

251.   Mahmood T, Yang PC. Western blot: technique, theory, and trouble shooting. N Am J Med Sci. 2012;4(9):429-34.

252.   Feoktistova M, Geserick P, Leverkus M. Crystal Violet Assay for Determining Viability of Cultured Cells. Cold Spring Harb Protoc. 2016;2016(4):pdb prot087379.

253.   Sanz G, Mir L, Jacquemin-Sablon A. Bleomycin resistance in mammalian cells expressing a genetic suppressor element derived from the SRPK1 gene. Cancer Res. 2002;62(15):4453-8.

254.   Yurchenko EA, Kolesnikova SA, Lyakhova EG, Menchinskaya ES, Pislyagin EA, Chingizova EA, et al. Lanostane Triterpenoid Metabolites from a Penares sp. Marine Sponge Protect Neuro-2a Cells against Paraquat Neurotoxicity. Molecules. 2020;25(22).

255.   Hara H, Araya J, Ito S, Kobayashi K, Takasaka N, Yoshii Y, et al. Mitochondrial fragmentation in cigarette smoke-induced bronchial epithelial cell senescence. Am J Physiol Lung Cell Mol Physiol. 2013;305(10):L737-46.

256.   Freschauf GK, Karimi-Busheri F, Ulaczyk-Lesanko A, Mereniuk TR, Ahrens A, Koshy JM, et al. Identification of a small molecule inhibitor of the human DNA repair enzyme polynucleotide kinase/phosphatase. Cancer Res. 2009;69(19):7739-46.

257.   Miller GW. Paraquat: the red herring of Parkinson's disease research. Toxicol Sci. 2007;100(1):1-2.

258.   Cocheme HM, Murphy MP. Complex I is the major site of mitochondrial superoxide production by paraquat. J Biol Chem. 2008;283(4):1786-98.

259.   Huang CL, Chao CC, Lee YC, Lu MK, Cheng JJ, Yang YC, et al. Paraquat Induces Cell Death Through Impairing Mitochondrial Membrane Permeability. Mol Neurobiol. 2016;53(4):2169-88.

260.   Watson JD, Milner-White EJ. A novel main-chain anion-binding site in proteins: the nest. A particular combination of phi,psi values in successive residues gives rise to anion-binding sites that occur commonly and are found often at functionally important regions. J Mol Biol. 2002;315(2):171-82.

261.   Bernstein NK, Hammel M, Mani RS, Weinfeld M, Pelikan M, Tainer JA, et al. Mechanism of DNA substrate recognition by the mammalian DNA repair enzyme, Polynucleotide Kinase. Nucleic acids research. 2009;37(18):6161-73.

262.   Kalasova I, Hailstone R, Bublitz J, Bogantes J, Hofmann W, Leal A, et al. Pathological mutations in PNKP trigger defects in DNA single-strand break repair but not DNA double-strand break repair. Nucleic Acids Res. 2020;48(12):6672-84.

263.   Coquerelle T, Bopp A, Kessler B, Hagen U. Strand breaks and K' end-groups in DNA of irradiated thymocytes. Int J Radiat Biol Relat Stud Phys Chem Med. 1973;24(4):397-404.

264.   Lennartz M, Coquerelle T, Bopp A, Hagen U. Oxygen--effect on strand breaks and specific end-groups in DNA of irradiated thymocytes. Int J Radiat Biol Relat Stud Phys Chem Med. 1975;27(6):577-87.

265.   Prinos P, Slack C, Lasko DD. 5'phosphorylation of DNA in mammalian cells: identification of a polymin P-precipitable polynucleotide kinase. J Cell Biochem. 1995;58(1):115-31.

266.   Watanabe N, Wachi S, Fujita T. Identification and characterization of BCL-3-binding protein: implications for transcription and DNA repair or recombination. J Biol Chem. 2003;278(28):26102-10.

267.   Bermudez-Guzman L, Leal A. DNA repair deficiency in neuropathogenesis: when all roads lead to mitochondria. Transl Neurodegener. 2019;8:14.

268.   Corasaniti MT, Strongoli MC, Rotiroti D, Bagetta G, Nistico G. Paraquat: a useful tool for the in vivo study of mechanisms of neuronal cell death. Pharmacol Toxicol. 1998;83(1):1-7.

269.   Drechsel DA, Patel M. Role of reactive oxygen species in the neurotoxicity of environmental agents implicated in Parkinson's disease. Free Radic Biol Med. 2008;44(11):1873-86.

270.   McCormack AL, Thiruchelvam M, Manning-Bog AB, Thiffault C, Langston JW, Cory-Slechta DA, et al. Environmental risk factors and Parkinson's disease: selective degeneration of nigral dopaminergic neurons caused by the herbicide paraquat. Neurobiol Dis. 2002;10(2):119-27.

271.   Liou HH, Tsai MC, Chen CJ, Jeng JS, Chang YC, Chen SY, et al. Environmental risk factors and Parkinson's disease: a case-control study in Taiwan. Neurology. 1997;48(6):1583-8.

272.   Castello PR, Drechsel DA, Patel M. Mitochondria are a major source of paraquat-induced reactive oxygen species production in the brain. J Biol Chem. 2007;282(19):14186-93.

273.   Jang YJ, Won JH, Back MJ, Fu Z, Jang JM, Ha HC, et al. Paraquat Induces Apoptosis through a Mitochondria-Dependent Pathway in RAW264.7 Cells. Biomol Ther (Seoul). 2015;23(5):407-13.

274.   Nowikovsky K, Reipert S, Devenish RJ, Schweyen RJ. Mdm38 protein depletion causes loss of mitochondrial K+/H+ exchange activity, osmotic swelling and mitophagy. Cell Death Differ. 2007;14(9):1647-56.

275.   Ahmad T, Aggarwal K, Pattnaik B, Mukherjee S, Sethi T, Tiwari BK, et al. Computational classification of mitochondrial shapes reflects stress and redox state. Cell Death Dis. 2013;4:e461.

276.   Xiong G, Zhao L, Yan M, Wang X, Zhou Z, Chang X. N-acetylcysteine alleviated paraquat-induced mitochondrial fragmentation and autophagy in primary murine neural progenitor cells. J Appl Toxicol. 2019;39(11):1557-67.

277.   Baloyannis SJ. Mitochondrial alterations in Alzheimer's disease. J Alzheimers Dis. 2006;9(2):119-26.

278.   Hirai K, Aliev G, Nunomura A, Fujioka H, Russell RL, Atwood CS, et al. Mitochondrial abnormalities in Alzheimer's disease. J Neurosci. 2001;21(9):3017-23.

279.   Zhang L, Trushin S, Christensen TA, Bachmeier BV, Gateno B, Schroeder A, et al. Altered brain energetics induces mitochondrial fission arrest in Alzheimer's Disease. Sci Rep. 2016;6:18725.

280.   Exner N, Treske B, Paquet D, Holmstrom K, Schiesling C, Gispert S, et al. Loss-of-function of human PINK1 results in mitochondrial pathology and can be rescued by parkin. J Neurosci. 2007;27(45):12413-8.

281.   Raimondi A, Mangolini A, Rizzardini M, Tartari S, Massari S, Bendotti C, et al. Cell culture models to investigate the selective vulnerability of motoneuronal mitochondria to familial ALS-linked G93ASOD1. Eur J Neurosci. 2006;24(2):387-99.

282.   Harmuth T, Prell-Schicker C, Weber JJ, Gellerich F, Funke C, Driessen S, et al. Mitochondrial Morphology, Function and Homeostasis Are Impaired by Expression of an N-terminal Calpain Cleavage Fragment of Ataxin-3. Front Mol Neurosci. 2018;11:368.

283.   Lakshmipathy U, Campbell C. Mitochondrial DNA ligase III function is independent of Xrcc1. Nucleic Acids Res. 2000;28(20):3880-6.

284.   Ghosh A, Bhattacharjee S, Chowdhuri SP, Mallick A, Rehman I, Basu S, et al. SCAN1-TDP1 trapping on mitochondrial DNA promotes mitochondrial dysfunction and mitophagy. Sci Adv. 2019;5(11):eaax9778.

285.   Chiang SC, Meagher M, Kassouf N, Hafezparast M, McKinnon PJ, Haywood R, et al. Mitochondrial protein-linked DNA breaks perturb mitochondrial gene transcription and trigger free radical-induced DNA damage. Sci Adv. 2017;3(4):e1602506.

286.   Rossi MN, Carbone M, Mostocotto C, Mancone C, Tripodi M, Maione R, et al. Mitochondrial localization of PARP-1 requires interaction with mitofilin and is involved in the maintenance of mitochondrial DNA integrity. J Biol Chem. 2009;284(46):31616-24.

287.   von der Malsburg K, Muller JM, Bohnert M, Oeljeklaus S, Kwiatkowska P, Becker T, et al. Dual role of mitofilin in mitochondrial membrane organization and protein biogenesis. Dev Cell. 2011;21(4):694-707.

288.   John GB, Shang Y, Li L, Renken C, Mannella CA, Selker JM, et al. The mitochondrial inner membrane protein mitofilin controls cristae morphology. Mol Biol Cell. 2005;16(3):1543-54.

289.   Madungwe NB, Feng Y, Lie M, Tombo N, Liu L, Kaya F, et al. Mitochondrial inner membrane protein (mitofilin) knockdown induces cell death by apoptosis via an AIF-PARP-dependent mechanism and cell cycle arrest. Am J Physiol Cell Physiol. 2018;315(1):C28-C43.
290.   Coleman WB, Tsongalis GJ. Essential concepts in molecular pathology. 2. ed. San Diego: Elsevier; 2019. pages cm p.
291.   Alper JS. Genetic complexity in single gene diseases. BMJ. 1996;312(7025):196-7.
292.   Snell RG, MacMillan JC, Cheadle JP, Fenton I, Lazarou LP, Davies P, et al. Relationship between trinucleotide repeat expansion and phenotypic variation in Huntington's disease. Nature genetics. 1993;4(4):393-7.
293.   Walker FO. Huntington's disease. Lancet. 2007;369(9557):218-28.
294.   Andrew SE, Goldberg YP, Kremer B, Telenius H, Theilmann J, Adam S, et al. The relationship between trinucleotide (CAG) repeat length and clinical features of Huntington's disease. Nature genetics. 1993;4(4):398-403.
295.   Taylor AM, Byrd PJ. Molecular pathology of ataxia telangiectasia. J Clin Pathol. 2005;58(10):1009-15.
296.   Riordan JR, Rommens JM, Kerem B, Alon N, Rozmahel R, Grzelczak Z, et al. Identification of the cystic fibrosis gene: cloning and characterization of complementary DNA. Science. 1989;245(4922):1066-73.
297.   Veit G, Avramescu RG, Chiang AN, Houck SA, Cai Z, Peters KW, et al. From CFTR biology toward combinatorial pharmacotherapy: expanded classification of cystic fibrosis mutations. Mol Biol Cell. 2016;27(3):424-33.
298.   Cutting GR. Cystic fibrosis genetics: from molecular understanding to clinical application. Nat Rev Genet. 2015;16(1):45-56.
299.   Dumitrache LC, McKinnon PJ. Polynucleotide kinase-phosphatase (PNKP) mutations and neurologic disease. Mech Ageing Dev. 2016.
300.   Milholland B, Dong X, Zhang L, Hao X, Suh Y, Vijg J. Differences between germline and somatic mutation rates in humans and mice. Nat Commun. 2017;8:15183.
301.   Lynch M. Evolution of the mutation rate. Trends Genet. 2010;26(8):345-52.
302.   Cairns J. Mutation selection and the natural history of cancer. Nature. 1975;255(5505):197-200.
303.   Lawrence MS, Stojanov P, Polak P, Kryukov GV, Cibulskis K, Sivachenko A, et al. Mutational heterogeneity in cancer and the search for new cancer-associated genes. Nature. 2013;499(7457):214-8.
304.   Vogelstein B, Papadopoulos N, Velculescu VE, Zhou S, Diaz LA, Jr., Kinzler KW. Cancer genome landscapes. Science. 2013;339(6127):1546-58.
305.   Shin W, Alpaugh W, Hallihan LJ, Sinha S, Crowther E, Martin GR, et al. PNKP is required for maintaining the integrity of progenitor cell populations in adult mice. Life Sci Alliance. 2021;4(9).
306.   Athma P, Rappaport R, Swift M. Molecular genotyping shows that ataxia-telangiectasia heterozygotes are predisposed to breast cancer. Cancer Genet Cytogenet. 1996;92(2):130-4.
307.   Geoffroy-Perez B, Janin N, Ossian K, Lauge A, Croquette MF, Griscelli C, et al. Cancer risk in heterozygotes for ataxia-telangiectasia. Int J Cancer. 2001;93(2):288-93.

308.   Hirai Y, Noda A, Kodama Y, Cordova KA, Cullings HM, Yonehara S, et al. Increased risk of skin cancer in Japanese heterozygotes of xeroderma pigmentosum group A. J Hum Genet. 2018;63(11):1181-4.

309.   Steffen J, Varon R, Mosor M, Maneva G, Maurer M, Stumm M, et al. Increased cancer risk of heterozygotes with NBS1 germline mutations in Poland. Int J Cancer. 2004;111(1):67-71.

310.   Seemanova E, Jarolim P, Seeman P, Varon R, Digweed M, Swift M, et al. Cancer risk of heterozygotes with the NBN founder mutation. J Natl Cancer Inst. 2007;99(24):1875-80.

311.   Coutinho P, Barbot C, Coutinho P. Ataxia with Oculomotor Apraxia Type 1. In: Adam MP, Ardinger HH, Pagon RA, Wallace SE, Bean LJH, Mirzaa G, et al., editors. GeneReviews((R)). Seattle (WA)1993.

312.   Nawathe A, Doherty J, Pandya P. Fetal microcephaly. BMJ. 2018;361:k2232.

313.   Choong CJ, Baba K, Mochizuki H. Gene therapy for neurological disorders. Expert Opin Biol Ther. 2016;16(2):143-59.

314.   Harper SQ, Staber PD, He X, Eliason SL, Martins IH, Mao Q, et al. RNA interference improves motor and neuropathological abnormalities in a Huntington's disease mouse model. Proc Natl Acad Sci U S A. 2005;102(16):5820-5.

315.   Loy CT, Schofield PR, Turner AM, Kwok JB. Genetics of dementia. Lancet. 2014;383(9919):828-40.

316.   Zhang J, Wu X, Qin C, Qi J, Ma S, Zhang H, et al. A novel recombinant adeno-associated virus vaccine reduces behavioral impairment and beta-amyloid plaques in a mouse model of Alzheimer's disease. Neurobiol Dis. 2003;14(3):365-79.

317.   Kells AP, Henry RA, Connor B. AAV-BDNF mediated attenuation of quinolinic acid-induced neuropathology and motor function impairment. Gene Ther. 2008;15(13):966-77.

318.   Deverman BE, Ravina BM, Bankiewicz KS, Paul SM, Sah DWY. Gene therapy for neurological disorders: progress and prospects. Nat Rev Drug Discov. 2018;17(10):767.

319.   Traber MG, Atkinson J. Vitamin E, antioxidant and nothing more. Free Radic Biol Med. 2007;43(1):4-15.

320.   Chow CK. Vitamin E regulation of mitochondrial superoxide generation. Biol Signals Recept. 2001;10(1-2):112-24.

321.   Schirinzi T, Martella G, Imbriani P, Di Lazzaro G, Franco D, Colona VL, et al. Dietary Vitamin E as a Protective Factor for Parkinson's Disease: Clinical and Experimental Evidence. Front Neurol. 2019;10:148.

322.   Zhou J, Wang H, Shen R, Fang J, Yang Y, Dai W, et al. Mitochondrial-targeted antioxidant MitoQ provides neuroprotection and reduces neuronal apoptosis in experimental traumatic brain injury possibly via the Nrf2-ARE pathway. Am J Transl Res. 2018;10(6):1887-99.

323.   Parsons JL, Khoronenkova SV, Dianova, II, Ternette N, Kessler BM, Datta PK, et al. Phosphorylation of PNKP by ATM prevents its proteasomal degradation and enhances resistance to oxidative stress. Nucleic Acids Res. 2012;40(22):11404-15.

324.   Yablonska S, Ganesan V, Ferrando LM, Kim J, Pyzel A, Baranova OV, et al. Mutant huntingtin disrupts mitochondrial proteostasis by interacting with TIM23. Proc Natl Acad Sci U S A. 2019;116(33):16593-602.

325.   Feng W, Liu HK, Kawauchi D. CRISPR-engineered genome editing for the next generation neurological disease modeling. Prog Neuropsychopharmacol Biol Psychiatry. 2018;81:459-67.

326.   Iyer V, Boroviak K, Thomas M, Doe B, Riva L, Ryder E, et al. No unexpected CRISPR-Cas9 off-target activity revealed by trio sequencing of gene-edited mice. PLoS Genet. 2018;14(7):e1007503.

327.   Hunker AC, Soden ME, Krayushkina D, Heymann G, Awatramani R, Zweifel LS. Conditional Single Vector CRISPR/SaCas9 Viruses for Efficient Mutagenesis in the Adult Mouse Nervous System. Cell Rep. 2020;30(12):4303-16 e6.

Appendix

Original article

Neurological disorders associated with DNA strand-break processing enzymes

Bingcheng Jiang[a], J.N. Mark Glover[b], Michael Weinfeld[a],*

[a] Department of Oncology, University of Alberta, Cross Cancer Institute, 11560 University Avenue, Edmonton, Alberta, T6G 1Z2, Canada
[b] Department of Biochemistry, Medical Sciences Building, University of Alberta, Edmonton, Alberta, T6G 2H7, Canada

ABSTRACT

The termini of DNA strand breaks induced by reactive oxygen species or by abortive DNA metabolic intermediates require processing to enable subsequent gap filling and ligation to proceed. The three proteins, tyrosyl DNA-phosphodiesterase 1 (TDP1), aprataxin (APTX) and polynucleotide kinase/phosphatase (PNKP) each act on a discrete set of modified strand-break termini. Recently, a series of neurodegenerative and neurodevelopmental disorders have been associated with mutations in the genes coding for these proteins. Mutations in *TDP1* and *APTX* have been linked to Spinocerebellar ataxia with axonal neuropathy (SCAN1) and Ataxia-ocular motor apraxia 1 (AOA1), respectively, while mutations in *PNKP* are considered to be responsible for Microcephaly with seizures (MCSZ) and Ataxia-ocular motor apraxia 4 (AOA4). Here we present an overview of the mechanisms of these proteins and how their impairment may give rise to their respective disorders.

© 2016 Elsevier Ireland Ltd. All rights reserved.

Contents

1. Introduction

DNA strand breaks continually arise in cells. The primary sources for this damage are endogenously produced reactive oxygen species (ROS). However, other factors can also contribute to strand break induction. These include DNA metabolic processes, such as DNA repair, topoisomerase-catalyzed DNA unwinding or

DNA ligase-catalyzed strand rejoining, that can be aborted prior to completion (Andres et al., 2015; Caldecott, 2008). The maintenance of the genome is therefore dependent on DNA repair pathways that respond to single- and double-strand breaks. Since the chemical makeup of the termini at many of these strand breaks precludes simple religation, a key component in the repair process is the restoration of the strand break chemistry to a form suitable for DNA polymerases and ligases, i.e. 3′-hydroxyl and 5′-phosphate termini (Andres et al., 2015). Several enzymes are now known to each act on a subset of strand-break termini including tyrosyl DNA-phosphodiesterase 1 (TDP1), aprataxin (APTX) and polynucleotide kinase/phosphatase (PNKP) (Pommier et al., 2014; Schellenberg et al., 2015; Weinfeld et al., 2011).

In addition to the roles these enzymes might play in preventing carcinogenesis and response to cancer therapy, recent studies have highlighted their importance in protection against neurological disorders. Because of their relatively long life span, neuronal cells may be especially sensitive to the deleterious consequences of endogenous DNA damage. Mutations in the genes coding for each of these enzymes are responsible for rare autosomal recessive diseases with varying degrees of severity. A mutation in *TDP1* gives rise to the neurodegenerative disorder Spinocerebellar ataxia with axonal neuropathy (SCAN1) (Takashima et al., 2002), while mutations in *APTX* are responsible for another neurodegenerative disorder, Ataxia-ocular motor apraxia 1 (AOA1) (Moreira et al., 2001). Mutations in *PNKP* underlie both a neurodevelopmental disorder, Microcephaly with seizures (MCSZ) (Shen et al., 2010) and a neurodegenerative disease, Ataxia-ocular motor apraxia 4 (AOA4) (Bras et al., 2015). Here we describe each of these enzymes including the DNA lesions that they act on, their mechanism of action, their role in DNA repair pathways in the nucleus and mitochondria, and how the disease-associated mutations impair their function and cause the observed neurological pathology.

2. Spinocerebellar ataxia with axonal neuropathy (SCAN1) and TDP1

SCAN1 is a neurological autosomal recessive disorder characterized by late childhood (13–15 years of age) onset of a series of symptoms starting with slowly progressing cerebellar ataxia causing unsteady gait, which ultimately leads to wheelchair dependency, followed by areflexia (loss of reflexes) and peripheral neuropathy. Additional symptoms include involuntary movements of the eye (gaze nystagmus) and slurred speech (cerebellar dysarthria). However, affected individuals retain normal intellect and lifespan with no indication of a higher incidence of cancer. Extra-neurological features of SCAN1 include hypoalbuminemia and hypercholesterolemia. SCAN1 is caused by a mutation of *TDP1*, the gene that encodes tyrosyl-DNA phosphodiesterase 1 (TDP1). To date only one mutation in *TDP1* has been linked to the disorder. The mutation results in an amino acid residue change (His493Arg) that disrupts a key active site of the enzyme (Davies et al., 2002; Takashima et al., 2002).

2.1. Tyrosyl-DNA phosphodiesterase 1

Tyrosyl-DNA phosphodiesterase 1 (TDP1) is involved in the repair of several DNA lesions either as the primary agent or in a backup capacity. It has a major role in processing specific types of DNA strand breaks in the nucleus and mitochondria and has more recently been implicated in the repair of abasic sites and ribonucleosides misincorporated into DNA (Andres et al., 2015; Pommier et al., 2014).

Tdp1 was originally isolated from *Saccharomyces cerevisiae* as an enzyme that hydrolyzed the bond between topoisomerase 1

(Top1) and DNA (Pouliot et al., 1999; Yang et al., 1996). During the course of its action Top1 incises one strand of the DNA by forming a transient covalent bond between a tyrosine residue (Y723 in human topoisomerase 1) and the 3′-phosphate terminus of the cleaved DNA (Champoux, 1977). Following relaxation of the DNA, the enzyme normally ligates the DNA. However, poisons such as camptothecin, or its clinical derivatives irinotecan and topotecan, can stall the process by preventing the second step and preserving the protein-DNA complex, often termed the Top1 "dead-end" or Top1 cleavage complex (Hsiang et al., 1985; Pommier et al., 2010). The removal of the "dead-end" complex is achieved by partial proteolysis of the trapped topoisomerase followed by Tdp1 cleavage of the residual peptide-DNA bond (Debethune et al., 2002; Interthal and Champoux, 2011). Processing by Tdp1 occurs in two steps (Fig. 1A); Tdp1 first displaces the Top1 fragment to form a covalent Tdp1-DNA intermediate, and then catalyzes the hydrolysis of the Tdp1-DNA bond (Davies et al., 2003; Raymond et al., 2004). The second step is driven by His493, which is the altered residue responsible for SCAN1. Because the Tdp1-incised DNA retains 3′-phosphate and 5′-hydroxyl termini, processing by PNKP is required before ligation can occur (Plo et al., 2003).

Importantly from the perspective of neurological damage, other, endogenous factors can also lead to stalling of topoisomerase 1. Preexisting lesions in the DNA in close proximity to the sites of topoisomerase 1-mediated incision serve as the main source preventing DNA religation by the enzyme. These lesions include abasic sites, mismatches, nicks or gaps opposite the top1 cleavage site, and certain DNA oxidative base lesions such as 7, 8-dihydro-8-oxoguanine and 5-hydroxycytosine (Pourquier et al., 1997a,b, 1999). In addition to preventing religation, 7, 8-dihydro-8-oxoguanine and 5-hydroxycytosine in certain positions in close proximity to the topoisomerase cleavage site can also enhance DNA scission by the enzyme (Pourquier et al., 1999).

The action of Tdp1 is not confined to Top1 dead-end complexes or to single-strand breaks (SSBs). It can release a variety of 3′-adducts including 3′-terminal abasic sites (Interthal et al., 2005a) and phosphoglycolates, which are strand-break termini generated by ROS and ionizing radiation (Inamdar et al., 2002; Zhou et al., 2009). While Ape1 efficiently removes 3′-phosphoglycolates from SSBs, Tdp1 plays a critical role in their removal at double-strand breaks (DSBs) by hydrolyzing the glycolic acid function. Tdp1 also displays 3′-exonuclease activity. It can remove terminal deoxy- and ribonucleotides leaving a 3′-phosphate terminus (Interthal et al., 2005a). The importance of this function has yet to be fully explored. TDP1 has also been shown to have AP endonuclease activity, and may act in a backup capacity for APE1 (Lebedeva et al., 2013, 2011). A role for TDP1 in the nonhomologous end-joining pathway (NHEJ) for double-strand break repair (DSBR) has been proposed based on the observation that it physically interacts with XLF in a TDP1-XLF-DNA complex, which stimulates TDP1 activity at DSBs (Heo et al., 2015). These investigators also observed that TDP1 promotes DNA binding by Ku70/80.

There is mounting evidence that TDP1 may act on stalled topoisomerase 2 cleavage sites, although this is still an area of controversy. Topoisomerase 2 cleaves both strands of the DNA through the formation of covalent phosphotyrosine bonds with the 5′-termini of the incised duplex DNA, thereby allowing changes to DNA topology prior to catalyzing DNA religation by the topoisomerase (Roca and Wang, 1994). As with Top1, the action of Top2 can be inhibited at the DNA cleavage stage by chemotherapeutic agents, such as etoposide (Pommier et al., 2010), and by preexisting abasic sites and nicks in the Top2 recognition sequence (Wilstermann and Osheroff, 2001). The primary pathway for the repair of these lesions involves 5′-tyrosyl phosphodiesterase activity of TDP2, which hydrolyzes the bond between the 5′-phosphate and Top2, followed by nonhomologous end-joining (Cortes Ledesma et al.,

A. TDP1
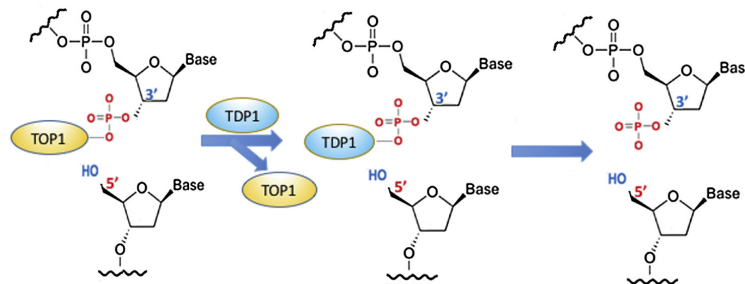
B. APTX
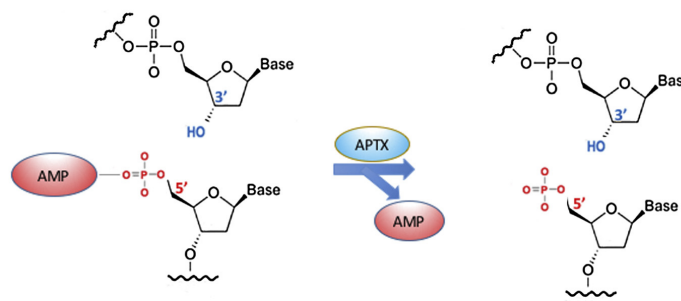
C. PNKP
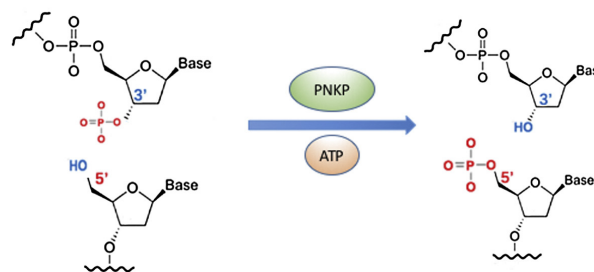
Fig. 1. Reactions catalyzed by DNA strand temini-processing enzymes. (A) TDP1 acts on stalled TOP1 cleavage complexes. Following partial proteolysis of TOP1 covalently bound to the 3′-phosphate, TDP1 carries out nucleophilic attack of the TOP1-DNA phosphotyrosyl bond to form a transient covalent TDP1-DNA intermediate, which subsequently undergoes hydrolysis catalyzed by TDP1 itself. (B) APTX catalyzes the removal of 5′-AMP from abortive ligation intermediates. (C) PNKP catalyzes the phosphorylation of 5′-OH termini, using ATP as the phosphate donor, and the dephosphorylation of 3′-phosphate termini.

2009; Gomez-Herreros et al., 2013). Biochemical analysis using a variety of substrates bearing 5′-phosphotyrosyl termini showed that purified human TDP1 was capable of hydrolyzing the tyrosine residue from a substrate bearing a 4-base overhang, which resembles the break induced by Top2, but not a blunt-ended substrate (Murai et al., 2012). Tdp1-depleted and overexpressing cells have provided mixed answers. Cells from Tdp1 knockout mice and MEFs showed no hypersensitivity to etoposide (Hirano et al., 2007b), while down-regulation of TDP1 in HeLa cells did confer hypersen-

sitivity (Borda et al., 2015). Furthermore, overexpression of TDP1 in HEK293 cells induced resistance to etoposide (Barthelmes et al., 2004).

2.2. Mitochondrial TDP1

Following up on the observation of a prominent TDP1 signal in the cytoplasm of some human neurons (Hirano et al., 2007b), Das et al. showed that a fraction of cellular human TDP1 localizes in
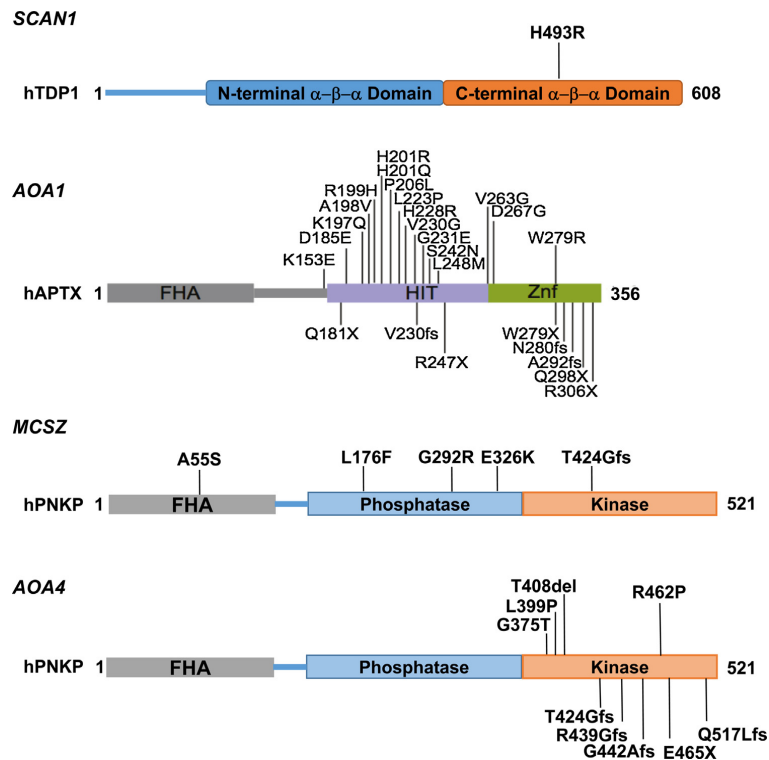
Fig. 2. Protein alterations as a result of mutations in *TDP1, APTX and PNKP* responsible for SCAN1, AOA1, MCSZ and AOA4. FHA represents the forkhead associated domains in APTX and PNKP, HIT and Znf represent the histidine triad and Zinc finger domains in APTX. Frameshifts are indicated by fs, nonsense mutations by an X and deletions by del. The numbers on the righthand side of each protein indicate the size of each protein in terms of the number of amino acid residues. Not shown in the MSCZ figure is a deletion of exon15 accompanied by a premature stop codon arising from a mutation in intron 15 that disrupts normal splicing. (Adapted from Schellenberg et al., 2015 and Bras et al., 2015).

the mitochondria (Das et al., 2010). Further analysis by Das et al. indicated that the mitochondrial protein appears to have a similar, if not identical, molecular weight as the nuclear protein, suggesting that mitochondrial TDP1 does not require post-translational modification, such as the N-terminal truncation seen with mitochondrial APE1 (Chattopadhyay et al., 2006). Mitochondrial TDP1 possesses the same biochemical activities as the nuclear protein and together with mitochondrial DNA ligase III plays a critical role in the base excision repair pathway in response to oxidative damage of mitochondrial DNA, and in the maintenance of mitochondrial DNA integrity in vivo (Das et al., 2010). Subsequently, an extensive histological analysis of human and mouse tissue revealed that Tdp1 is present in the nuclei and mitochondria of many tissues, although interestingly, only cytoplasmic TDP1 was observed in human skeletal muscle (Fam et al., 2013). This group also observed a dramatic increase in the cytoplasmic level of TDP1 in cultured human dermal fibroblasts in response to oxidative stress elicited by treatment with menadione or hydrogen peroxide (Fam et al., 2013).

2.3. SCAN1 cells and model organisms

At the DNA level, a single mutation of the *TDP1* gene (1478A > G) is the cause of SCAN1. Importantly, the resulting His493Arg alteration in TDP1 from SCAN1 patients (Fig. 2), prevents the second step in the processing of the Top1-cleavage complex by TDP1, i.e.

the self-catalyzed hydrolysis of the TDP1-DNA complex, and as a consequence TDP1 remains bound at the 3′-terminus of the strand break (Interthal et al., 2005b). SCAN1 cells are defective in the repair of transcription-dependent topoisomerase I cleavage complexes (Miao et al., 2006) and single strand-break repair (SSBR) (El-Khamisy et al., 2005), as well as the removal of phosphoglycolates at DSBs (Akopiants et al., 2015; Zhou et al., 2005). Interestingly, in contrast to its displacement of Top1 and aberrant formation of a TDP1-DNA complex when handling Top1-DNA complexes, the failure of the mutant TDP1 to process phosphoglycolates is not due to the formation of a stalled TDP1-DNA complex, but rather an inability to initially displace the glycolate group (Hawkins et al., 2009; Zhou et al., 2005).

Tdp1 has been knocked out in several organisms in order to define the role of Tdp1 at the cellular level and model various facets of SCAN1. Three groups generated *Tdp1* knockout mice (Hawkins et al., 2009; Hirano et al., 2007b; Katyal et al., 2007). All reported that cells derived from these *Tdp*$^{-/-}$ mice display a greatly reduced capacity to remove Top1-cleavage complexes. Hawkins et al. observed a failure of extracts of their *Tdp1*$^{-/-}$ cells to remove phosphoglycolates from double-stranded substrates (Hawkins et al., 2009), but, perhaps surprisingly, neural cells derived from *Tdp1*$^{-/-}$ mice failed to show any measurable defect in DSBR in response to ionizing radiation (Katyal et al., 2007). None of the groups observed any overt physiological or behavioural dif-

166

ferences between the $Tdp1^{-/-}$ mice and their wild-type littermates including their CNS system. One study did note a slow progressive reduction of the cerebellum with age in the $Tdp1^{-/-}$ mice (Katyal et al., 2007), but this was not observed in the knockout mice generated by Hawkins et al. even after 22 months (Hawkins et al., 2009). In particular, the latter group found that the granule and Purkinje cells in the cerebellum were present in equal numbers and appeared morphologically similar in the brains of the wildtype and *Tdp1*-/- mice. The failure of the knockout mice to fully recapitulate SCAN1, particularly the failure to develop ataxia, was attributed to the difference between the obstruction to alternative repair processes imposed by the H493R Tdp1-DNA complex compared to the complete loss of Tdp1 (Hawkins et al., 2009; Hirano et al., 2007b).

Studies of glaikit (gkt), the *Drosphila melanogaster* ortholog of *Tdp1* resulted in starker inter-laboratory differences than observed with *Tdp1* knockout mice phenotypes (Dunlop et al., 2004; Guo et al., 2014). The earlier report indicated that loss of gkt severely impairs neuronal development (Dunlop et al., 2004), while the more recent study noted a comparatively benign phenotype (only in mutant females) consisting of shortened lifespan and a late onset reduced climbing ability, both of which could be rescued by expression of *TDP1* (Guo et al., 2014). The reasons for the divergent phenotypes have yet to be resolved.

2.4. Mechanism underlying SCAN1 neuronal atrophy

The question remains as to why inactivation of TDP1 gives rise to the neurological symptoms of SCAN1. The question can be broken down into two components. First, why would neuronal cells be the major target, and second, what is the underlying mechanism responsible for their demise when TDP1 is mutated?

SCAN1 is a neurodegenerative disorder, rather than a neurodevelopmental disorder, and is therefore considered a disease of differentiated post-mitotic neuronal cells. Several key features of neuronal cells may make them especially susceptible to death arising from endogenous damage including (i) their longevity, (ii) their high energy requirement and therefore elevated generation of oxidative free radicals (Bolanos, 2016), (iii) their high transcriptional activity, which will necessitate increased processing by topoisomerases, and (iv) unlike most other non-cycling cells neurons have a capacity to regenerate (Steward et al., 2013). Based on these properties of neuronal cells a number of possible explanations for their degeneration in SCAN1 have been put forward. Not surprisingly, most are predicated on an inability to fully repair DNA strand breaks, but a key issue has been the mechanism for formation of DSBs in non-replicating cells and the subsequent signaling leading to cell death. One source for the induction of DSBs in neurons is transcription arrest by Top1-cleavage complexes (Sordet et al., 2010, 2009), which instigates the formation of triple-stranded DNA/RNA hybrid structures termed R-loops (Aguilera and Garcia-Muse, 2012). These DSBs activate ATM (Cristini et al., 2016; Sordet et al., 2009). While ATM is normally considered protective, it has been shown that in response to damage by camptothecin, ATM in post-mitotic neurons is phosphorylated by Cdk5 at Ser794, promoting further ATM activity that triggers cell death, possibly as a result of re-entry of the neurons into the cell cycle (Tian et al., 2009). Support for this proposed mechanism has been provided from studies with *Schizosaccharomyces pombe*. Like SCAN1 neuronal cells, quiescent *tdp1* mutated *S. pombe* cells accumulate strand breaks and undergo cell death over a period of several days through ATM/Tel1-dependent nuclear DNA degradation (Arcangioli and Ben Hassine, 2009; Ben Hassine and Arcangioli, 2009). In addition, since cell death of the *tdp1 S. pombe* mutants is not dependent on top1 function, it implies that the toxic DNA lesions are most likely strand breaks caused by reactive oxygen species (Ben Hassine and

Arcangioli, 2009). This led the authors to propose that mitochondrial respiration is responsible for the neuronal cell death in SCAN1 patients. Since the mitochondrial form of TDP1 appears to be identical to the nuclear protein (Das et al., 2010), the mitochondrial TDP1 in SCAN1 is also mutated, which raises the possibility that mitochondrial DNA damage contributes to SCAN1 (Sykora et al., 2012).

3. Ataxia-ocular motor apraxia 1 (AOA1) and APTX

In 1988, Aicardi et al. reported a novel neurological syndrome in 14 patients from 10 families (Aicardi et al., 1988). The syndrome, whose symptoms included progressive ataxia, choreoathetosis (irregular movements such as twisting and writhing) and ocular motor apraxia (defective control of eye movement), was termed Ataxia-ocular motor apraxia (AOA). Since then four distinct AOA disorders have been identified, each associated with mutations in different genes: AOA1 is linked to mutations in APTX (Aprataxin) (Date et al., 2001; Moreira et al., 2001), AOA2 is linked to mutations in SETX (Senataxin) (Moreira et al., 2004), AOA3 is linked to mutations in PIK3R5 (Phosphoinositide-3-kinase regulatory subunit 5) (Al Tassan et al., 2012), and AOA4 is linked to mutations in PNKP (Polynucleotide phosphatase/kinase) (Bras et al., 2015).

The mean age of onset of AOA1 is 4.3 years and additional symptoms include cerebellar atrophy, hypoalbuminemia and hypercholesterolemia. Unlike SCAN1, for which only a single mutation has been observed in TDP1, over 20 distinct mutations in APTX have been identified in different AOA1 individuals (Fig. 2), including base substitution and frameshift mutations, and there is some evidence that the nature and site of the mutation may influence the severity of the disorder and age of onset (Le Ber et al., 2003). For example, the A198V mutation is associated with a more choreic phenotype (Le Ber et al., 2003).

3.1. Aprataxin

Following from an observation that APTX possesses an AMP-lysine hydrolase activity (Seidle et al., 2005), Ahel et al. discovered a role for APTX in the resolution of stalled DNA ligation intermediates that contain an adenosine monophosphate moiety covalently linked to the 5′-phosphate terminus of the strand break (Ahel et al., 2006). These intermediates can arise when DNA lesions, such as 8-oxoguanine or an abasic site, at the 3′-terminus of the strand break prevent the second step of the ligation process, which involves phosphodiester formation between the DNA 3′-OH and 5′-phosphate termini and displacement of the AMP (Harris et al., 2009). Under normal circumstances, however, these lesions are considered to be a rare occurrence, but recent evidence has shown that 5′-adenylated termini frequently arise at ribonucleotide terminated strand breaks induced by RNaseH2 incision at sites of ribonucleotide misincorporation into DNA (Tumbale et al., 2014). APTX may also have the capacity to act on 3′-phosphate and 3′-phosphoglycolate termini (Takahashi et al., 2007), but this requires further validation.

APTX is composed of three major domains: an N-terminal forkhead associated (FHA) domain, and a histidine triad (HIT) domain linked to a C-terminal Cys_2His_2 Zn-finger (Znf) domain, which together comprise the catalytic domain and DNA interaction scaffold (Kijas et al., 2006; Rass et al., 2007a; Tumbale et al., 2011). The FHA domain interacts with phosphorylated XRCC1 and XRCC4 (Ahel et al., 2006; Clements et al., 2004; Sano et al., 2004) and PARP (Gueven et al., 2004; Harris et al., 2009), and mediates recruitment of APTX to DNA SSBs (Harris et al., 2009; Hirano et al., 2007a). The finding that the FHA domain also interacts with mediator of DNA-damage checkpoint protein 1 (MDC1) suggests that APTX is

167

involved in the repair of a subset of DSBs (Becherel et al., 2010), in agreement with the observation that APTX hydrolyzes adenylated DSBs in vitro (Rass et al., 2007a). APTX acts by initially displacing the adenylate moiety from the 5′-terminus through nucleophilic attack by the His260 residue to generate a transient covalent protein-AMP complex, which is then hydrolyzed to release the free enzyme and AMP (Fig. 1B) (Rass et al., 2008; Tumbale et al., 2014).

3.2. Mitochondrial APTX

At least one isoform of APTX, containing an N-terminal mitochondrial targeting sequence, has been shown to localize to mitochondria (Sykora et al., 2011). Knockdown of *APTX* expression resulted in mitochondrial dysfunction as indicated by altered ROS production, reduced citrate synthase activity, and lower mitochondrial DNA copy number (Sykora et al., 2011). The knockdown cells also accumulated a significantly higher level of strand breaks in their mitochondrial DNA than in their nuclear DNA (Sykora et al., 2011). The possibility that mitochondria, in comparison to nuclei, do not possess an efficient backup pathway to handle adenylated-DNA termini in the absence of APTX was recently confirmed (Akbari et al., 2015).

3.3. AOA1 cells and APTX knockout mice

To date, the *APTX* mutations found in AOA1 patients are distributed in the HIT and Znf domain, including nonsense truncations, frameshifts and missense mutations, as shown in Fig. 2. No mutations linked to AOA1 have been found in the FHA domain. Using their assay for lysine-AMP hydrolysis, Seidle et al. examined several of the APTX mutations found in AOA1 (Seidle et al., 2005) and found that the A198V, P206L, V263G, D267G, 689insT, W279X, and 840delT proteins to be functionally inactive, while the W279R protein retained a very low level of activity and the K197Q protein was more active, possibly reflecting its milder phenotype (Tranchant et al., 2003).

Cells derived from AOA1 patients have been widely used to study the cellular role of APTX in response to a variety of genotoxic agents, sometimes with seemingly contradictory results. There is little evidence for sensitivity of AOA1 cells to ionizing radiation (Clements et al., 2004; Gueven et al., 2004; Moreira et al., 2001; Mosesso et al., 2005), although APTX colocalizes with XRCC1 and MDC1 along tracks induced by high LET radiation (Becherel et al., 2010; Gueven et al., 2004). Several studies indicated that AOA1 cells are modestly hypersensitive to hydrogen peroxide (Clements et al., 2004; Gueven et al., 2004) and methyl methanesulfonate (MMS) (Clements et al., 2004) consistent with a role in base excision and/or SSBR. However, AOA1 cells bearing the 892C > T (Gln298X) nonsense mutation do not display hypersensitivity to hydrogen peroxide or MMS, but in both cases the repair of SSBs is much slower than in normal cells, suggesting that alternative repair pathways prevent toxicity by these agents (Crimella et al., 2011). This has been substantiated by recent findings showing that DNA polymerase β can remove 5′-adenylated-deoxyribose phosphate groups through its lyase activity and that the long-patch SSBR enzyme flap endonuclease (FEN1) can also remove this end group together with one or two additional nucleotides (Caglayan et al., 2014, 2015). Daley et al. similarly suggested that long patch repair may serve as a backup pathway for removal of 5′-adenylated strand-break termini based on their observation that combined loss of *HNT3* (Aprataxin homolog) and *rad27* (FEN1 homolog) in *S. cerevisiae* induces synergistic sensitivity to hydrogen peroxide and MMS (Daley et al., 2011).

Aptx$^{-/-}$ mice show no overt phenotype (Ahel et al., 2006), although murine *Aptx*$^{-/-}$ primary neural astrocytes respond similarly to genotoxic agents as AOA1 human cells and depend on long-patch SSBR as a back up to the loss of Aptx (Reynolds et al., 2009). Murine *Aptx*$^{-/-}$ embryonic fibroblasts (MEFs) cultured over 2 months showed reduced population doubling and a progressive increase in senescence in comparison to wild-type MEFs, which was ascribed to a progressive build up of DNA damage (Carroll et al., 2015). In order to augment the chances of observing a more obvious phenotype, Carroll et al. generated an *Aptx*$^{-/-}$ mouse expressing a mutant form of superoxide dismutase (*SOD1*^{G93A}) thereby reducing cellular antioxidant homeostasis to increase the constitutive level of oxidative DNA damage (Carroll et al., 2015). Although this model still did not recapitulate the neurological symptoms of AOA1, spinal cord sections from the *APTX*$^{-/-}$*SOD1*^{G93A} mice exhibited a reduction in motor neuron survival compared with sections from *SOD1*^{G93A} mice. Interestingly, the *APTX*$^{-/-}$*SOD1*^{G93A} mice also displayed down-regulation of insulin-like growth factor 1 indicative of premature aging. The *APTX*$^{-/-}$*SOD1*^{G93A} MEFs were slightly more sensitive to hydrogen peroxide than the *APTX*$^{-/-}$ or *SOD1*^{G93A} MEFs and showed slower strand break repair.

3.4. Mechanism underlying AOA1

This still remains an open area of research, in part because of the lack of a suitable animal model. At the molecular level, most attention has focused on the idea of a progressive accumulation of DNA lesions due to mutations in the catalytic/DNA interacting domain of APTX (Rass et al., 2007b; Schellenberg et al., 2015; Tada et al., 2010). If this is the case, another question arises as to what form of DNA damage is critical, single or double-strand breaks in nuclear or mitochondrial DNA (Akbari et al., 2015; Iyama and Wilson, 2013). Aside from the mitochondrial targeting sequence, the mitochondrial isoform of APTX is essentially the same as the nuclear protein and thus will carry the same mutations in AOA1, and so faulty repair of mitochondrial DNA strand breaks may contribute to AOA1 (Sykora et al., 2012). A consequence of accumulated DNA damage is its impact on transcription, which tends to be high in neuronal cells (Sarkander and Dulce, 1978). Inhibition of transcription may lead to apoptosis (Ljungman and Lane, 2004) or, potentially, altered neuronal development and plasticity (Borquez et al., 2016).

Several groups have observed that cells derived from individuals with the W279X stop-codon mutation of APTX also have markedly reduced levels of the antioxidant and electron transporter coenzyme Q10 (CoQ$_{10}$) (Castellotti et al., 2011; Le Ber et al., 2007; Quinzii et al., 2005). A detailed analysis of the underlying mechanism for the diminished CoQ$_{10}$ biosynthesis indicated that APTX depletion leads to reduced levels of APE1, which in turn downregulates NRF1 and NRF2 and downstream biomolecules including CoQ$_{10}$, and led to the suggestion that this pathway, and not the lack of mitochondrial DNA repair, is responsible for the mitochondrial dysfunction seen in AOA1 cells (Garcia-Diaz et al., 2015).

4. Microcephaly with seizures (MCSZ) and ataxia-ocular motor apraxia 4 (AOA4) and PNKP

Mutations in the *PNKP* gene coding for polynucleotide kinase/phosphatase are responsible for both MCSZ and AOA4. MCSZ is a rare autosomal recessive neurodevelopmental disorder. In addition to microcephaly and early-onset seizures, the children display developmental delay and hyperactivity (Nakashima et al., 2014; Shen et al., 2010). To date the disease has been recorded in 8 families. The disease can vary from severe microcephaly and difficult to control seizures to moderate microcephaly with seizures that can be effectively controlled. Up to 21 years of age (the oldest patient discussed in the literature) there was no indication of ataxia, immunodeficiency or cancer in any affected individual (Shen et al., 2010). One child with MCSZ was also found to carry muta-

tions in PCDH15, the gene responsible for Usher syndrome type 1F, and the child showed symptoms of both disorders (Nakashima et al., 2014). Importantly, MCSZ patients do not show signs of neurodegeneration. AOA4, on the other hand, is a rare autosomal neurodegenerative disorder with onset between 1 and 9 years of age (Bras et al., 2015). The symptoms include ataxia, oculomotor apraxia, and peripheral neuropathy. Muscle weakness progresses so that most individuals become wheelchair bound by the second or third decade. Some patients suffer cognitive impairment, and brain scans have revealed cerebellar atrophy in all patients (Bras et al., 2015; Paucar et al., 2016; Tzoulis et al., 2016).Two brothers with a *PNKP* mutation appear to show compound symptoms encompassing both conditions, i.e. microcephaly, epileptic seizures, progressive polyneuropathy and progressive cerebellar atrophy (Poulton et al., 2013).

4.1. Polynucleotide kinase/phosphatase

PNKP is a bifunctional enzyme that catalyzes the phosphorylation of 5′-hydroxyl termini and the dephosphorylation of 3′-phosphate termini (Fig. 1C) (Jilani et al., 1999; Karimi-Busheri et al., 1999; Pheiffer and Zimmerman, 1982). It is a nuclear and mitochondrial protein involved in SSBR, NHEJ and Alt-NHEJ (Audebert et al., 2006; Chappell et al., 2002; Karimi-Busheri et al., 1998; Whitehouse et al., 2001), but is not required for homologous recombination (Karimi-Busheri et al., 2007; Shimada et al., 2015). Strand breaks with 5′-hydroxyl and 3′-phosphate termini are commonly produced by hydroxyl radicals and ionizing radiation (Dedon, 2008; Henner et al., 1983), and they are also the product of Top1 dead-end complexes following removal of the covalently bound Top1 by proteolysis and the action of Tdp1 (Plo et al., 2003). In addition, strand breaks with 3′-phosphate termini are generated after removal of the glycolate moiety from phosphoglycolate termini at DSB termini by TDP1 (Inamdar et al., 2002; Zhou et al., 2009), and by several DNA glycosylases, such as NEIL1 and 2, that cleave abasic sites by β,δ-elimination (Hazra et al., 2002a,b; Rosenquist et al., 2003). The capacity of these glycosylases to act on abasic sites provides an alternative base excision repair pathway to the canonical APE1-dependent mechanism (Wiederhold et al., 2004). Down-regulation of *PNKP* expression increases spontaneous mutation frequency, indicating the importance of PNKP in protecting the genome following endogenous DNA damage (Rasouli-Nia et al., 2004). PNKP depletion also increases the sensitivity of cells to ionizing radiation, hydrogen peroxide and the topoisomerase 1 poison camptothecin (Rasouli-Nia et al., 2004).

PNKP is composed of three domains, an FHA domain at the N-terminus, similar to the APTX FHA domain, and the phosphatase domain and C-terminal kinase domain that together constitute the catalytic domain (Bernstein et al., 2005). The FHA domain is not required for enzyme activity, but, as with the APTX FHA domain, it binds to phosphorylated XRCC1 and XRCC4 for optimal response in SSBR and NHEJ, respectively (Koch et al., 2004; Loizou et al., 2004). Interaction of non-phosphorylated XRCC1 and XRCC4 with PNKP also stimulates PNKP catalytic activity although the binding is to the catalytic domain rather than the FHA domain (Lu et al., 2010; Mani et al., 2007; Whitehouse et al., 2001).

The *PNKP* mutations identified in the MSCZ patients to date appear mostly in the phosphatase and kinase domains (Fig. 2) (Nakashima et al., 2014; Shen et al., 2010). The patient with the 163G > T (p.A55S) mutation in the FHA domain also carries a 874G > A (p.G292R) mutation in the phosphatase domain (Nakashima et al., 2014). The mutations responsible for AOA4, in contrast, all appear in the kinase domain (Bras et al., 2015; Paucar et al., 2016; Tzoulis et al., 2016). Intriguingly, the mutation giving rise to the T424G-frameshift was found in four of the MCSZ families and in an AOA4 proband and in the brothers exhibiting the com-

bined symptoms of MSCZ and AOA4 (Bras et al., 2015; Poulton et al., 2013; Shen et al., 2010). In addition, a homozygous recessive missense mutation in the FHA domain of *PNKP* (58G > A, p.P20S) was identified in a proband with epileptic encephalopathy but with no sign of microcephaly or developmental delay (Carvill et al., 2013).

4.2. Mitochondrial PNKP

PNKP localizes to mitochondria as well as the nucleus (Mandal et al., 2012; Tahbaz et al., 2012). The mitochondrial PNKP appears to be the same full-length isoform as the nuclear protein (Tahbaz et al., 2012) and thus any mutations in *PNKP* will affect the mitochondrial protein as well as the nuclear protein. In mitochondria PNKP binds to NEIL2 and to DNA polymerase γ, indicating a role for PNKP in mitochondrial BER (Mandal et al., 2012). Depletion of cellular PNKP increased the levels of SSBs in untreated as well as hydrogen peroxide-treated cells (Mandal et al., 2012; Tahbaz et al., 2012). Both the kinase and phosphatase activities were required to fully restore the DNA in the hydrogen peroxide-treated cells (Tahbaz et al., 2012).

4.3. MCSZ cells and PNKP knockout mice

Mutations in PNKP that give rise to neurological disorders are shown in Fig. 2. An examination of Epstein-Barr virus-transformed lymphocytes derived from affected MCSZ individuals indicated a substantial decrease in their PNKP protein content, and their repair of damage induced by either hydrogen peroxide or camptothecin was severely impaired (Reynolds et al., 2012; Shen et al., 2010). Analysis of the kinase activity of the mutated proteins revealed that the frameshift mutations in the kinase domain abrogated kinase activity, while the E326K protein had similar activity as the wild-type protein (Reynolds et al., 2012). Interestingly, the L176K protein showed reduced kinase activity despite being located in the phosphatase domain. A similar analysis revealed that only the L176K mutation resulted in a partial decrease in phosphatase activity (Reynolds et al., 2012). Skin fibroblasts isolated from the two affected brothers exhibiting the combined symptoms of MSCZ and AOA4 also displayed reduced PNKP protein content and increased apoptosis in response to stress induced by serum starvation followed by treatment with dithiothreitol (Poulton et al., 2013).

Unlike *Tdp1* and *Aptx*, embryo-wide knockout of *Pnkp* is embryonic lethal in mice, as is homozygous introduction of the murine T424G-frameshift mutation (Shimada et al., 2015). However, Shimada et al. were able to generate a Nestin-cre knockout just targeting the nervous system that died 5 days after birth, and more importantly, a viable hypomorphic conditional knockout with a smaller brain that more closely mimics MCSZ (Shimada et al., 2015). Analysis of neurogenesis in these mice revealed increased DNA damage and apoptosis in the neocortex of E13.5 embryos and a reduction in proliferating cells. Apoptosis was shown to be dependent on p53. A less overt, but nonetheless discernable, response was observed when the loss of PNKP commenced after birth. For example, there was a significant reduction in the level of myelin basic protein required for myelination of oligodendrocytes.

4.4. Mechanism underlying MCSZ and AOA4

Several mutations in *PNKP* give rise to MCSZ and AOA4. Those responsible for MCSZ lead to a decrease in the cellular levels of PNKP, down to 5–10% of wild-type levels in EBV-transformed lymphocytes (Reynolds et al., 2012; Shen et al., 2010). The reduction is probably not due to lower transcriptional levels (Shen et al., 2010), but more likely due to protein instability (Reynolds et al., 2012). At this point it is understandable that the proteins produced by the frameshift mutations would show reduced stability, but it is

less clear why the L176F and E326K modified proteins should be less stable than the wild-type protein. In addition, the L176F modified protein showed reduced phosphatase activity (Reynolds et al., 2012). Leu176 is packed in the hydrophobic core of the phosphatase domain, and positioned immediately under the phosphatase active site cleft. Mutation to the slightly larger phenylalanine residue could introduce steric clashes that may distort the phosphatase active site geometry (Reynolds et al., 2012). The E326K mutation does not appear to interfere with the catalytic activity of recombinant PNKP and yet the severity of the resultant MCSZ is similar to that arising from the other mutations. This may be due to an intrinsic loss of stability, but we speculate that it is also possible that in the wild-type protein the Glu326, which is exposed on the surface of the phosphatase domain distant from the active site and DNA binding surface (Bernstein et al., 2005), may interact with XRCC4-Lig4 in a way that modulates PNKP function. The fact that the E326K MCSZ mutation is a charge swap is consistent with an electrostatic interaction between this region and a partner in XRCC4-Lig4. It is instructive that none of the mutations in either MSCZ or AOA4 abolish the PNKP phosphatase activity, perhaps indicating that complete loss of this function would be lethal during neurogenesis as a result of the frequency of generating 3'-phosphate termini and lack of an efficient backup pathway.

The murine *Pnkp* knockout model clearly established that loss of Pnkp is considerably more detrimental than loss of either Tdp1 or Aptx and this may explain why mutations in *PNKP* give rise to a severe neurodevelopmental disorder as well as a neurodegenerative disorder. Mechanistically, this may be due to the important role PNKP plays in both SSBR, the loss of which may underlie AOA4, and NHEJ, which if partially abrogated may be the cause of MCSZ. In a similar vein, Shen et al. suggested that the symptoms of MCSZ itself reflected PNKP's participation in both repair pathways by pointing out that mutations to the NHEJ proteins LIG4 and XRCC4 also cause microcephaly while mutations to the SSBR protein XRCC1 causes seizure-like behavior (Shen et al., 2010). However, it is hard to reconcile these ideas with the perplexing T424G-frameshift mutation common to both MCSZ and AOA4 patients. It implies that factors beyond the site of mutation in *PNKP* contribute to the disease process. For example, it has recently been shown that exposure of cells to cholesterol, which is abundant in the brain, stimulates PNKP expression in a human lymphoblastic lymphoma cell line (Codini et al., 2016).

The hypomorphic *Pnkp* model was able to partially recapitulate the symptoms of MCSZ (Shimada et al., 2015). Importantly, it revealed that the reduction of functional PNKP during neural development led to increased DNA damage and p53-dependent apoptosis in neural progenitor cells. Deleting PNKP postnatally also caused progressive damage to post-mitotic neurons, although it was not clear to what extent this mimics AOA4. Nonetheless, the investigators suggested that the loss of oligodendrocytes might be due to disruption of transcription in the DNA damaged cells.

5. Conclusions

Neurological problems are a common consequence of mutations in genes encoding DNA repair proteins in several DNA repair pathways. Here we have discussed the neurodegenerative and neurodevelopmental diseases arising from mutations in genes coding for proteins that process DNA strand-break termini. Many outstanding issues remain before we obtain a complete picture of the link between DNA damage and neurodegeneration and neurodevelopment. From the perspective of molecular mechanism(s), we still need to clarify the respective roles of single and double-strand break repair and the relative importance of damage to nuclear vs mitochondrial DNA. Most attention has focused on nuclear DNA,

but it is clear that mitochondria pathology contributes significantly to neurodegenerative diseases including Parkinson's disease (Ryan et al., 2015) and disorders involving epilepsy (Zsurka and Kunz, 2015). We then need to understand the consequences of unrepaired damage – are the downstream consequences related to one or a specific set of genes or proteins or are the responses driven by a global effect such as inhibition of transcription? Next we have to consider the subset of cells that appear to be affected by each of the disorders discussed. This will require new tools such as murine cerebellar organotypic cultures (Tzur-Gilat et al., 2013), and alternative animal models, especially for SCAN1, AOA1 and AOA4.

References

Aguilera, A., Garcia-Muse, T., 2012. R loops: from transcription byproducts to threats to genome stability. Mol. Cell 46, 115–124.

Ahel, I., Rass, U., El-Khamisy, S.F., Katyal, S., Clements, P.M., McKinnon, P.J., Caldecott, K.W., West, S.C., 2006. The neurodegenerative disease protein aprataxin resolves abortive DNA ligation intermediates. Nature 443, 713–716.

Aicardi, J., Barbosa, C., Andermann, E., Andermann, F., Morcos, R., Ghanem, Q., Fukuyama, Y., Awaya, Y., Moe, P., 1988. Ataxia-ocular motor apraxia: a syndrome mimicking ataxia-telangiectasia. Ann. Neurol. 24, 497–502.

Akbari, M., Sykora, P., Bohr, V.A., 2015. Slow mitochondrial repair of 5'-AMP renders mtDNA susceptible to damage in APTX deficient cells. Sci. Rep. 5, 12876.

Akopiants, K., Mohapatra, S., Menon, V., Zhou, T., Valerie, K., Povirk, L.F., 2015. Tracking the processing of damaged DNA double-strand break ends by ligation-mediated PCR: increased persistence of 3'-phosphoglycolate termini in SCAN1 cells. Nucleic Acids Res. 42, 3125–3137.

Al Tassan, N., Khalil, D., Shinwari, J., Al Sharif, L., Bavi, P., Abduljaleel, Z., Abu Dhaim, N., Magrashi, A., Bobis, S., Ahmed, H., et al., 2012. A missense mutation in PIK3R5 gene in a family with ataxia and oculomotor apraxia. Hum. Mutat. 33, 351–354.

Andres, S.N., Schellenberg, M.J., Wallace, B.D., Tumbale, P., Williams, R.S., 2015. Recognition and repair of chemically heterogeneous structures at DNA ends. Environ. Mol. Mutagen. 56, 1–21.

Arcangioli, B., Ben Hassine, S., 2009. Unrepaired oxidative DNA damage induces an ATR/ATM apoptotic-like response in quiescent fission yeast. Cell Cycle 8, 2326–2331.

Audebert, M., Salles, B., Weinfeld, M., Calsou, P., 2006. Involvement of polynucleotide kinase in a poly(ADP-ribose) polymerase-1-dependent DNA double-strand breaks rejoining pathway. J. Mol. Biol. 356, 257–265.

Barthelmes, H.U., Habermeyer, M., Christensen, M.O., Mielke, C., Interthal, H., Pouliot, J.J., Boege, F., Marko, D., 2004. TDP1 overexpression in human cells counteracts DNA damage mediated by topoisomerases I and II. J. Biol. Chem. 279, 55618–55625.

Becherel, O.J., Jakob, B., Cherry, A.L., Gueven, N., Fusser, M., Kijas, A.W., Peng, C., Katyal, S., McKinnon, P.J., Chen, J., et al., 2010. CK2 phosphorylation-dependent interaction between aprataxin and MDC1 in the DNA damage response. Nucleic Acids Res. 38, 1489–1503.

Ben Hassine, S., Arcangioli, B., 2009. Tdp1 protects against oxidative DNA damage in non-dividing fission yeast. EMBO J. 28, 632–640.

Bernstein, N.K., Williams, R.S., Rakovszky, M.L., Cui, D., Green, R., Karimi-Busheri, F., Mani, R.S., Galicia, S., Koch, C.A., Cass, C.E., et al., 2005. The molecular architecture of the mammalian DNA repair enzyme, polynucleotide kinase. Mol. Cell 17, 657–670.

Bolanos, J.P., 2016. Bioenergetics and redox adaptations of astrocytes to neuronal activity. J. Neurochem.

Borda, M.A., Palmitelli, M., Veron, G., Gonzalez-Cid, M., de Campos Nebel, M., 2015. Tyrosyl-DNA-phosphodiesterase I (TDP1) participates in the removal and repair of stabilized-Top2alpha cleavage complexes in human cells. Mutat. Res. 781, 37–48.

Borquez, D.A., Urrutia, P.J., Wilson, C., van Zundert, B., Nunez, M.T., Gonzalez-Billault, C., 2016. Dissecting the role of redox signaling in neuronal development. J. Neurochem. 137, 506–517.

Bras, J., Alonso, I., Barbot, C., Costa, M.M., Darwent, L., Orme, T., Sequeiros, J., Hardy, J., Coutinho, P., Guerreiro, R., 2015. Mutations in PNKP cause recessive ataxia with oculomotor apraxia type 4. Am. J. Hum. Genet. 96, 474–479.

Caglayan, M., Batra, V.K., Sassa, A., Prasad, R., Wilson, S.H., 2014. Role of polymerase beta in complementing aprataxin deficiency during abasic-site base excision repair. Nat. Struct. Mol. Biol. 21, 497–499.

Caglayan, M., Horton, J.K., Prasad, R., Wilson, S.H., 2015. Complementation of aprataxin deficiency by base excision repair enzymes. Nucleic Acids Res. 43, 2271–2281.

Caldecott, K.W., 2008. Single-strand break repair and genetic disease. Nat. Rev. Genet. 9, 619–631.

Carroll, J., Page, T.K., Chiang, S.C., Kalmar, B., Bode, D., Greensmith, L., McKinnon, P.J., Thorpe, J.R., Hafezparast, M., El-Khamisy, S.F., 2015. Expression of a pathogenic mutation of SOD1 sensitizes aprataxin-deficient cells and mice to oxidative stress and triggers hallmarks of premature ageing. Hum. Mol. Genet. 24, 828–840.

Carvill, G.L., Heavin, S.B., Yendle, S.C., McMahon, J.M., Cook, J., Khan, A., Dorschner, M.O., Weaver, M., Calvert, S., et al., 2013. Targeted resequencing in epileptic encephalopathies identifies de novo mutations in CHD2 and SYNGAP1. Nat. Genet. 45, 825–830.

Castellotti, B., Mariotti, C., Rimoldi, M., Fancellu, R., Plumari, M., Caimi, S., Uziel, G., Nardocci, N., Moroni, I., Zorzi, G., et al., 2011. Ataxia with oculomotor apraxia type1 (AOA1): novel and recurrent aprataxin mutations, coenzyme Q10 analyses, and clinical findings in Italian patients. Neurogenetics 12, 193–201.

Champoux, J.J., 1977. Strand breakage by the DNA untwisting enzyme results in covalent attachment of the enzyme to DNA. Proc. Natl. Acad. Sci. U. S. A. 74, 3800–3804.

Chappell, C., Hanakahi, L.A., Karimi-Busheri, F., Weinfeld, M., West, S.C., 2002. Involvement of human polynucleotide kinase in double-strand break repair by non-homologous end joining. EMBO J. 21, 2827–2832.

Chattopadhyay, R., Wiederhold, L., Szczesny, B., Boldogh, I., Hazra, T.K., Izumi, T., Mitra, S., 2006. Identification and characterization of mitochondrial abasic (AP)-endonuclease in mammalian cells. Nucleic Acids Res. 34, 2067–2076.

Clements, P.M., Breslin, C., Deeks, E.D., Byrd, P.J., Ju, L., Bieganowski, P., Brenner, C., Moreira, M.C., Taylor, A.M., Caldecott, K.W., 2004. The ataxia-oculomotor apraxia 1 gene product has a role distinct from ATM and interacts with the DNA strand break repair proteins XRCC1 and XRCC4. DNA Repair (Amst) 3, 1493–1502.

Codini, M., Cataldi, S., Lazzarini, A., Tasegian, A., Ceccarini, M.R., Floridi, A., Lazzarini, R., Ambesi-Impiombato, F.S., Curcio, F., Beccari, T., et al., 2016. Why high cholesterol levels help hematological malignancies: role of nuclear lipid microdomains. Lipids Health Dis. 15, 4.

Cortes Ledesma, F., El Khamisy, S.F., Zuma, M.C., Osborn, K., Caldecott, K.W., 2009. A human 5′-tyrosyl DNA phosphodiesterase that repairs topoisomerase-mediated DNA damage. Nature 461, 674–678.

Crimella, C., Cantoni, O., Guidarelli, A., Vantaggiato, C., Martinuzzi, A., Fiorani, M., Azzolini, C., Orso, G., Bresolin, N., Bassi, M.T., 2011. A novel nonsense mutation in the APTX gene associated with delayed DNA single-strand break removal fails to enhance sensitivity to different genotoxic agents. Hum. Mutat. 32, E2118–2133.

Cristini, A., Park, J.H., Capranico, G., Legube, G., Favre, G., Sordet, O., 2016. DNA-PK triggers histone ubiquitination and signaling in response to DNA double-strand breaks produced during the repair of transcription-blocking topoisomerase I lesions. Nucleic Acids Res. 44, 1161–1178.

Daley, J.M., Wilson, T.E., Ramotar, D., 2011. Genetic interactions between HNT3/Aprataxin and RAD27/FEN1 suggest parallel pathways for 5′ end processing during base excision repair. DNA Repair (Amst) 9, 690–699.

Das, B.B., Dexheimer, T.S., Maddali, K., Pommier, Y., 2010. Role of tyrosyl-DNA phosphodiesterase (TDP1) in mitochondria. Proc. Natl. Acad. Sci. U. S. A. 107, 19790–19795.

Date, H., Onodera, O., Tanaka, H., Iwabuchi, K., Uekawa, K., Igarashi, S., Koike, R., Hiroi, T., Yuasa, T., Awaya, Y., et al., 2001. Early-onset ataxia with ocular motor apraxia and hypoalbuminemia is caused by mutations in a new HIT superfamily gene. Nat. Genet. 29, 184–188.

Davies, D.R., Interthal, H., Champoux, J.J., Hol, W.G., 2002. The crystal structure of human tyrosyl-DNA phosphodiesterase, Tdp1. Structure 10, 237–248.

Davies, D.R., Interthal, H., Champoux, J.J., Hol, W.G., 2003. Crystal structure of a transition state mimic for Tdp1 assembled from vanadate DNA, and a topoisomerase I-derived peptide. Chem. Biol. 10, 139–147.

Debethune, L., Kohlhagen, G., Grandas, A., Pommier, Y., 2002. Processing of nucleopeptides mimicking the topoisomerase I-DNA covalent complex by tyrosyl-DNA phosphodiesterase. Nucleic Acids Res. 30, 1198–1204.

Dedon, P.C., 2008. The chemical toxicology of 2-deoxyribose oxidation in DNA. Chem. Res. Toxicol. 21, 206–219.

Dunlop, J., Morin, X., Corominas, M., Serras, F., Tear, G., 2004. Glaikit is essential for the formation of epithelial polarity and neuronal development. Curr. Biol. 14, 2039–2045.

El-Khamisy, S.F., Saifi, G.M., Weinfeld, M., Johansson, F., Helleday, T., Lupski, J.R., Caldecott, K.W., 2005. Defective DNA single-strand break repair in spinocerebellar ataxia with axonal neuropathy-1. Nature 434, 108–113.

Fam, H.K., Chowdhury, M.K., Walton, C., Choi, K., Boerkoel, C.F., Hendson, G., 2013. Expression profile and mitochondrial colocalization of Tdp1 in peripheral human tissues. J. Mol. Histol. 44, 481–494.

Garcia-Diaz, B., Barca, E., Balreira, A., Lopez, L.C., Tadesse, S., Krishna, S., Naini, A., Mariotti, C., Castellotti, B., Quinzii, C.M., 2015. Lack of aprataxin impairs mitochondrial functions via downregulation of the APE1/NRF1/NRF2 pathway. Hum. Mol. Genet. 24, 4516–4529.

Gomez-Herreros, F., Romero-Granados, R., Zeng, Z., Alvarez-Quilon, A., Quintero, C., Ju, L., Umans, L., Vermeire, L., Huylebroeck, D., Caldecott, K.W., et al., 2013.

TDP2-dependent non-homologous end-joining protects against topoisomerase II-induced DNA breaks and genome instability in cells and in vivo. PLoS Genet. 9, e1003226.

Gueven, N., Becherel, O.J., Kijas, A.W., Chen, P., Howe, O., Rudolph, J.H., Gatti, R., Date, H., Onodera, O., Taucher-Scholz, G., et al., 2004. Aprataxin, a novel protein that protects against genotoxic stress. Hum. Mol. Genet. 13, 1081–1093.

Guo, D., Dexheimer, T.S., Pommier, Y., Nash, H.A., 2014. Neuroprotection and repair of 3′-blocking DNA ends by glaikit (gkt) encoding drosophila tyrosyl-DNA phosphodiesterase 1 (TDP1). Proc. Natl. Acad. Sci. U. S. A. 111, 15816–15820.

Harris, J.L., Jakob, B., Taucher-Scholz, G., Dianov, G.L., Becherel, O.J., Lavin, M.F., 2009. Aprataxin, poly-ADP ribose polymerase 1 (PARP-1) and apurinic endonuclease 1 (APE1) function together to protect the genome against oxidative damage. Hum. Mol. Genet. 18, 4102–4117.

Hawkins, A.J., Subler, M.A., Akopiants, K., Wiley, J.L., Taylor, S.M., Rice, A.C., Windle, J.J., Valerie, K., Povirk, L.F., 2009. In vitro complementation of Tdp1 deficiency indicates a stabilized enzyme-DNA adduct from tyrosyl but not glycolate lesions as a consequence of the SCAN1 mutation. DNA Repair (Amst) 8, 654–663.

Hazra, T.K., Izumi, T., Boldogh, I., Imhoff, B., Kow, Y.W., Jaruga, P., Dizdaroglu, M., Mitra, S., 2002a. Identification and characterization of a human DNA glycosylase for repair of modified bases in oxidatively damaged DNA. Proc. Natl. Acad. Sci. U. S. A. 99, 3523–3528.

Hazra, T.K., Kow, Y.W., Hatahet, Z., Imhoff, B., Boldogh, I., Mokkapati, S.K., Mitra, S., Izumi, T., 2002b. Identification and characterization of a novel human DNA glycosylase for repair of cytosine-derived lesions. J. Biol. Chem. 277, 30417–30420.

Henner, W.D., Grunberg, S.M., Haseltine, W.A., 1983. Enzyme action at 3′ termini of ionizing radiation-induced DNA strand breaks. J. Biol. Chem. 258, 15198–15205.

Heo, J., Li, J., Summerlin, M., Hays, A., Katyal, S., McKinnon, P.J., Nitiss, K.C., Nitiss, J.L., Hanakahi, L.A., 2015. TDP1 promotes assembly of non-homologous end joining protein complexes on DNA. DNA Repair (Amst) 30, 28–37.

Hirano, M., Yamamoto, A., Mori, T., Lan, L., Iwamoto, T.A., Aoki, M., Shimada, K., Furiya, Y., Kariya, S., Asai, H., et al., 2007a. DNA single-strand break repair is impaired in aprataxin-related ataxia. Ann. Neurol. 61, 162–174.

Hirano, R., Interthal, H., Huang, C., Nakamura, T., Deguchi, K., Choi, K., Bhattacharjee, M.B., Arimura, K., Umehara, F., Izumo, S., et al., 2007b. Spinocerebellar ataxia with axonal neuropathy: consequence of a Tdp1 recessive neomorphic mutation? EMBO J. 26, 4732–4743.

Hsiang, Y.H., Hertzberg, R., Hecht, S., Liu, L.F., 1985. Camptothecin induces protein-linked DNA breaks via mammalian DNA topoisomerase I. J. Biol. Chem. 260, 14873–14878.

Inamdar, K.V., Pouliot, J.J., Zhou, T., Lees-Miller, S.P., Rasouli-Nia, A., Povirk, L.F., 2002. Conversion of phosphoglycolate to phosphate termini on 3′ overhangs of DNA double strand breaks by the human tyrosyl-DNA phosphodiesterase hTdp1. J. Biol. Chem. 277, 27162–27168.

Interthal, H., Champoux, J.J., 2011. Effects of DNA and protein size on substrate cleavage by human tyrosyl-DNA phosphodiesterase 1. Biochem. J 436, 559–566.

Interthal, H., Chen, H.J., Champoux, J.J., 2005a. Human Tdp1 cleaves a broad spectrum of substrates: including phosphoamide linkages. J. Biol. Chem. 280, 36518–36528.

Interthal, H., Chen, H.J., Kehl-Fie, T.E., Zotzmann, J., Leppard, J.B., Champoux, J.J., 2005b. SCAN1 mutant Tdp1 accumulates the enzyme–DNA intermediate and causes camptothecin hypersensitivity. EMBO J. 24, 2224–2233.

Iyama, T., Wilson 3rd, D.M., 2013. DNA repair mechanisms in dividing and non-dividing cells. DNA Repair (Amst) 12, 620–636.

Jilani, A., Ramotar, D., Slack, C., Ong, C., Yang, X.M., Scherer, S.W., Lasko, D.D., 1999. Molecular cloning of the human gene PNKP, encoding a polynucleotide kinase 3′-phosphatase and evidence for its role in repair of DNA strand breaks caused by oxidative damage. J. Biol. Chem. 274, 24176–24186.

Karimi-Busheri, F., Lee, J., Tomkinson, A.E., Weinfeld, M., 1998. Repair of DNA strand gaps and nicks containing 3′-phosphate and 5′-hydroxyl termini by purified mammalian enzymes. Nucleic Acids Res. 26, 4395–4400.

Karimi-Busheri, F., Daly, G., Robins, P., Canas, B., Pappin, D.J., Sgouros, J., Miller, G.G., Fakhrai, H., Davis, E.M., Le Beau, M.M., 1999. Molecular characterization of a human DNA kinase. J. Biol. Chem. 274, 24187–24194.

Karimi-Busheri, F., Rasouli-Nia, A., Allalunis-Turner, J., Weinfeld, M., 2007. Human polynucleotide kinase participates in repair of DNA double-strand breaks by nonhomologous end joining but not homologous recombination. Cancer Res. 67, 6619–6625.

Katyal, S., el-Khamisy, S.F., Russell, H.R., Li, Y., Ju, L., Caldecott, K.W., McKinnon, P.J., 2007. TDP1 facilitates chromosomal single-strand break repair in neurons and is neuroprotective in vivo. EMBO J. 26, 4720–4731.

Kijas, A.W., Harris, J.L., Harris, J.M., Lavin, M.F., 2006. Aprataxin forms a discrete branch in the HIT (histidine triad) superfamily of proteins with both DNA/RNA binding and nucleotide hydrolase activities. J. Biol. Chem. 281, 13939–13948.

Koch, C.A., Agyei, R., Galicia, S., Metalnikov, P., O'Donnell, P., Starostine, A., Weinfeld, M., Durocher, D., 2004. Xrcc4 physically links DNA end processing by polynucleotide kinase to DNA ligation by DNA ligase IV. EMBO J. 23, 3874–3885.

Le Ber, I., Moreira, M.C., Rivaud-Pechoux, S., Chamayou, C., Ochsner, F., Kuntzer, T., Tardieu, M., Said, G., Habert, M.O., Demarquay, G., et al., 2003. Cerebellar ataxia with oculomotor apraxia type 1: clinical and genetic studies. Brain 126, 2761–2772.

171

Le Ber, I., Dubourg, O., Benoist, J.F., Jardel, C., Mochel, F., Koenig, M., Brice, A., Lombes, A., Durr, A., 2007. Muscle coenzyme Q10 deficiencies in ataxia with oculomotor apraxia 1. Neurology 68, 295–297.

Lebedeva, N.A., Rechkunova, N.I., Lavrik, O.I., 2011. AP-site cleavage activity of tyrosyl-DNA phosphodiesterase 1. FEBS Lett. 585, 683–686.

Lebedeva, N.A., Rechkunova, N.I., Ishchenko, A.A., Saparbaev, M., Lavrik, O.I., 2013. The mechanism of human tyrosyl-DNA phosphodiesterase 1 in the cleavage of AP site and its synthetic analogs. DNA Repair (Amst) 12, 1037–1042.

Ljungman, M., Lane, D.P., 2004. Transcription – guarding the genome by sensing DNA damage. Nat. Rev. Cancer 4, 727–737.

Loizou, J.I., El-Khamisy, S.F., Zlatanou, A., Moore, D.J., Chan, D.W., Qin, J., Sarno, S., Meggio, F., Pinna, L.A., Caldecott, K.W., 2004. The protein kinase CK2 facilitates repair of chromosomal DNA single-strand breaks. Cell 117, 17–28.

Lu, M., Mani, R.S., Karimi-Busheri, F., Fanta, M., Wang, H., Litchfeld, D.W., Weinfeld, M., 2010. Independent mechanisms of stimulation of polynucleotide kinase/phosphatase by phosphorylated and non-phosphorylated XRCC1. Nucleic Acids Res. 38, 510–521.

Mandal, S.M., Hegde, M.L., Chatterjee, A., Hegde, P.M., Szczesny, B., Banerjee, D., Boldogh, I., Gao, R., Falkenberg, M., Gustafsson, C.M., et al., 2012. Role of human DNA glycosylase Nei-like 2 (NEIL2) and single strand break repair protein polynucleotide kinase 3'-phosphatase in maintenance of mitochondrial genome. J. Biol. Chem. 287, 2819–2829.

Mani, R.S., Fanta, M., Karimi-Busheri, F., Silver, E., Virgen, C.A., Caldecott, K.W., Cass, C.E., Weinfeld, M., 2007. XRCC1 stimulates polynucleotide kinase by enhancing its damage discrimination and displacement from DNA repair intermediates. J. Biol. Chem. 282, 28004–28013.

Miao, Z.H., Agama, K., Sordet, O., Povirk, L., Kohn, K.W., Pommier, Y., 2006. Hereditary ataxia SCAN1 cells are defective for the repair of transcription-dependent topoisomerase I cleavage complexes. DNA Repair (Amst) 5, 1489–1494.

Moreira, M.C., Barbot, C., Tachi, N., Kozuka, N., Uchida, E., Gibson, T., Mendonca, P., Costa, M., Barros, J., Yanagisawa, T., et al., 2001. The gene mutated in ataxia-ocular apraxia 1 encodes the new HIT/Zn-finger protein aprataxin. Nat. Genet. 29, 189–193.

Moreira, M.C., Klur, S., Watanabe, M., Nemeth, A.H., Le Ber, I., Moniz, J.C., Tranchant, C., Aubourg, P., Tazir, M., Schols, L., et al., 2004. Senataxin, the ortholog of a yeast RNA helicase, is mutant in ataxia-ocular apraxia 2. Nat. Genet. 36, 225–227.

Mosesso, P., Piane, M., Palitti, F., Pepe, G., Penna, S., Chessa, L, 2005. The novel human gene aprataxin is directly involved in DNA single-strand-break repair. Cell. Mol. Life Sci.: CMLS 62, 485–491.

Murai, J., Huang, S.Y., Das, B.B., Dexheimer, T.S., Takeda, S., Pommier, Y., 2012. Tyrosyl-DNA phosphodiesterase 1 (TDP1) repairs DNA damage induced by topoisomerases I and II and base alkylation in vertebrate cells. J. Biol. Chem. 287, 12848–12857.

Nakashima, M., Takano, K., Osaka, H., Aida, N., Tsurusaki, Y., Miyake, N., Saitsu, H., Matsumoto, N., 2014. Causative novel PNKP mutations and concomitant PCDH15 mutations in a patient with microcephaly with early-onset seizures and developmental delay syndrome and hearing loss. J. Human Genet. 59, 471–474.

Paucar, M., Malmgren, H., Taylor, M., Reynolds, J.J., Svenningsson, P., Press, R., Nordgren, A., 2016. Expanding the ataxia with oculomotor apraxia type 4 phenotype. Neurol. Genet. 2, e49.

Pheiffer, B.H., Zimmerman, S.B., 1982. 3'-Phosphatase activity of the DNA kinase from rat liver. Biochem. Biophys. Res. Commun. 109, 1297–1302.

Plo, I., Liao, Z.Y., Barcelo, J.M., Kohlhagen, G., Caldecott, K.W., Weinfeld, M., Pommier, Y., 2003. Association of XRCC1 and tyrosyl DNA phosphodiesterase (Tdp1) for the repair of topoisomerase I-mediated DNA lesions. DNA Repair (Amst) 2, 1087–1100.

Pommier, Y., Leo, E., Zhang, H., Marchand, C., 2010. DNA topoisomerases and their poisoning by anticancer and antibacterial drugs. Chem. Biol. 17, 421–433.

Pommier, Y., Huang, S.Y., Gao, R., Das, B.B., Murai, J., Marchand, C., 2014. Tyrosyl-DNA-phosphodiesterases (TDP1 and TDP2). DNA Repair (Amst) 19, 114–129.

Pouliot, J.J., Yao, K.C., Robertson, C.A., Nash, H.A., 1999. Yeast gene for a Tyr-DNA phosphodiesterase that repairs topoisomerase I complexes. Science 286, 552–555.

Poulton, C., Oegema, R., Heijsman, D., Hoogeboom, J., Schot, R., Stroink, H., Willemsen, M.A., Verheijen, F.W., van de Spek, P., Kremer, A., et al., 2013. Progressive cerebellar atrophy and polyneuropathy: expanding the spectrum of PNKP mutations. Neurogenetics 14, 43–51.

Pourquier, P., Pilon, A.A., Kohlhagen, G., Mazumder, A., Sharma, A., Pommier, Y., 1997a. Trapping of mammalian topoisomerase I and recombinations induced by damaged DNA containing nicks or gaps. Importance of DNA end phosphorylation and camptothecin effects. J. Biol. Chem. 272, 26441–26447.

Pourquier, P., Ueng, L.M., Kohlhagen, G., Mazumder, A., Gupta, M., Kohn, K.W., Pommier, Y., 1997b. Effects of uracil incorporation, DNA mismatches and abasic sites on cleavage and religation activities of mammalian topoisomerase I. J. Biol. Chem. 272, 7792–7796.

Pourquier, P., Ueng, L.M., Fertala, J., Wang, D., Park, H.J., Essigmann, J.M., Bjornsti, M.A., Pommier, Y., 1999. Induction of reversible complexes between eukaryotic DNA topoisomerase I and DNA-containing oxidative base damages. 7, 8-dihydro-8-oxoguanine and 5-hydroxycytosine. J. Biol. Chem. 274, 8516–8523.

Quinzii, C.M., Kattah, A.G., Naini, A., Akman, H.O., Mootha, V.K., DiMauro, S., Hirano, M., 2005. Coenzyme Q deficiency and cerebellar ataxia associated with an aprataxin mutation. Neurology 64, 539–541.

Rasouli-Nia, A., Karimi-Busheri, F., Weinfeld, M., 2004. Stable down-regulation of human polynucleotide kinase enhances spontaneous mutation frequency and sensitizes cells to genotoxic agents. Proc. Natl. Acad. Sci. U. S. A. 101, 6905–6910.

Rass, U., Ahel, I., West, S.C., 2007a. Actions of aprataxin in multiple DNA repair pathways. J. Biol. Chem. 282, 9469–9474.

Rass, U., Ahel, I., West, S.C., 2007b. Defective DNA repair and neurodegenerative disease. Cell 130, 991–1004.

Rass, U., Ahel, I., West, S.C., 2008. Molecular mechanism of DNA deadenylation by the neurological disease protein aprataxin. J. Biol. Chem. 283, 33994–34001.

Raymond, A.C., Rideout, M.C., Staker, B., Hjerrild, K., Burgin Jr., A.B., 2004. Analysis of human tyrosyl-DNA phosphodiesterase I catalytic residues. J. Mol. Biol. 338, 895–906.

Reynolds, J.J., El-Khamisy, S.F., Katyal, S., Clements, P., McKinnon, P.J., Caldecott, K.W., 2009. Defective DNA ligation during short-patch single-strand break repair in ataxia oculomotor apraxia 1. Mol. Cell. Biol. 29, 1354–1362.

Reynolds, J.J., Walker, A.K., Gilmore, E.C., Walsh, C.A., Caldecott, K.W., 2012. Impact of PNKP mutations associated with microcephaly, seizures and developmental delay on enzyme activity and DNA strand break repair. Nucleic Acids Res. 40, 6608–6619.

Roca, J., Wang, J.C., 1994. DNA transport by a type II DNA topoisomerase: evidence in favor of a two-gate mechanism. Cell 77, 609–616.

Rosenquist, T.A., Zaika, E., Fernandes, A.S., Zharkov, D.O., Miller, H., Grollman, A.P., 2003. The novel DNA glycosylase NEIL1, protects mammalian cells from radiation-mediated cell death. DNA Repair (Amst) 2, 581–591.

Ryan, B.J., Hoek, S., Fon, E.A., Wade-Martins, R., 2015. Mitochondrial dysfunction and mitophagy in Parkinson's: from familial to sporadic disease. Trends Biochem. Sci. 40, 200–210.

Sano, Y., Date, H., Igarashi, S., Onodera, O., Oyake, M., Takahashi, T., Hayashi, S., Morimatsu, M., Takahashi, H., Makifuchi, T., et al., 2004. Aprataxin, the causative protein for EAOH is a nuclear protein with a potential role as a DNA repair protein. Ann. Neurol. 55, 241–249.

Sarkander, H.I., Dulce, H.J., 1978. Studies on the regulation of RNA synthesis in neuronal and glial nuclei isolated from rat brain. Exp. Brain Res. 31, 317–327.

Schellenberg, M.J., Tumbale, P.P., Williams, R.S., 2015. Molecular underpinnings of Aprataxin RNA/DNA deadenylase function and dysfunction in neurological disease. Prog. Biophys. Mol. Biol.

Seidle, H.F., Bieganowski, P., Brenner, C., 2005. Disease-associated mutations inactivate AMP-lysine hydrolase activity of Aprataxin. J. Biol. Chem. 280, 20927–20931.

Shen, J., Gilmore, E.C., Marshall, C.A., Haddadin, M., Reynolds, J.J., Eyaid, W., Bodell, A., Barry, B., Gleason, D., Allen, K., et al., 2010. Mutations in PNKP cause microcephaly, seizures and defects in DNA repair. Nat. Genet. 42, 245–249.

Shimada, M., Dumitrache, L.C., Russell, H.R., McKinnon, P.J., 2015. Polynucleotide kinase-phosphatase enables neurogenesis via multiple DNA repair pathways to maintain genome stability. EMBO J. 34, 2465–2480.

Sordet, O., Redon, C.E., Guirouilh-Barbat, J., Smith, S., Solier, S., Douarre, C., Conti, C., Nakamura, A.J., Das, B.B., Nicolas, E., et al., 2009. Ataxia telangiectasia mutated activation by transcription- and topoisomerase I-induced DNA double-strand breaks. EMBO Rep. 10, 887–893.

Sordet, O., Nakamura, J., Redon, C.E., Pommier, Y., 2010. DNA double-strand breaks and ATM activation by transcription-blocking DNA lesions. Cell Cycle 9, 274–278.

Steward, M.M., Sridhar, A., Meyer, J.S., 2013. Neural regeneration. Curr. Top. Microbiol. Immunol. 367, 163–191.

Sykora, P., Croteau, D.L., Bohr, V.A., Wilson 3rd, D.M., 2011. Aprataxin localizes to mitochondria and preserves mitochondrial function. Proc. Natl. Acad. Sci. U. S. A. 108, 7437–7442.

Sykora, P., Wilson 3rd, D.M., Bohr, V.A., 2012. Repair of persistent strand breaks in the mitochondrial genome. Mech. Ageing Dev. 133, 169–175.

Tada, M., Yokoseki, A., Sato, T., Makifuchi, T., Onodera, O., 2010. Early-onset ataxia with ocular motor apraxia and hypoalbuminemia/ataxia with oculomotor apraxia 1. Adv. Exp. Med. Biol. 685, 21–33.

Tahbaz, N., Subedi, S., Weinfeld, M., 2012. Role of polynucleotide kinase/phosphatase in mitochondrial DNA repair. Nucleic Acids Res. 40, 3484–3495.

Takahashi, T., Tada, M., Igarashi, S., Koyama, A., Date, H., Yokoseki, A., Shiga, A., Yoshida, Y., Tsuji, S., Nishizawa, M., et al., 2007. Aprataxin, causative gene product for EAOH/AOA1, repairs DNA single-strand breaks with damaged 3'-phosphate and 3'-phosphoglycolate ends. Nucleic Acids Res. 35, 3797–3809.

Takashima, H., Boerkoel, C.F., John, J., Saifi, G.M., Salih, M.A., Armstrong, D., Mao, Y., Quiocho, F.A., Roa, B.B., Nakagawa, M., et al., 2002. Mutation of TDP1, encoding a topoisomerase I-dependent DNA damage repair enzyme, in spinocerebellar ataxia with axonal neuropathy. Nat. Genet. 32, 267–272.

Tian, B., Yang, Q., Mao, Z., 2009. Phosphorylation of ATM by Cdk5 mediates DNA damage signalling and regulates neuronal death. Nat. Cell Biol. 11, 211–218.

Tranchant, C., Fleury, M., Moreira, M.C., Koenig, M., Warter, J.M., 2003. Phenotypic variability of aprataxin gene mutations. Neurology 60, 868–870.

Tumbale, P., Appel, C.D., Kraehenbuehl, R., Robertson, P.D., Williams, J.S., Krahn, J., Ahel, I., Williams, R.S., 2011. Structure of an aprataxin-DNA complex with insights into AOA1 neurodegenerative disease. Nat. Struct. Mol. Biol. 18, 1189–1195.

Tumbale, P., Williams, J.S., Schellenberg, M.J., Kunkel, T.A., Williams, R.S., 2014. Aprataxin resolves adenylated RNA-DNA junctions to maintain genome integrity. Nature 506, 111–115.

Tzoulis, C., Sztromwasser, P., Johansson, S., Gjerde, I.O., Knappskog, P., Bindoff, L.A., 2016. PNKP mutations identified by whole-exome sequencing in a norwegian patient with sporadic ataxia and edema. Cerebellum.

Tzur-Gilat, A., Ziv, Y., Mittelman, L., Barzilai, A., Shiloh, Y., 2013. Studying the cerebellar DNA damage response in the tissue culture dish. Mech. Ageing Dev. 134, 496–505.

Weinfeld, M., Mani, R.S., Abdou, I., Aceytuno, R.D., Glover, J.N., 2011. Tidying up loose ends: the role of polynucleotide kinase/phosphatase in DNA strand break repair. Trends Biochem. Sci. 36, 262–271.

Whitehouse, C.J., Taylor, R.M., Thistlethwaite, A., Zhang, H., Karimi-Busheri, F., Lasko, D.D., Weinfeld, M., Caldecott, K.W., 2001. XRCC1 stimulates human polynucleotide kinase activity at damaged DNA termini and accelerates DNA single-strand break repair. Cell 104, 107–117.

Wiederhold, L., Leppard, J.B., Kedar, P., Karimi-Busheri, F., Rasouli-Nia, A., Weinfeld, M., Tomkinson, A.E., Izumi, T., Prasad, R., Wilson, S.H., et al., 2004. AP endonuclease-independent DNA base excision repair in human cells. Mol. Cell 15, 209–220.

Wilstermann, A.M., Osheroff, N., 2001. Base excision repair intermediates as topoisomerase II poisons. J. Biol. Chem. 276, 46290–46296.

Yang, S.W., Burgin Jr., A.B., Huizenga, B.N., Robertson, C.A., Yao, K.C., Nash, H.A., 1996. A eukaryotic enzyme that can disjoin dead-end covalent complexes between DNA and type I topoisomerases. Proc. Natl. Acad. Sci. U. S. A. 93, 11534–11539.

Zhou, T., Lee, J.W., Tatavarthi, H., Lupski, J.R., Valerie, K., Povirk, L.F., 2005. Deficiency in 3'-phosphoglycolate processing in human cells with a hereditary mutation in tyrosyl-DNA phosphodiesterase (TDP1). Nucleic Acids Res. 33, 289–297.

Zhou, T., Akopiants, K., Mohapatra, S., Lin, P.S., Valerie, K., Ramsden, D.A., Lees-Miller, S.P., Povirk, L.F., 2009. Tyrosyl-DNA phosphodiesterase and the repair of 3'-phosphoglycolate-terminated DNA double-strand breaks. DNA Repair (Amst) 8, 901–911.

Zsurka, G., Kunz, W.S., 2015. Mitochondrial dysfunction and seizures: the neuronal energy crisis. Lancet Neurol. 14, 956–966.